

การพัฒนาโครงเลี้ยงเซลล์สามมิติที่ทำจากไฟโบรอินจากไหมไทยและเจลาติน

นางสาวจิตติมา ชำของเกษตร

ศูนย์วิทยทรัพยากร
จุฬาลงกรณ์มหาวิทยาลัย

วิทยานิพนธ์นี้เป็นส่วนหนึ่งของการศึกษาตามหลักสูตรปริญญาวิศวกรรมศาสตรมหาบัณฑิต

สาขาวิชาวิศวกรรมเคมี ภาควิชาวิศวกรรมเคมี

คณะวิศวกรรมศาสตร์ จุฬาลงกรณ์มหาวิทยาลัย


ปีการศึกษา 2550

ลิขสิทธิ์ของจุฬาลงกรณ์มหาวิทยาลัย



4 8 7 0 2 5 1 5 2 1

DEVELOPMENT OF THREE-DIMENSIONAL GELATIN/THAI SILK FIBROIN SCAFFOLDS



Miss Jitima Chamchongkaset

ศูนย์วิทยทรัพยากร

A Thesis Submitted in Partial Fulfillment of the Requirements
for the Degree of Master of Engineering Program in Chemical Engineering

Department of Chemical Engineering

Faculty of Engineering

Chulalongkorn University

Academic Year 2007

Copyright of Chulalongkorn University


502107

Thesis Title DEVELOPMENT OF THREE-DIMENSIONAL GELATIN/THAI SILK
FIBROIN SCAFFOLDS
By Miss. Jitima Chamchongkaset
Field of Study Chemical Engineering
Thesis Advisor Associate Professor Siriporn Damrongsakkul, Ph.D.


Accepted by the Faculty of Engineering, Chulalongkorn University in Partial
Fulfillment of the Requirements for the Master 's Degree

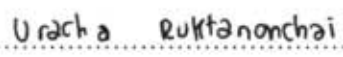

.....Dean of the Faculty of Engineering
(Professor Direk Lavansiri, Ph.D.)

THESIS COMMITTEE


.....Chairman
(Associate Professor Prasert Pavasant, Ph.D.)


.....Thesis Advisor
(Associate Professor Siriporn Damrongsakkul, Ph.D.)


.....Member
(Sorada Kanokpanont, Ph.D.)


.....Member
(Uracha Ruktanonchai, Ph.D.)

จิตินา ชำของเกษร : การพัฒนาโครงเลี้ยงเซลล์สามมิติที่ทำจากไฟโบรอินจากไหมไทย และเจลาติน. (DEVELOPMENT OF THREE-DIMENSIONAL GELATIN/THAI SILK FIBROIN SCAFFOLDS) อ. ที่ปรึกษา : รศ.ดร.ศิริพร คำรงค์ศักดิ์กุล, อ. ที่ปรึกษาร่วม : PROF.DAVID L. KAPLAN, Ph.D., 106 หน้า.

งานวิจัยนี้มุ่งเน้นพัฒนาโครงเลี้ยงเซลล์สามมิติที่ทำจากไฟโบรอินจากไหมไทย โดยนำเจลาติน ซึ่งเป็นอนุพันธ์ย่อยของคอลลาเจน ที่มีความเข้ากันได้ทางชีวภาพ ไม่ก่อให้เกิดการต่อต้านภายในร่างกาย มาผสมเพื่อช่วยเพิ่มคุณสมบัติทางชีวภาพให้กับโครงเลี้ยงเซลล์สามมิติไฟโบรอิน โดยโครงเลี้ยงเซลล์สามมิติจะเตรียมโดย 2 วิธีคือ วิธีการทำแห้งด้วยความเย็นและวิธีการกำจัดเกลือออก (salt-leaching) โครงเลี้ยงเซลล์สามมิติแบบทำแห้งด้วยความเย็น ถูกเตรียมจากสารละลายผสมและเชื่อมโยงพันธะระหว่างสายโซ่โพลีเมอร์โดยการให้ความร้อนภายใต้สภาวะสูญญากาศและการใช้สารเคมี ซึ่งพบว่า ลักษณะพื้นฐานของโครงเลี้ยงเซลล์สามมิติไฟโบรอินมีรูพรุนที่มีความเชื่อมต่อกัน ส่วนการกำจัดเกลือออกภายหลังจากไฟโบรอินเกิดการเจล จะได้โครงเลี้ยงเซลล์สามมิติที่มีขนาดรูพรุนประมาณ 600-710 ไมครอนตามขนาดของผลึกเกลือที่ใช้ ภายหลังจากปรับปรุงพื้นผิวด้วยการคอนจูเกตกับเจลาตินพบว่า ลักษณะพื้นฐานของโครงเลี้ยงเซลล์สามมิติไฟโบรอินมีลักษณะเป็นเส้นใยที่เชื่อมโยงต่อกันอย่างมาก ผลการทดสอบด้วยเทคนิคฟูเรียร์ทรานส์ฟอร์มอินฟราเรดสเปกโทรสโกปีและเอ็กซ์เรย์ดิฟแฟรกชัน พิสูจน์ให้เห็นว่า โครงสร้างของไฟโบรอินที่ขึ้นรูปด้วยวิธีทำแห้งด้วยความเย็นเป็น random coil ในขณะที่การขึ้นรูปด้วยวิธีการกำจัดเกลือออก โครงสร้างของไฟโบรอินมีลักษณะเป็น β -sheet จากการทดสอบค่ามอดูลัสของการกดพบว่าโครงเลี้ยงเซลล์สามมิติที่มีปริมาณไฟโบรอิน 80-100 เปอร์เซ็นต์โดยน้ำหนักที่ขึ้นรูปโดยการทำแห้งด้วยความเย็นมีค่ามอดูลัสประมาณ 350 กิโลปาสคาล และความสามารถในการบวมตัวของโครงเลี้ยงเซลล์สามมิติลดลงเมื่อปริมาณไฟโบรอินเพิ่มขึ้น ในกรณีโครงเลี้ยงเซลล์ที่ผลิตโดยการกำจัดเกลือออกพบว่า การคอนจูเกตเจลาตินและการสะสมของไฮดรอกซีเอปอไทต์ ช่วยเสริมความแข็งแรงให้กับโครงเลี้ยงเซลล์สามมิติไฟโบรอิน ผลการเลี้ยงเซลล์ต้นกำเนิดจากไขกระดูกของหนู และเซลล์กระดูก (MC3T3-E1) ในระดับห้องปฏิบัติการพบว่า เซลล์ต้นกำเนิดจากไขกระดูกของหนู สามารถเจริญเติบโตได้ดีบนโครงเลี้ยงเซลล์ไฟโบรอินที่ผลิตโดยการทำแห้งด้วยความเย็น นอกจากนี้พบว่า เจลาตินมีส่วนส่งเสริมการเจริญเติบโตของเซลล์กระดูกบนโครงเลี้ยงเซลล์ไฟโบรอิน เห็นได้จากจำนวนเซลล์ที่เพิ่มขึ้นและลักษณะพื้นฐานของเซลล์บนพื้นผิวของโครงเลี้ยงเซลล์ ซึ่งชัดเจนอย่างมากในกรณีของโครงเลี้ยงเซลล์ที่ผลิตโดยการกำจัดเกลือออกและคอนจูเกตกับเจลาติน ผลการทดลองแสดงถึงความเป็นไปได้ในการประยุกต์ใช้ไฟโบรอินจากไหมไทยในงานวิศวกรรมเนื้อเยื่อ

ภาควิชา.....วิศวกรรมเคมี..... ลายมือชื่อนิสิต..... จิตินา ชำของเกษร.....
 สาขาวิชา.....วิศวกรรมเคมี.....ลายมือชื่ออาจารย์ที่ปรึกษา.....
 ปีการศึกษา.....2550.....

4870251521 : MAJOR CHEMICAL ENGINEERING

KEY WORD: SILK FIBROIN / GELATIN / SCAFFOLD / OSTEOBLAST / TISSUE ENGINEERING

JITIMA CHAMCHONGKASET : DEVELOPMENT OF THREE-DIMENSIONAL
GELATIN/THAI SILK FIBROIN SCAFFOLDS. THESIS ADVISOR :
ASSOC.PROF.SIRIPORN DAMRONGSAKKUL, Ph.D., THESIS COADVISOR :
PROF.DAVID L. KAPLAN, Ph.D., 106 pp.

The aim of this study was to develop three-dimensional silk fibroin-based (SF) scaffolds from Thai yellow cocoon "Nangnoi-Srisaket" of *Bombyx mori* silkworms. To enhance the biological properties of Thai silk fibroin-based scaffolds, type A gelatin, the denature form of collagen having good biocompatibility, was used to blend with silk fibroin. Three-dimensional scaffolds were prepared by two methods; freeze-drying and salt-leaching. Freeze-dried scaffolds were prepared from blended solutions and crosslinked by dehydrothermal and chemicals. It was found that pure silk fibroin scaffolds possessed highly interconnected porous network. For salt-leached scaffolds, the pore size of silk fibroin scaffold structure represented the size of salt crystals used (600-710 μ m). After gelatin conjugating, gelatin was partly formed fibers inside the pores of silk fibroin scaffolds resulting in fiber-like structure with highly interconnection. The results on ATR-FTIR and XRD proved that the structure of freeze-dried silk fibroin scaffolds was random coil while that of salt-leached silk fibroin scaffolds was β -sheet. The compressive modulus of freeze-dried scaffolds having high silk fibroin contents (80-100wt%) was about 350 kPa. Swelling ability of freeze-dried scaffolds decreased as increasing silk fibroin content. For salt-leached scaffolds, gelatin conjugating and hydroxyapatite deposition enhanced the compressive modulus of silk fibroin scaffolds. The results on *in vitro* culture using bone-marrow derived mesenchymal stem cells (MSCs) on freeze-dried silk fibroin showed that silk fibroin scaffolds were more effective to promote cell proliferation than pure gelatin and blended scaffolds. Mouse osteoblast-like cells (MC3T3-E1) culture showed that gelatin blending and gelatin conjugating could enhance the cell proliferation on silk fibroin scaffolds as noticed from the number of cells and the cell morphology on the surface of scaffolds. This was more distinct in the case of conjugated gelatin/silk fibroin scaffolds. The results implied that Thai silk fibroin looked promising to be applied in tissue engineering.

Department..... Chemical Engineering.....Student's signature.....
Field of study..... Chemical Engineering.....Advisor's signature.....
Academic year... 2007.....

ACKNOWLEDGEMENTS

This research is completed with the aid and support of many people. The author would like to express her deepest gratitude to Associate Professor Dr. Siriporn Damrongsakkul, her advisor, for her continuous guidance, helpful suggestions and warm encouragement. She wishes to give her gratitude to Professor Dr. David L. Kaplan, the thesis co-advisor, for his kind guidance and invaluable discussions. In addition, she is also grateful to Associate Professor Dr. Prasert Pavasant, Dr. Sorada Kanokpanont and Dr. Uracha Ruktanonchai for serving as the chairman and the members of the thesis committee, respectively, whose comments were constructively and especially helpful.

The author would like to thank Associate Professor Dr. Prasit Pavasant and the Department of Anatomy, Faculty of Dentistry, Chulalongkorn University for his assistance in cell sources and Associate Professor Dr. Sanong Ekgasit and the Department of Chemistry, Faculty of Science, Chulalongkorn University for his provision of Fourier Transform Infrared (FTIR) spectrophotometer.

The author would like to thank Miss. Juthamas Ratanavaraporn for her kind attentions and suggestions in cell culture as well as facilities and Mr. Isarawut Prasertsung for his helps and suggestions with experiments.

The author would like to thank the staffs of Analytical Instrument Center and Laboratory for their helps with experiments. She would like to extend her grateful thanks to all members of Polymer Engineering Research Group and Center of Excellence on Catalysis and Catalytic Reaction Engineering at the Department of Chemical Engineering as well as all members of i-Tissue Laboratory at the Department of Medicine, Chulalongkorn University.

Finally, the author expresses her sincere thanks to her parents and everyone in her family for their unflinching understanding and affectionate encouragement.

CONTENTS

	PAGE
ABSTRACT (IN THAI)	iv
ABSTRACT (IN ENGLISH)	v
ACKNOWLEDGEMENTS	vi
CONTENTS.....	vii
LIST OF TABLES	xi
LIST OF FIGURES	xii
CHAPTER	
I. INTRODUCTION.....	1
1.1 Background.....	1
1.2 Objectives.....	2
1.3 Scopes of research.....	3
II. RELEVANT THEORY.....	4
2.1 Three-dimensional scaffolds.....	4
2.2 Biomaterials for scaffold fabrication.....	4
2.2.1 Synthetic polymers.....	5
2.2.2 Inorganic materials or ceramics.....	5
2.2.3 Natural macromolecules.....	5
2.2.3.1 Silk.....	6
2.2.3.2 Gelatin.....	13
2.3 Scaffold fabrication techniques.....	16
2.3.1 Particulate leaching.....	16
2.3.2 Gas foaming.....	17
2.3.3 Fiber meshes/fiber bonding.....	17
2.3.4 Phase separation.....	18
2.3.5 Melt molding.....	18
2.3.6 Freeze drying.....	19
2.4 Crosslinking techniques.....	19
2.4.1 Ultraviolet irradiation.....	19

2.4.2	Electron beam irradiation.....	20
2.4.3	Dehydrothermal crosslinking.....	20
2.4.4	Chemical crosslinking.....	20
2.5	<i>In vitro</i> cell culture.....	21
2.5.1	Types of cell cultures.....	21
2.5.1.1	Primary cell cultures.....	21
2.5.1.2	Permanent cultures or cell lines cultures.....	22
2.5.2	MTT assay for cell viability.....	22
III.	LITERATURE REVIEWS.....	24
IV.	EXPERIMENTAL WORK.....	39
4.1	Materials and reagents.....	39
4.2	Equipments.....	40
4.3	Experimental procedures.....	41
4.3.1	Preparation of silk fibroin and gelatin solutions.....	42
4.3.1.1	Preparation of silk fibroin solution.....	42
4.3.1.2	Preparation of gelatin solution.....	42
4.3.2	Preparation of silk fibroin and silk fibroin-based scaffolds.....	42
4.3.2.1	Preparation of silk fibroin and gelatin/silk fibroin scaffolds via freeze-drying.....	42
4.3.2.2	Preparation of silk fibroin and conjugated gelatin/silk fibroin scaffolds via salt-leaching.....	43
4.3.2.3	Preparation of hydroxyapatite/silk fibroin and hydroxyapatite-conjugated gelatin/silk fibroin scaffolds.....	43
4.3.3	Characterization of scaffolds.....	44
4.3.3.1	Chemical characterization.....	44
4.3.3.1.1	Attenuated total reflection fourier transform infrared (ATR-FTIR) spectrophotometric measurements.....	44
4.3.3.1.2	X-ray diffraction (XRD) measurements.....	44
4.3.3.2	Physical characterization.....	44
4.3.3.2.1	Morphology.....	44

	4.3.3.2.2 Compressive modulus.....	45
	4.3.3.2.3 Swelling property.....	45
	4.3.3.3 Biological characterization.....	45
	4.3.3.3.1 MSCs isolation and culture.....	46
	4.3.3.3.2 MC3T3-E1 culture.....	46
	4.3.3.3.3 <i>In vitro</i> cell proliferation tests.....	46
	4.3.3.3.4 MC3T3-E1 Migration and morphological observation	47
	4.3.4 Statistical analysis.....	47
V.	RESULTS AND DISCUSSION.....	49
	5.1 Degummed silk fiber.....	49
	5.2 Chemical characteristics of silk fibroin scaffolds.....	51
	5.2.1 Structural analysis of silk fibroin scaffolds.....	51
	5.2.1.1 Attenuated total reflection fourier transform infrared (ATR-FTIR) spectrophotometric analysis.....	51
	5.2.1.2 X-ray diffraction (XRD) analysis.....	52
	5.2.2 LiBr residual in silk fibroin scaffolds.....	55
	5.3 Comparison of type A and type B gelatin blending in silk fibroin.....	55
	5.4 Silk fibroin and gelatin/silk fibroin scaffolds via freeze-drying.....	61
	5.4.1 Compressive modulus of scaffolds.....	61
	5.4.2 Swelling property of scaffolds.....	62
	5.4.3 Biological property of scaffolds.....	64
	5.4.3.1 MSCs proliferation tests.....	64
	5.4.3.2 MC3T3-E1 proliferation tests.....	64
	5.4.3.3 MC3T3-E1 migration and morphological observation.....	67
	5.5 Silk fibroin and conjugated gelatin/silk fibroin scaffolds via salt-leaching.....	71
	5.5.1 Morphology of scaffolds.....	72
	5.5.1.1 Hydroxyapatite/silk fibroin scaffolds.....	72
	5.5.1.2 Hydroxyapatite-conjugated gelatin/silk fibroin scaffolds.....	73

5.5.2 Compressive modulus of scaffolds.....	80
5.5.3 Swelling property of scaffolds.....	82
5.5.4 Biological property of scaffolds.....	83
5.5.4.1 MC3T3-E1 proliferation tests.....	83
5.5.4.2 MC3T3-E1 migration and morphological observation.....	84
VI. CONCLUSIONS AND RECOMMENDATIONS.....	90
6.1 Conclusions.....	90
6.2 Recommendations.....	92
REFERENCES.....	93
APPENDICES.....	99
APPENDIX A: Raw data of compressive modulus	100
APPENDIX B: Raw data of swelling ratios	102
APPENDIX C: Standard curve of <i>in vitro</i> cell culture test.....	104
VITAE.....	106



 ศูนย์วิทยทรัพยากร
 จุฬาลงกรณ์มหาวิทยาลัย

LIST OF TABLES

TABLE	PAGE
2.1 Amino Acid Compositions of <i>Bombyx mori</i> silk fibroin	8
2.2 Typical specifications for gelatins	14
2.3 Amino acids essential for humans	15
5.1 pI and charges of silk fibroin and gelatin	56
5.2 Salt-leached scaffolds prepared in this work	72
A-1 Mean and SD of Compressive modulus of gelatin/silk fibroin scaffolds with DHT treatment for 24 h.....	100
A-2 Mean and SD of Compressive modulus of gelatin/silk fibroin scaffolds with DHT treatment for 48 h	100
A-3 Mean and SD of compressive modulus of hydroxyapatite/silk fibroin scaffolds	100
A-4 Mean and SD compressive modulus of hydroxyapatite-conjugated gelatin/silk fibroin scaffolds.....	101
B-1 Mean and SD of swelling ratios of gelatin/silk fibroin scaffolds with DHT treatment for 24 h	102
B-2 Mean and SD of swelling ratios of gelatin/silk fibroin scaffolds with DHT treatment for 48 h.....	102
B-3 Mean and SD of swelling ratios of hydroxyapatite/silk fibroin scaffolds.....	102
B-4 Mean and SD of swelling ratios of hydroxyapatite-conjugated gelatin/silk fibroin scaffolds.....	103
C-1 Absorbance at 570 nm from MTT assay for standard curve of bone-marrow derived mesenchymal stem cells (MSCs).....	104
C-2 Absorbance at 570 nm from MTT assay for mouse osteoblast-like cells (MC3T3-E1).....	105

LIST OF FIGURES

FIGURE	PAGE
2.1 β -sheet secondary structure of silk	6
2.2 Structure of raw silk fiber	7
2.3 SEM micrographs of fiber (a) cocoon raw material, and (b) degummed fiber...10	10
2.4 Illustration of a Donnan dialysis experiment to separate and concentrate uranyl nitrate, $UO_2(NO_3)_2$	12
2.5 Charge mosaic membranes, consisting of finely dispersed domains containing fixed negatively and fixed positively charged groups, are salt permeable	13
2.6 The structural unit of gelatin	14
2.7 Applications of gelatin	16
2.8 Porous polymer foams produced by different techniques. (a) phase separation, (b) particulate leaching, (c) solid freeform fabrication technique, and (d) microsphere sintering	17
2.9 Crosslinking of protein with EDC and NHS	21
2.10 Molecular structure of MTT (3-(4, 5-dimethyl-2-thiazolyl)-2, 5-diphenyl tetrazolium bromide).....	23
4.1 Diagram of experimental procedures.	41
4.2 Schematic diagram of cross-sectional plane prior to observe cell-scaffold interaction.....	48
5.1 SEM micrographs of silk fiber: (a)-(b) cocoon fiber, (c)-(d) degummed silk fiber with Na_2CO_3 , and (e)-(f) degummed silk fiber with $NaOH$	50
5.2 ATR-FTIR spectra of freeze-dried silk fibroin scaffolds from dialyzed solution (a) after freeze-drying (before any treatments), (b) after DHT treatment for 48 h, (c) after DHT and EDC treatments, and (d) air-dried silk fibroin obtained after gelling.....	53
5.3 XRD patterns of freeze-dried silk fibroin scaffolds from dialyzed solution (a) after freeze-drying (before any treatments), (b) after DHT treatment for 48 h, (c) after DHT and EDC treatment, and (d) air-dried silk fibroin	

obtained after gelling.....	54
5.4 XRD pattern of lithium bromide (LiBr) powder	55
5.5 SEM micrographs of freeze-dried type B gelatin/silk fibroin (GB/SF) scaffolds (a), (b) 0/100, (c)-(e) 20/80, (f)-(h) 40/60, (i)-(k) 60/40, (l)-(n) 80/20, and (o), (p) 100/0.....	57
5.6 SEM micrographs of freeze-dried type A gelatin/silk fibroin (GA/SF) scaffolds (a) 0/100, (b) 20/80, (c) 40/60, (d) 60/40, (e) 80/20, and (f)100/0.....	60
5.7 Compressive modulus of freeze-dried gelatin/silk fibroin scaffolds with various DHT treatment periods: (◆) 24 h, and (■) 48 h.....	62
5.8 Swelling ratios of freeze-dried gelatin/silk fibroin scaffolds with various DHT treatment periods: (◆) 24 h, and (■) 48 h.....	63
5.9 Number of MSCs on freeze-dried gelatin/silk fibroin scaffolds after 3 and 7 days of the culture (seeding: 2×10^4 cells/scaffold).....	66
5.10 Number of MC3T3-E1 on freeze-dried gelatin/silk fibroin scaffolds after 1, 7 and 14 days of the culture (seeding: 2×10^4 cells/scaffold).....	67
5.11 SEM micrographs of cross-sectional plane of freeze-dried 20/80 gelatin/silk fibroin scaffolds at position (a) 1 (cell seeding side), (b) 2, (c) 3, and (d) 4 (plate-exposed side) after 14 days of MC3T3-E1 culture	68
5.12 SEM micrographs of cross-sectional plane of freeze-dried pure silk fibroin scaffolds at position (a) 1 (cell seeding side), (b) 2, (c) 3, and (d) 4 (plate- exposed side) after 14 days of MC3T3-E1 culture	69
5.13 SEM micrographs of MC3T3-E1 morphology after 14 days cultured on freeze-dried gelatin/silk fibroin scaffolds: (a) 20/80, and (b) 0/100	70
5.14 SEM micrograph of NaCl crystals.....	71
5.15 SEM micrographs of silk fibroin scaffolds (a)-(c) before soaking, after (d)-(f) 2 cycles, (g)-(i) 4 cycles, and (j)-(l) 6 cycles of alternate soaking in calcium and phosphate solutions.....	75
5.16 SEM micrographs of hydroxyapatite crystals in silk fibroin scaffolds (a)-(b) 2 cycles, (c)-(d) 4 cycles, and (e)-(f) 6 cycles of alternate soaking.....	76
5.17 SEM micrographs of conjugated gelatin/silk fibroin scaffolds (a)-(c) before soaking, after (d)-(f) 2 cycles, (g)-(i) 4 cycles, and (j)-(l) 6 cycles of alternate soaking in calcium and phosphate solutions.....	77

5.18 SEM micrographs of hydroxyapatite crystals in conjugated gelatin/ silk fibroin scaffolds (a)-(b) 2 cycles, (c)-(d) 4 cycles, and (e)-(f) 6 cycles of alternate soaking.....	78
5.19 Increasing weights of scaffolds as a function of alternate soaking cycles (◆) silk fibroin scaffolds, and (■) conjugated gelatin/silk fibroin scaffold.....	79
5.20 Compressive modulus of (◆) hydroxyapatite/silk fibroin scaffolds, and (■) hydroxyapatite-conjugated gelatin/silk fibroin scaffolds.....	81
5.21 Swelling properties of (◆) hydroxyapatite/silk fibroin scaffolds, and (■) hydroxyapatite-conjugated gelatin/silk fibroin scaffolds.....	83
5.22 Number of MC3T3-E1 on hydroxyapatite/silk fibroin scaffolds, and hydroxyapatite-conjugated gelatin/silk fibroin scaffolds after 1, 7 and 14 days of the culture (seeding: 2×10^4 cells/scaffold).....	86
5.23 SEM micrographs of cross-sectional plane of silk fibroin scaffolds at position (a) 1 (cell seeding side), (b) 2, (c) 3, and (d) 4 (plate-exposed side) after 14 days of MC3T3-E1 culture	87
5.24 SEM micrographs of cross-sectional plane of conjugated-gelatin silk fibroin scaffolds at position (a) 1 (cell seeding side), (b) 2, (c) 3, and (d) 4 (plate- exposed side) after 14 days of MC3T3-E1 culture	88
5.25 SEM micrographs of cell morphology on scaffolds: (a) silk fibroin, and (b) conjugated-gelatin silk fibroin after 14 days of MC3T3-E1 culture	89
C-1 Standard curve for MSCs.....	104
C-2 Standard curve for MC3T3-E1.....	105

CHAPTER I

INTRODUCTION

1.1 Background

Three-dimensional scaffolds are required in tissue engineering to support for the formation of tissue as well as to promote cell migration, adherence, and formation of new extracellular matrix and to foster the transport of nutrients and metabolic wastes. Porous structure with interconnected pores and appropriated pore size is usually requested for scaffolds. Sufficient mechanical properties of the scaffolds are also necessary to support tissue function and integration. Scaffolds also have to biodegrade at a rate comparable with new tissue growth [1]. As a result, types of biodegradable materials suitable to fabricate such scaffolds are widely explored. Typical material used is collagen.

As silk fibroin has been used commercially as biomedical sutures for decades, recently it has been explored for many biomedical applications, because of its impressive biological compatibility and mechanical properties. For example, silk fibroin from *Bombyx mori* silkworm is reported to support matrixes and ligament using osteoblast, hepatocyte and fibroblast cell for tissue engineering [2-5]. Therefore, the preparation of silk fibroin porous scaffolds, having high porosity and interconnected pores, has become one of the major challenges in tissue engineering.

In Thailand, Thai native silkworms have been long cultivated and Thai silk is well known in textile industry for many decades. Distinct characteristics of cocoon Thai silk are its yellow color and coarse filament. There is more sericin or silk gum in Thai silk (e.g. up to 38%) than in normal *Bombyx mori* silk (e.g. 20-25%) [6]. These characteristics provide Thai silk a unique texture for textile industry. However, Thai silk fibers have not much been reported for biomedical uses, especially in tissue

engineering application. It is therefore of our interest to explore the uses of Thai silk fibroin as three-dimensional scaffolds for tissue engineering applications.

In addition, to enhance the biological properties of Thai silk fibroin-based scaffolds, the concept of blending with gelatin is employed. This due to the fact that gelatin is a derivative of collagen which is a major constituent of skin, bones and connective tissue. Gelatin contains arginine-glycine-aspartic acid (RGD)-like sequence that promotes cell adhesion and migration [7]. Particularly, it does not exhibit antigenicity and it is widely applied in many industries such as pharmaceutical, cosmetics, food and tissue engineering. Recently, crosslinked gelatin-based scaffolds have been reported as a potential wound substitute [8].

Moreover, as known that natural bone comprises about 70wt% of a mineral phase, primarily hydroxyapatite, and 30wt% of an organic matrix [9]. Hydroxyapatite was employed to strengthen scaffolds used for bone tissue engineering [10-12].

The purpose of this study is to develop silk fibroin and gelatin/silk fibroin scaffolds using silk fibroin extracted from cocoon of Thai silkworm. The influence of the type of gelatin (i.e. type A and type B) and hydroxyapatite on scaffold fabrication are studied. Chemical, physical, and biological properties of scaffolds will be investigated in order to evaluate the applicability of Thai silk fibroin and gelatin/Thai silk fibroin scaffolds as a biomaterial for tissue engineering.

1.2 Objectives

- 1.2.1 To develop three-dimensional Thai silk fibroin and gelatin/Thai silk fibroin scaffolds for tissue engineering applications.
- 1.2.2 To study chemical, physical, and biological properties of Thai silk fibroin and gelatin/Thai silk fibroin scaffolds.

1.3 Scopes of Research

- 1.3.1 Prepare silk fibroin solution from cocoons of Thai silkworm.
- 1.3.2 Prepare Thai silk fibroin and gelatin/Thai silk fibroin scaffolds via freeze-drying.
- 1.3.3 Prepare Thai silk fibroin, conjugated gelatin/Thai silk fibroin, and hydroxyapatite-conjugated gelatin/Thai silk fibroin scaffolds via salt-leaching.
- 1.3.4 Characterize the chemical properties of Thai silk fibroin scaffolds including:
 - 1.3.4.1 Attenuated total reflection fourier transforms infrared (ATR-FTIR) spectroscopy
 - 1.3.4.2 X-ray diffraction (XRD)
- 1.3.5 Characterize the physical properties of Thai silk fibroin, gelatin/Thai silk fibroin and hydroxyapatite-conjugated gelatin/Thai silk fibroin scaffolds including:
 - 1.3.5.1 Morphology (porous structure analysis)
 - 1.3.5.2 Compression modulus
 - 1.3.5.3 Water swelling
- 1.3.6 Characterize the biological properties of Thai silk fibroin and gelatin/Thai silk fibroin scaffolds including *in vitro* biocompatibility of bone-marrow derived mesenchymal stem cells (MSCs) and mouse osteoblasts-like cells (MC3T3-E1).

จุฬาลงกรณ์มหาวิทยาลัย

CHAPTER II

RELEVANT THEORY

2.1 Three-dimensional scaffolds [1, 5]

Three-dimensional scaffolds are required in tissue engineering to support the formation of tissue relevant mimics as well as to promote cellular migration, adherence, formation of new extracellular matrix, tissue ingrowth and to foster the transport of nutrients and metabolic wastes. Ideally, scaffolds should:

- support cell attachment, migration, cell–cell interactions, cell proliferation and differentiation;
- be biocompatible to the host immune system where the engineered tissue will be implanted;
- biodegrade at a controlled rate to match the rate of neotissue growth and facilitate the integration of engineered tissue into the surrounding host tissue;
- provide structural support for cells and neotissue formed in the scaffold during the initial stages of post-implantation, and
- have versatile processing options to alter structure and morphology related to tissue-specific needs.

2.2 Biomaterials for scaffold fabrication [13]

There are many natural, synthetic polymers and ceramics which have high potential as biocompatible and biodegradable materials for scaffolding.

2.2.1 Synthetic polymers

Poly(glycolic acid) (PGA), poly(lactic acid) (PLA), and their copolymers poly(lactic acid-co-glycolic acid) (PLGA) are a family of linear aliphatic polyesters, which are most frequently used in tissue engineering. These polymers degrade through hydrolysis of ester bonds. There are other linear aliphatic polyesters, such as poly(ϵ -caprolactone) (PCL) and poly(hydroxy butyrate) (PHB), which are also used in tissue engineering.

2.2.2 Inorganic materials or ceramics

These materials can be categorized as porous bioactive glasses and calcium phosphates. Within the calcium phosphates, β -tricalcium phosphate (β -TCP), hydroxyapatite (HAp) and its derivatives, and their combinations are the most frequently used. In many natural material such as bone, cartilage, shells, and skin, are composed of inorganic minerals and organic molecules. These inorganic materials are widely considered to be osteoconductive (their surface properties support osteoblastic cells adhesion, growth, and differentiation). However, these inorganic materials are often difficult to process into highly porous structures and are mechanically brittle. To overcome these disadvantages, composite materials with synthetic or natural polymers have been explored for bone tissue engineering.

2.2.3 Natural macromolecules

Natural polymers, such as proteins and polysaccharides, have also been used for tissue engineering applications. Collagen is a fibrous protein and a major natural extracellular matrix component. It has been used for various tissue regeneration applications. Another category of well-known natural fibrous proteins is silk. Silkworm silk has been used in textile production for centuries, and has been used as nondegradable sutures for decades because of its excellent tensile mechanical property. Polysaccharides such as alginate, chitosan, and hyaluronate are another class

of natural polymers that have been used as porous solid-state tissue engineering scaffolds.

2.2.3.1 Silk [14-15]

Silk is generally defined as a protein polymer that is spun into fibers by some lepidoptera larvae such as silkworms, spiders, scorpions, mites and flies. Silk proteins are usually produced within specialized glands after biosynthesis in epithelial cells, followed by secretion into the lumen of these glands where the proteins are stored prior to spinning into fibers. Silks differ widely in composition, structure and properties depending on the specific source. The most extensively characterized silks are from the domesticated silkworm, *Bombyx mori*, and from spiders (*Nephila clavipes* and *Araneus diadematus*).

Fibrous proteins, such as silks and collagens, are characterized by a highly repetitive primary sequence that leads to significant homogeneity in secondary structure, i.e., triple helices in the case of collagens and β -sheets (Figure 2.1) in the case of many types of silks.

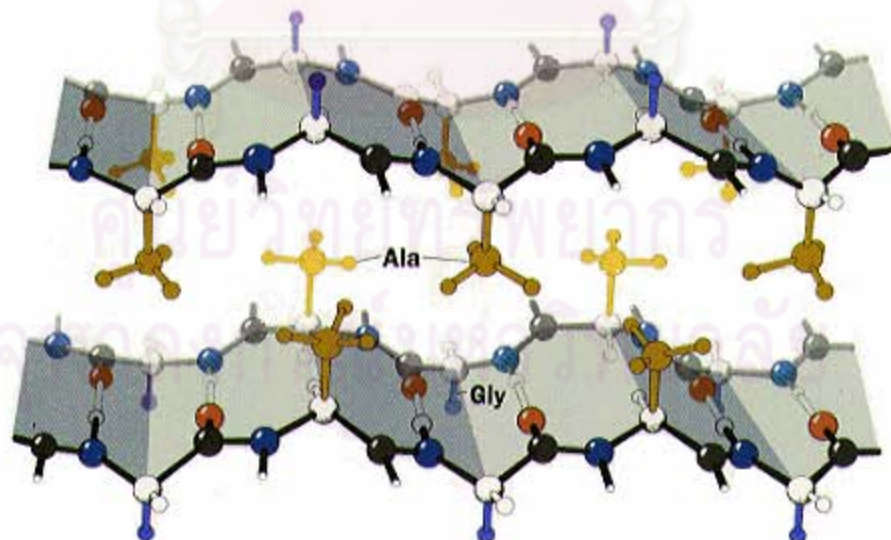


Figure 2.1 β -sheet secondary structure of silk [16]

Silk consists of two main parts called silk sericin and silk fibroin.

(a) Silk sericin

Silk sericin or silk gum is a minor component of fiber (i.e. 20-25 wt% of raw silk) and it also has some impurities such as waxes, fats, and pigments. Sericin is a yellow, brittle, and inelastic substance. It acts as an adhesive for the twin silk fibroin filaments and covers the luster of silk fibroin as shown in Figure 2.2. Sericin is known as an amorphous structure. It can be dissolved in a hot soap solution.

(b) Silk fibroin

A major constituent of raw silk fiber, about 75-80 wt%, is silk fibroin is an insoluble protein in most solvents, including water, dilute acid, and alkaline.

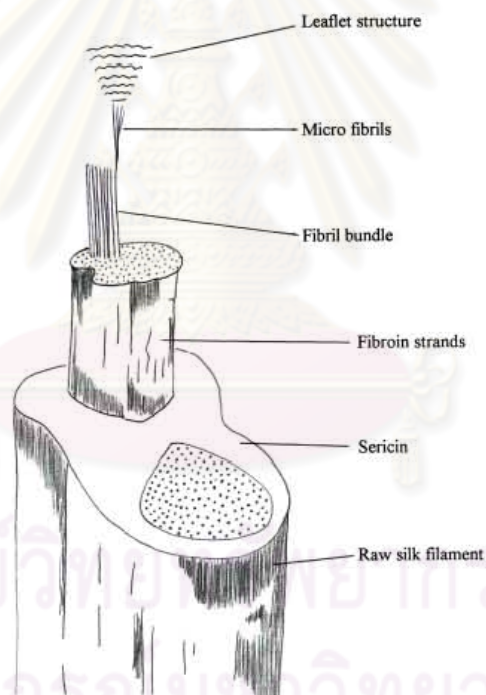


Figure 2.2 Structure of raw silk fiber [6]

Structure of silk fibroin

Silk fibroin contains at least two major proteins, light and heavy chains, 25 and 325 kDa, respectively. The heavy chain protein consists of 12 repetitive regions called crystalline regions and 11 non-repetitive interspaced regions called amorphous regions. The crystalline regions of the domestic silk proteins contain several

repetitions of the basic sequence $-(\text{Gly-Ala-Gly-X})_n-$, with X: Ser or Tyr. The amorphous regions contain most of the amino acid residues with bulky and polar side chains. Silk fibroin has a highly oriented and crystalline structure.

Amino acid compositions of silk fibroin

Silk fibroin is composed of 18 amino acids (Table 2.1). The isoelectric point is around 5.

Table 2.1 Amino Acid Compositions of *Bombyx mori* silk fibroin [17]

Amino Acid	Symbol	Charge	Hydrophobic/ Hydrophilic	Amount (g/100 g silk fibroin)
Alanine	Ala	neutral	hydrophobic	32.4
Glycine	Gly	neutral	hydrophilic	42.8
Tyrosine	Tyr	neutral	hydrophilic	11.8
Serine	Ser	neutral	hydrophilic	14.7
Aspartate	Asp	negative	hydrophilic	1.73
Arginine	Arg	positive	hydrophilic	0.90
Histidine	His	positive	hydrophilic	0.32
Glutamate	Glu	negative	hydrophilic	1.74
Lysine	Lys	positive	hydrophilic	0.45
Valine	Val	neutral	hydrophobic	3.03
Leucine	Leu	neutral	hydrophobic	0.68
Isoleucine	Ile	neutral	hydrophobic	0.87
Phenylalanine	Phe	neutral	hydrophobic	1.15
Proline	Pro	neutral	hydrophobic	0.63
Threonine	Thr	neutral	hydrophilic	1.51
Methionine	Met	neutral	hydrophobic	0.10
Cysteine	Cys	neutral	hydrophobic	0.03
Tryptophan	Trp	neutral	hydrophilic	0.36

Characteristics of silk fibroin

Characteristics of silk fibroin as for industrial materials can be summarized as follows.

- Pure silk proteins can be obtained from silkworms.
- Silk fibers from *Bombyx mori* silkworms can be dissolved in concentrated neutral salt solutions. After dialyzing against water a pure silk fibroin solution can be obtained.
- Various forms of silk proteins, such as powder, gel and film can be produced by controlling the cast-dry speed of the silk fibroin solution.
- Silk protein can be made insoluble by immersing it in alcohol solution. This technique is interesting for the application of silk fibroin as a biomaterial since this agent is not harmful to living tissues.

Applications of silk fibroin as a biomaterial

Silk fibers have been used as sutures for a long time in the surgical field, due to the biocompatibility of silk fibroin fibers with human living tissues and its good tensile properties. In addition, it has been demonstrated that silk fibroin can be used as a substrate for enzyme immobilization in biosensors and as a blood-compatible material. A more complete understanding of silk structure provided the possibility to exploit silk fibroin for new uses, such as the production of oxygen-permeable membranes and biocompatible materials for various medical applications.

Degradation of silk fiber

Treatment of silk fibers with acid or alkaline substances causes hydrolysis of peptide linkages. The degree of hydrolysis is based on pH factor, which is at minimum between 4 and 8. Degradation of the fiber is exhibited by loss of tensile strength or change in the viscosity of the solution.

Hydrolysis by acid is more extensive than alkaline. Acid hydrolysis occurs at linkages widely distributed along protein chains, whereas the early stages of alkaline hydrolysis happens at the end of chains. Hydrochloric acid readily dissolves silk fibroin especially when heated. Hot concentrated sulphuric acid, while rapidly

dissolving and hydrolyzing silk fibroin, also causes sulphation tyrosine. Nitric acid readily decomposes silk fibroin, due to its powerful oxidizing properties and concurrently causes nitration of the benzene nuclei. Organic acids have few effects at room temperature when diluted, but in a concentrated form, silk fibroin may be dissolved, along with a certain amount of decomposition.

Proteolytic enzymes do not apparently attack silk fibroin in fibrous form because the protein chains in silk are densely packed without bulky side chains. Serious degradation may be caused by water or steam at 100°C.

Silk protein processing [6, 18]

(a) Degummed process

As mentioned before, sericin layers contain some impurities. Therefore, sericin layers must be removed to receive purified fibroin fiber. Sericin removal affected surface of fiber as shown in Figure 2.3. This process is called degumming. The degummed processes are classified into five methods as follows:

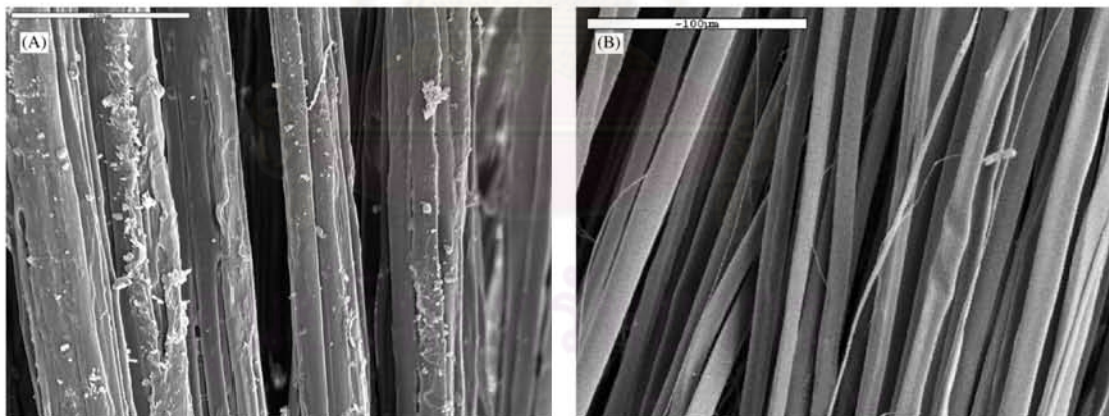


Figure 2.3 SEM micrographs of fiber (a) cocoon raw material, and (b) degummed fiber [15].

- Degummed with hot water

Sericin can easily soluble in boiling water. However, this process gives a risk of the fibroin being damaged when the treatment time is prolonged. Another disadvantage is that this process gives incomplete degumming.

- Degummed with soap

Marseilles soap, olive oil soap, is a favorable soap for degumming. For example, this process may be carried out using 10-20g/l soap at 92-98°C for 2-4 hours. Significantly, this process should use a soft water to avoid the formation of calcium soap.

- Degummed with synthetic detergent

Synthetic detergents have some advantages over soap such as reduction of the treatment time. This process is carried out using 2.5g/l non-ionic synthetic detergent for 30-40 min at 98°C.

- Degummed with acid

Some acids such as sulphuric, hydrochloric, tartaric, and citric acid can be used as degummed agent. This process is not favorable because acid conditions are more harmful to fibroin than alkaline conditions.

- Degummed with enzymes

Trypsin, papain, and bacterial enzymes are the main types of enzymes for silk degummed. These enzymes are called proteases because they degrade proteins and their degradation products are polypeptides, peptides and other substances. This process is a very slow reaction compared to alkaline soap degumming.

(b) Dialysis process

Dialysis was also used in the laboratory in the 1950s and 1960s, mainly to purify biological solutions or to fractionate macromolecules. Now the major application of dialysis is the artificial kidney more than 100 million of these devices are used annually. The dialysis processes divide into many types such as Donnan dialysis, diffusion dialysis and piezodialysis are described in the following section:

- Donnan dialysis and diffusion dialysis

One dialysis process for which the membrane does have sufficient selectivity to achieve useful separations is Donnan dialysis. Salt solutions are separated by a membrane permeable only one charge ion, such as a cation exchange membrane

containing fixed negatively charged groups. Donnan dialysis process is shown in Figure 2.4.

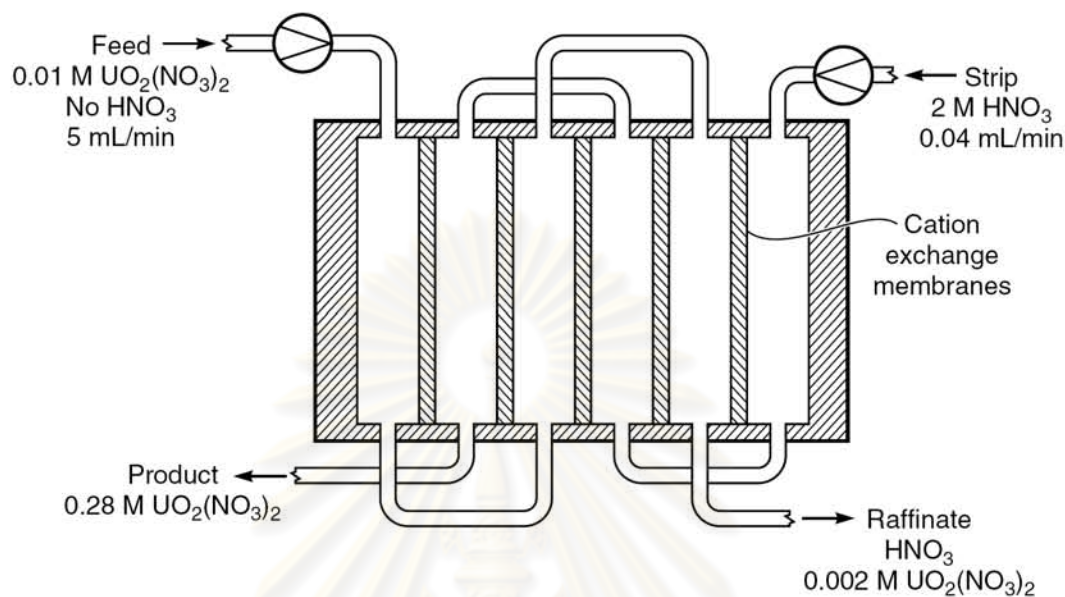


Figure 2.4. Illustration of a Donnan dialysis experiment to separate and concentrate uranyl nitrate, $\text{UO}_2(\text{NO}_3)_2$ [18].

- Charge Mosaic Membranes and Piezodialysis

Ion exchange membranes consisting of separated small domains of anionic and cationic membranes, which would be permeable to both anions and cations. These membranes are now called charge mosaic membranes. The concept is illustrated in Figure 2.5. Cations permeate the cationic membrane domain; anions permeate the anionic domain.

Thai silk [19]

Thai silk is the type of *Bombyx mori* silkworm silks. It is mainly produced by domestic industries in the northern and north-eastern parts of Thailand. Yellow color and coarse filaments are the main characteristics of Thai silk. It also contains more silk gum (e.g. up to 38%) than other types of *Bombyx mori* silk (e.g. 20-25%). There are many species of Thai silk such as, Nangnoi Srisaket, and Nangnoi Sakolnakorn including other species of blended-Thai silk such as blended-Sakolnakorn and blended-Ubonratchathani, cultivated all years.

(a) Nangnoi Srisaket

This specie is easily cultivated. The life cycle is short (about 18 days). The color of the cocoon is dark yellow.

(b) Nangnoi Sakolnakorn

The color of the cocoon is light yellow. Cocoon produced by this specie is more than that by Nangnoi Srisaket about 5-8 kilograms.

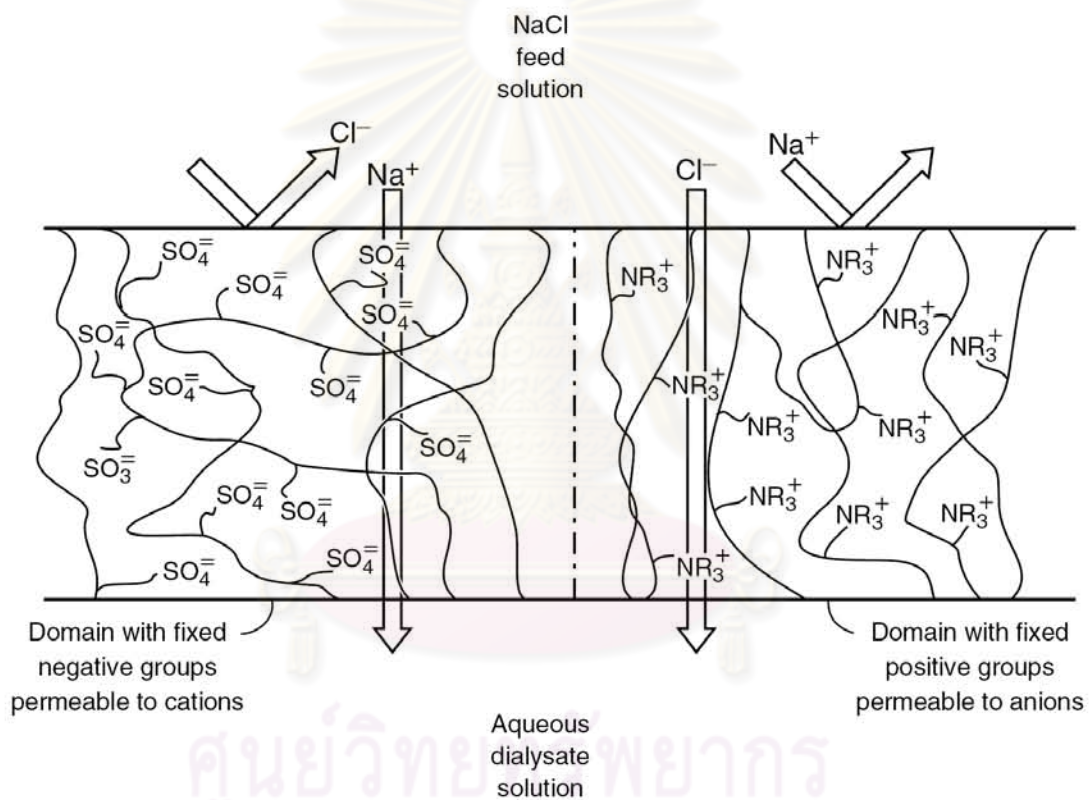


Figure 2.5. Charge mosaic membranes, consisting of finely dispersed domains containing fixed negatively and fixed positively charged groups, are salt permeable [18].

2.2.3.2 Gelatin [20-21]

Gelatin, also called gelatine, is prepared by the thermal and enzymatic denaturation of collagen, isolated from animal skin, bones, cartilage, and ligaments.

Gelatin is a vitreous, brittle solid that is faintly yellow to white and nearly tasteless and odorless.

There are two types of gelatin dependent on preparation method. Type A, with isoionic point of 7 to 9, is derived from acid treatment of collagen. Type B, with isoionic point of 4.8 to 5.2, is the result of an alkaline treatment, such as caustic lime or sodium carbonate, of collagen.

Typical specifications for type A and B gelatin are shown in Table 2.2.

Table 2.2 Typical specifications for gelatins [22]

	Type A	Type B
pH	3.8-5.5	5.0-7.5
Isoelectric Point	7.0-9.0	4.7-6.0
Gel strength (bloom)	50-300	50-300
Viscosity (mps)	15-75	20-75
Ash (%)	0.3-2.0	0.5-2.0

Structure and composition

Gelatin contains a large number of glycine (almost 1 in 3 residues, arranged every third residue), proline and 4-hydroxyproline residues. A typical structure is -Ala-Gly-Pro-Arg-Gly-Glu-4Hyp-Gly-Pro- as shown in Figure 2.6.

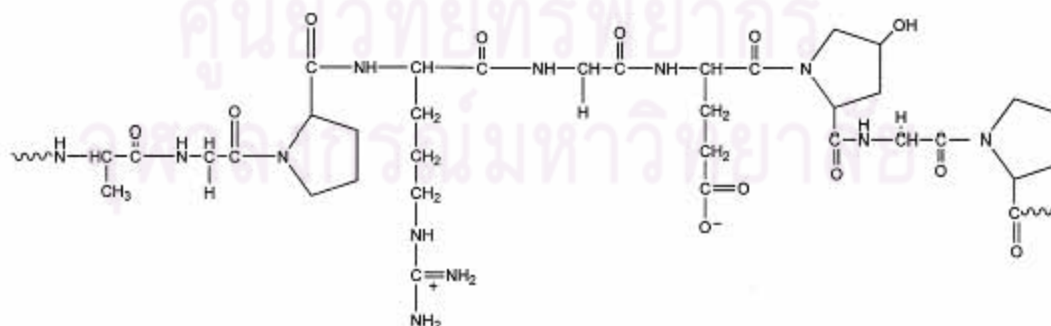


Figure 2.6 The structural unit of gelatin. [23]

Gelatin is composed of 9 amino acids essential for humans as shown in Table 2.3. Gelatin contains 84-90% protein, 1-2% mineral salts and 8-15% water. The natural molecular bonds between individual collagen strands are broken down into a form that rearranges more easily. Gelatin melts when heated and solidifies when cooled again. Together with water it forms a semi-solid colloidal gel.

Table 2.3 Amino acids essential for humans [24]

Amino Acid	g amino acids per 100 g pure protein
Alanine	11.3
Arginine *	9.0
Aspartic Acid	6.7
Glutamic Acid	11.6
Glycine	27.2
Histidine *	0.7
Proline	15.5
Hydroxyproline	13.3
Hydroxylysine	0.8
Isoleucine *	1.6
Leucine *	3.5
Lysine *	4.4
Methionine *	0.6
Phenylalanine	2.5
Serine	3.7
Threonine *	2.4
Tryptophan *	0.0
Tyrosine	0.2
Valine	2.8

* Essential Amino Acid

Applications of gelatin

Gelatin is used extensively in food industries including cake preparation, jelly, aspic, ice cream, and nougat confectionaries etc (see Figure 2.7). Gelatin is also used to make hard and soft capsules in pharmaceutical and medical applications because of its biodegradability and biocompatibility in physiological environments. Therefore, gelatin has become the interesting natural choice in tissue engineering application.



Figure 2.7 Applications of gelatin [25]

2.3 Scaffold fabrication techniques [26-27]

In the body, tissues are organized into three-dimensional structures as functional organs and organ systems. To engineer functional tissues and organs successfully, the scaffolds have to be designed to facilitate cell distribution and guide tissue regeneration in three dimensions. Many methods to prepare porous three-dimensional biodegradable scaffolds have been developed in tissue engineering as shown in Figure 2.8.

2.3.1 Particulate leaching

Particulate leaching is a technique that has been widely used to fabricate scaffolds for tissue engineering applications. Salt is first ground into small particles and those of the desired size are transferred into a mold. A polymer solution is then cast into the salt-filled mold. After the evaporation of the solvent, the salt crystals are leached away using water to form the pores of the scaffold. The pore size can be controlled by the size of the salt crystals and the porosity by the salt/polymer solution ratio. Another particle is used such as monosodium glutamate, alginate hydrogel.

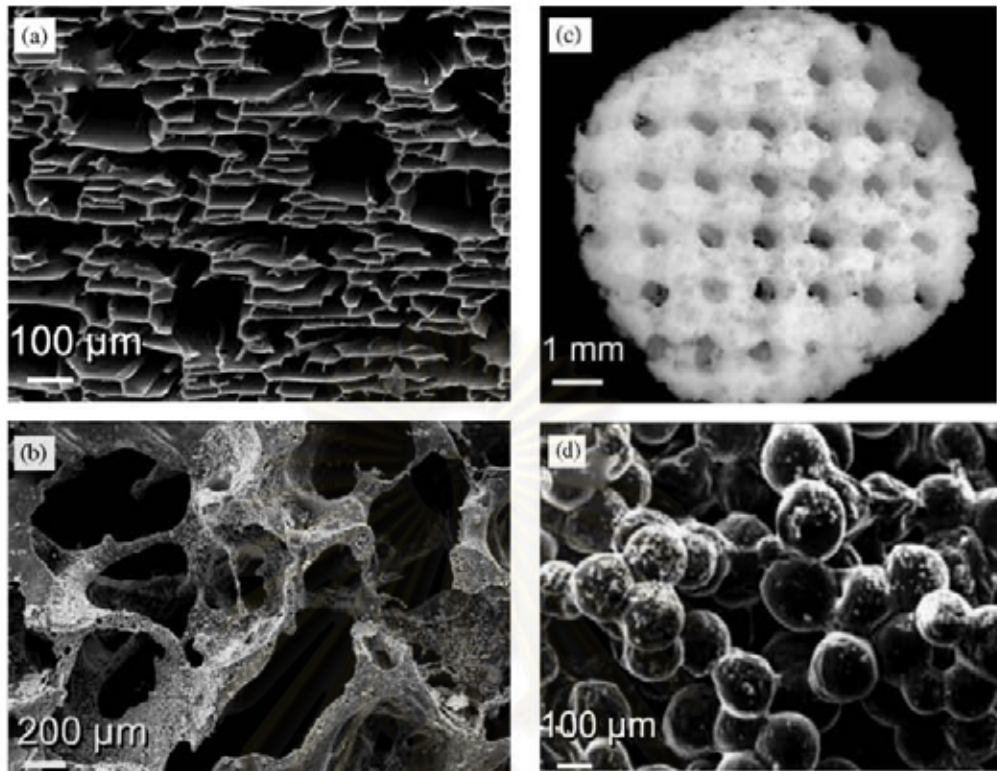


Figure 2.8 Porous polymer foams produced by different techniques. (a) phase separation, (b) particulate leaching, (c) solid freeform fabrication technique, and (d) microsphere sintering [28].

2.3.2 Gas foaming

A biodegradable polymer, such as poly(lactic-co-glycolic acid) (PLGA) is saturated with carbon dioxide (CO_2) at high pressures. The solubility of the gas in the polymer is then decreased rapidly by bringing CO_2 pressure back to atmospheric level. This results in nucleation and growth of gas bubbles, or cells, with sizes ranging between 100-500 μm in the polymer.

2.3.3 Fiber meshes/fiber bonding

Fibers, produced by textile technology, have been used to make non-woven scaffolds from polyglycolic acid (PGA) and poly-L-lactides (PLLA). The lack of structural stability of these non-woven scaffolds, often resulted in significant deformation due to contractile forces of the cells that have been seeded on the

scaffold. This led to the development of a fiber bonding technique to increase the mechanical properties of the scaffolds. This is achieved by dissolving PLLA in methylene chloride and casting over the PGA mesh. The solvent is allowed to evaporate and the construct is then heated above the melting point of PGA. Once the PGA-PLLA construct has cooled, the PLLA is removed by dissolving in methylene chloride again. This treatment results in a mesh of PGA fibers joined at the cross-points.

2.3.4 Phase separation

A biodegradable synthetic polymer is dissolved in molten phenol or naphthalene and biologically active molecules such as alkaline phosphates can be added to the solution. The temperature is then lowered to produce a liquid-liquid phase separation and quenched to form a two-phase solid. The solvent is removed by sublimation to give a porous scaffold with bioactive molecules incorporated in the structure.

2.3.5 Melt molding

This process involves filling a Teflon mould with PLGA powder and gelatin microspheres and then heating the mould above the glass-transition temperature of PLGA while applying pressure to the mixture. This treatment causes the PLGA particles to bond together. Once the mold is removed, the gelatin component is leached out by immersing in water and the scaffold is then dried. Scaffolds produced this way assume the shape of the mould. The melt molding process was modified to incorporate short fibers of hydroxyapatite (HAp). A uniform distribution of HAp fibers throughout the PLGA scaffold could only be accomplished by using a solvent-casting technique to prepare a composite material of HAp fibers, PLGA matrix and gelatin or salt porogen, which was then used in the melt molding process.

2.3.6 Freeze drying

Synthetic polymers, such as PLGA, are dissolved in glacial acetic acid or benzene. The resultant solution is then frozen and freeze-dried to yield porous matrices. Similarly, collagen scaffolds have been made by freezing a dispersion or solution of collagen and then freeze-drying. Freezing the dispersion or solution results in the formation of ice crystals that force and aggregate the collagen molecules into the interstitial spaces. The ice crystals are then removed by freeze-drying. The pore size can be controlled by the freezing rate and pH. A fast freezing rate produces smaller pores.

2.4 Crosslinking techniques [29-30]

Scaffolds can be crosslink to increase mechanical properties and reduce degradation rate. Crosslinking can be done by various methods such as ultraviolet irradiation, electron beam irradiation, dehydrothermal treatment, and chemical treatment.

2.4.1 Ultraviolet irradiation

UV irradiation generates radicals at the aromatic residues of amino acids, such as tyrosin and phenylalanine. The binding of these radicals will react to each other, resulting in crosslinking formation. The crosslinking density largely changes depending on UV irradiation time. However, it is possible that irradiation for longer time preferably acts on the chain scission of molecules. A balance of the crosslinking and chain scission will result in unchanged density of crosslinking.

2.4.2 Electron beam irradiation

Electron beam irradiation also produces radicals. The number of crosslinks is not large and the water content does not decrease very much. This is because the chain scission by the over dose of electron beam also occurs.

2.4.3 Dehydrothermal crosslinking

Scaffolds can be crosslinked by the method of dehydrothermal (DHT) treatment in a vacuum oven at temperature above 100°C. Dehydrothermal treatment brings about chemical bonding between the amino and carboxyl groups within molecule of polypeptide. Dehydrothermal crosslinking can occur only if the amino and carboxyl groups are close to each other. Therefore, it is believed that dehydrothermal treatment have crosslink extent less than chemical treatment.

2.4.4 Chemical crosslinking

There are many types of chemical crosslinking agents such as, glutaraldehyde, formaldehyde, and carbodiimide solution (1-ethyl-3-(3-dimethylaminopropyl) carbodiimide hydrochloride (EDC) with N-hydroxy-succinimide (NHS)).

The EDC crosslinking mechanism is showed in Figure 2.9. EDC activates the carboxyl group of glutamic or aspartic acid to form an active O-acylisourea intermediate. This intermediate can then react with an amino group to form an isopeptide bond or with a water molecule to regenerate the original COOH. Crosslinks are formed after nucleophilic attack by free amine groups of lysine or hydroxylysine. Addition of the nucleophile NHS to the EDC containing solution was very effective in increasing the number of crosslinked matrix. In addition, water can act as a nucleophile, resulting in the hydrolysis of the O-acylisourea group to give the substituted urea. The crosslink reaction is usually performed between pH 4.5-5. The disadvantage of chemical crosslinking is the toxicity to cells. Therefore, the scaffolds should be rinsed thoroughly to remove overall agents.

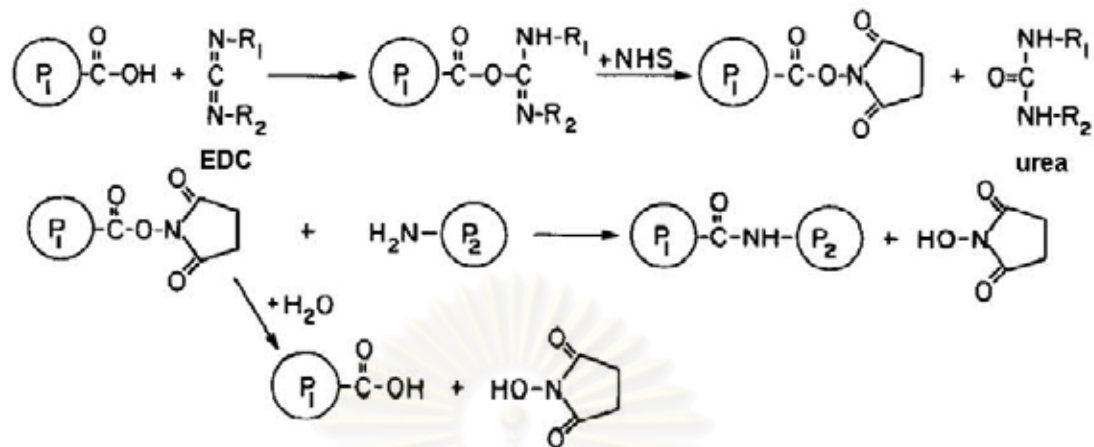


Figure 2.9 Crosslinking of protein with EDC and NHS [31].

2.5 *In vitro* cell culture

2.5.1 Types of cell cultures [5, 32-34]

Types of cell cultures are classified into two types as follow:

2.5.1.1 Primary cell cultures

Primary cell cultures are obtained directly from multiple species including mouse, guinea pig, rat, rabbit, dog, horse, and human. These cells can be kept at the differentiated state for a short period.

Mesenchymal stem cells (MSCs), one type of primary cells, can be isolated from a wide variety of tissues including bone marrow, periosteum, synovium, muscle, adipose tissue, lung, bone, deciduous teeth, dermis, and articular cartilage. Among these, bone marrow is the major source of MSCs. MSCs can be expanded and differentiated into cells of different connective tissue lineages including bone, cartilage, fat, and muscle upon proper stimulation.

These cells also have the potential for a wide range of therapeutic applications through autologous, allogeneic or xenogeneic stem cell transplantation. Bone marrow-derived MSCs have been used to treat a variety of defects and diseases, including

critical size segmental bone defects, full thickness cartilage defects, tendon defects, myocardial infarction and even nerve defects.

2.5.1.2 Permanent cultures or cell lines cultures

Cell lines cultures have an unlimited proliferation capacity. They are derived from embryos, tumors or transformed cells. Examples of cell lines are L929 mouse skin fibroblast, MC3T3-E1 mouse osteoblast, HeLa, MDCK, etc.

Proliferation and differentiation depending on the cell type. Numerous publications [35-37] provide protocols for the isolation of different cell types, their culture conditions, and for the evaluation of the degree of differentiation.

MC3T3-E1, preosteoblastic cell line, was derived from mouse calvaria. Culture conditions can be induced to undergo a developmental sequence leading to the formation of multilayered bone nodules. This sequence is characterized by the replication of preosteoblasts followed by growth arrest and expression of mature osteoblastic characteristics such as matrix maturation and eventual formation of multilayered nodules with a mineralized extracellular matrix. This cell line has become the standard *in vitro* model of osteogenesis and has found widespread use in studies examining many aspects and applications of osteogenesis, including transcriptional regulation, mineralization and tissue engineering.

2.5.2 MTT assay for cell viability [38]

MTT assay is a quantitative colorimetric assay for mammalian cell survival and cell proliferation. It is an indirect method for assessing cell growth and proliferation. MTT [3-(4,5-dimethylthiazol-2-yl)-2,5-diphenyltetrazolium bromide] (Figure 2.10) is a water soluble tetrazolium salt yielding a yellowish solution when prepared in media without phenol red. MTT solution is converted to an insoluble purple formazan by cleavage of the tetrazolium ring by dehydrogenase enzyme from mitochondria. The yellow tetrazolium MTT is reduced by metabolically active cells. The insoluble purple formazan can be solubilized using isopropanol or other solvents

such as dimethyl sulfoxide (DMSO). The absorbance of the resulting solution can be measured and used to quantify the number of cells using a spectrophotometer.

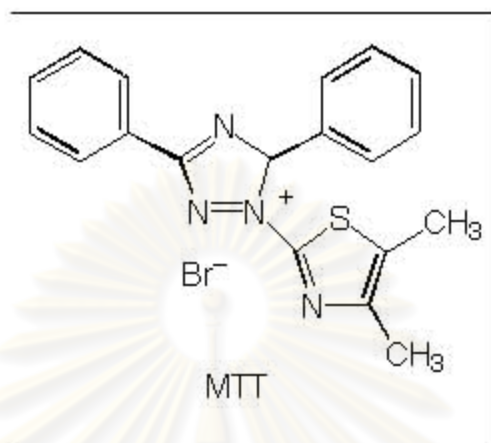


Figure 2.10 Molecular structure of MTT (3-(4,5-dimethyl-2-thiazolyl)-2,5-diphenyl tetrazolium bromide) [39].

ศูนย์วิทยทรัพยากร
จุฬาลงกรณ์มหาวิทยาลัย

CHAPTER III

LITERATURE REVIEWS

In this chapter, the literature reviews are summarized into four parts as follows:

1. Characterization and processing of silk fibroin.
2. *In vitro* and *in vivo* studies of silk fibroin.
3. Preparation and characterization of silk fibroin blends.
4. Preparation and characterization of hydroxyapatite-deposited biomaterials.

3.1 Characterization and processing of silk fibroin

Tsukada, M. *et al.* [40]

In 1994, Masuhiro Tsukada *et al.* studied the structural changes of two different kinds of silk fibroin membranes obtained by casting from native and regenerated silk fibroin solutions. The structural changes of these membranes were discussed as a function of immersion time in methanol and methanol concentration. X-ray diffractometry and infrared spectroscopy results showed that transition from random coil to β -sheet structure, which became water insoluble, is independent to immersion time. Only native silk membrane treated with pure methanol for 2 min, maintained its original amorphous structure, as demonstrated by differential scanning calorimetric (DSC) curves. SDS-PAGE pattern showed that the molecular weight of native silk fibroin was 350 kDa, while the regenerated sample was formed by a large number of polypeptides in the range of 50-200 kDa.

Chen, X. *et.al.* [41]

In 2001, Xin Chen *et.al.* studied differences in the rheological behavior of regenerated silk fibroin and secondary structure of membranes in four solvent systems: $\text{CaCl}_2\text{-EtOH-H}_2\text{O}$; $\text{Ca(NO}_3)_2\text{-MeOH-H}_2\text{O}$; LiBr-EtOH (with and without water); and $\text{LiBr-H}_2\text{O}$. The results demonstrated that $\text{Ca(NO}_3)_2\text{-MeOH-H}_2\text{O}$ and $\text{LiBr-EtOH-H}_2\text{O}$ had the strongest salivation on silk fibroin chains, as shown in an almost constant viscosity (Newtonian behavior) over most of the shear rate range (0.1 to 500s^{-1}). In contrast, 9.5M aqueous LiBr appeared to have the weakest salivation with similar effects on the silk molecules to pure water. FTIR results also showed that the silk fibroin membranes prepared using all four solvent systems showed mainly random coil conformation with a small proportion of β -sheet.

Li, M. *et.al.* [42]

In 2001, Ming Zhong Li *et.al.* studied the relationship between freeze-drying conditions, structural characteristics and physical properties of silk fibroin aqueous solution. Porous silk fibroin materials, with average pore size of 10 to $300\mu\text{m}$, pore density at 1 to 2000mm^{-2} , and porosity at 35 to 70% , were prepared by freeze-drying aqueous solution obtained by dissolving silk fibroin in ternary solvent $\text{CaCl}_2\text{-CH}_3\text{CH}_2\text{OH-H}_2\text{O}$. Pore size distribution of such materials mostly accorded with logarithmic normal distribution. Freezing temperature and concentration of silk fibroin solution were adjusted to control structural parameter (pore size, pore density, and porosity) and the physical properties of moisture permeability, compressibility, strength, elongation, etc. Above glass transition zone (-34 to -20°C) of silk fibroin, the freezing temperature has more significant effect on the structure and properties of porous silk fibroin materials.

Yamada, H. *et.al.* [43]

In 2001, Hiromi Yamada *et.al.* examined the factors affecting the molecular mass of fibroin in the dissolved process, and describes a procedure for obtaining

fibroin solutions from cocoons without incurring molecular degradation. The molecular mass of fibroin solutions prepared from silk was analyzed by SDS-PAGE. It was found that fibroin molecule was degraded during reeling, degumming, and dissolution of silk fiber. A method for the preparation of fibroin solution conserving its native molecular size was offered: (1) use only fresh cocoons, after the completion of spinning without reeling as a starting material, (2) degum without breaking the fibroin molecule, and (3) dissolve by saturated aqueous lithium thiocyanate at room temperature.

Wang, H. *et.al.* [44]

In 2005, Hong Wang *et.al.* investigated the influences of temperature and silk fibroin concentration on the flow stability of the solution to obtain optimal storing conditions for silk fibroin aqueous solution. It was found that the flow stability decreased quickly with the increase of solution concentration and temperature. X-ray diffraction, Fourier transform infrared (FTIR) and Raman spectroscopy analysis showed that silk fibroin in aqueous solution was mainly in random coil conformation. After gelation process, it turned into α -helix and β -sheet conformation. The investigation implied that the original dilute regenerated silk fibroin aqueous solution should be stored under low temperature and concentration.

Kim, U.J. *et.al.* [1]

In 2005, Ung Jin Kim *et.al.* developed a new strategy for silk fibroin processing that avoided the use of organic solvents or harsh chemicals. A new mechanism was employed to promote water solubility and then stability of the assembled silk fibroin without the use of hexafluoroisopropanol (HFIP) or methanol. The result of this process showed that adjusting the concentration of silk fibroin in water, and the particle size of granular NaCl used in the process, leads to the control of morphological and functional properties of the scaffolds. The aqueous-derived scaffolds had highly homogeneous and interconnected pores with pore sizes ranging from 470 to 940 μ m, depending on the particle size of granular NaCl. At 10% silk

fibroin aqueous solutions, the porosity of scaffolds obtained was more than 90% and compressive strength and modulus up to 320 ± 10 and 3330 ± 500 kPa, respectively. The aqueous-derived scaffolds fully degraded upon exposure to protease during 21 days, while HFIP-derived scaffolds showed slow degradation. This new process offered an entirely new window of material properties when compared with traditional silk fibroin-based materials.

Horan, R.L. *et.al.* [45]

In 2005, Rebecca L. Horan *et.al.* demonstrated *in vitro* proteolytic degradation of silk fibroin and its predictable mechanical behavior including tensile and fatigue properties. *Bombyx mori* silk fibroin yarns were incubated in 1 mg/ml Protease XIV at 37°C to create an *in vitro* model system of proteolytic degradation. Control samples were incubated in phosphate-buffered saline. Scanning electron microscopy (SEM) indicated increasing fragmentation of individual fibroin filaments from protease-digested samples with time of exposure to the enzyme. Particulate debris was presented within 7 days of incubation. Gel electrophoresis indicated a decreasing amount of silk 25 kDa light chain and the molecular weight of the heavy chain shifted to a lower molecular weight range with increasing incubation time in protease.

3.2 *In vitro* and *in vivo* studies of silk fibroin

Minoura, N. *et.al.* [46]

In 1995, Norihiko Minoura *et.al.* investigated the cell attachment and growth on silk fibroin from *Bombyx mori* domestic silkworm (DSF) and *Antheraea pernyi* wild silkworm (WSF) and compared the performance to that on collagen. Two kinds of silkworm had a difference in their amino acid sequences. The sequence of WSF contains not only a large number of basic amino acids same as DSF but also the tripeptide sequence arginine-glycine-aspartic acid (RGD). The results on the culture of L929 cells showed that cell attachment and growth on DSF was as good as on collagen. The cells attached to DSF were extensively spread out and their filopodia

were observed in SEM micrographs. On the other hand, WSF displayed much better cell attachment and growth than DSF. The cells attached on WSF became virtually flat and their filopodia could be seen, indicating that they were strongly held on the surface.

Sofia, S. *et.al.* [47]

In 2001, Susan Sofia *et.al.* studied the attachment, growth, differentiation, and bone-forming capacities of human osteoblast cells (Saos-2 line) on *Bombyx mori* silk films. Silk films were prepared to be free of sericin and decorated by covalently coupled peptides included GRGDS containing the adhesion ligand RGD. Response of saos-2 to the decorated silk films indicated that the proteins served as suitable bone-inducing matrices. Osteoblast-like cell adhesion was significantly increased on RGD-modified silk film and parathyroid hormone (PTH) compared to plastic, a modified PTH (mPTH), and the control peptide RAD. At 2 weeks of culture, alkaline phosphatase levels were similar on all substrates but were greatest on RGD-modified silk film by 4 weeks. At 2 weeks of culture, $\alpha 1(I)$ procollagen mRNA was elevated on silk film, RGD-modified, RAD-modified, and PTH-modified, and hardly detectable on mPTH and plastic. However, by 4 weeks RGD-modified silk film demonstrated the highest level of $\alpha 1(I)$ procollagen mRNA compared to the other substrates. Osteocalcin levels detected by RT-PCR were greatest on RGD-modified at both 2 and 4 weeks of cultures. Calcification was also significantly elevated on RGD-modified compared to the other substrates with an increase in number and size of the mineralized nodules in culture. Therefore, RGD covalently decorated silk appears to stimulate osteoblast-based mineralization *in vitro*.

Panilaitis, B. *et.al.* [48]

In 2003, Bruce Panilaitis *et.al.* examined the direct activation of the innate immune response by silk fibers in order to understand the relationship between fibers and biological responses. The results indicated that silk fibers are largely immunologically inert in short- and long-term culture with murine macrophage cell

line while fibroin particles induced significant tumor necrosis factor release. Sericin proteins extracted from native silk fibers did not induce significant macrophage activation. While sericin did not activate macrophages by itself, it demonstrated a synergistic effect with bacterial lipopolysaccharide. The low level of inflammatory potential of silk fibers makes them promising candidates in future biomedical applications.

Kim, U.J. *et.al.* [49]

In 2004, Ung Jin Kim *et.al.* studied the environmental factors that influence silk fibroin sol-gel transitions. Using osmotic stress to generate highly concentrated fibroin aqueous solutions provided the opportunity to explore sol-gel transitions. It was found that gelation of silk fibroin aqueous solutions was affected by temperature, Ca^{2+} , pH, and polyethylene oxide (PEO). Gelation time decreased with an increase in protein concentration, decrease in pH, increase in temperature, addition of Ca^{2+} , and addition of PEO. No change of gelation time was observed with the addition of K^+ . Upon gelation, a random coil structure of the silk fibroin was transformed into a β -sheet structure. Hydrogels with fibroin concentrations $>4\text{wt}\%$ exhibited network and spongelike structures. Pore sizes of the freeze-dried hydrogels were smaller as the silk fibroin concentration or gelation temperature was increased. Freeze-dried hydrogels formed in the presence of Ca^{2+} exhibited larger pores as the concentration of the ion was increased. Mechanical compressive strength and modulus of the hydrogels increased with an increase in protein concentration and gelation temperature. The results provided an insight into the silk fibroin sol-gel transitions which is the important insight in the *in vitro* processing of these proteins into useful new materials.

Meinel, L. *et.al.* [36]

In 2004, Lorenz Meinel *et.al.* examined porous silk scaffolds for tissue engineered human bone using human mesenchymal stem cells (hMSCs). The differentiation of hMSCs along osteogenic lineage, and the formation of bonelike tissue *in vitro* on porous scaffolds made of silk (slow degrading), silk-RGD (slow

degrading, enhanced cell attachment), and collagen (fast degrading) in control and osteogenic medium was studied. Histological analysis and microcomputer tomography showed the development of up to 1.2mm long interconnected and organized bonelike trabeculae with cuboid cells on the silk-RGD scaffolds. X-ray diffraction pattern of the deposited bone corresponded to hydroxyapatite presented in native bone. Biochemical analysis showed increased mineralization on silk-RGD scaffolds compared with either silk or collagen scaffolds after 4 weeks. Expression of bone sialoprotein, osteopontin, and bone morphogenetic protein 2 was significantly higher for hMSCs cultured in osteogenic than control medium both after 2 and 4 weeks of culture. The results illustrated that RGD-silk scaffolds are particularly suitable for autologous bone tissue engineering because of their stable macroporous structure, mechanical properties matching those of native bone, and slow degradation.

Meinel, L. *et.al.* [50]

In 2005, Lorenz Meinel *et.al.* studied the inflammatory reactions by hMSCs seeded on silk films and silk films covalently decorated with cell attachment sequences (RGD) *in vitro*. *In vitro* responses of hMSCs on silk were compared with the responses on tissue culture plastic (TCP; negative control), TCP with lipopolysaccharide (LPS) in the cell culture medium (positive control), and collagen films. After 9 h, it was found that the rate of cell proliferation was higher on silk films than either on collagen or TCP. *In vivo*, films made of silk, collagen or PLA were seeded with rat MSCs, implanted intramuscularly in rats and harvested after 6 weeks. Histological and immunohistochemical evaluation of silk explants revealed the presence of circumferentially oriented fibroblasts, few blood vessels, macrophages at the implant-host interface, and the absence of giant cells. Inflammatory tissue reaction was more conspicuous around collagen films and even more around PLA films when compared to silk. These data illustrated that purified degradable silk is biocompatible and the *in vitro* cell culture model (hMSC seeded and cultured on biomaterial films) gave inflammatory responses that were comparable to those observed *in vivo*.

Kim, H.J. *et.al.* [37]

In 2005, Hyeon Joo Kim *et.al.* compared two types of silk fibroin scaffolds prepared from hexafluoro-2-propanal (HFIP) and water, on human bone marrow stem cells (hMSCs) responses toward osteogenic outcomes. hMSCs were seeded on the scaffolds and cultured up to 28 days. It was found that hMSCs seeded onto the water-based silk scaffolds showed a significant increase in cell numbers compared to HFIP-based silk scaffolds. The results demonstrated that three-dimensional aqueous-derived silk fibroin scaffolds provided improved bone-related outcomes in comparison to the HFIP-derived systems. These data illustrated the importance of materials processing on biological outcomes of the same silk fibroin.

Tamada, Y. *et.al.* [51]

In 2005, Yasushi Tamada *et.al.* presented the new processes to form the fibroin sponge. The process involves freezing and thawing fibroin aqueous solution in the presence of a small amount of an organic solvent. The new process did not require freeze-drying, chemical cross-linking, or other polymeric materials. Solvent concentration, fibroin concentration, freezing temperature, and freezing duration affected sponge formation, porous structure, and mechanical properties. XRD and FTIR results indicated that silk I and silk II crystalline structures exist in the fibroin sponge and that the secondary structure of fibroin is transformed from a random coil to a β -sheet during this process. The tensile strength of fibroin sponge decreased slightly because of autoclave treatment. Prior to *in vitro* culture, the fibroin sponge was sterilized using an autoclave. At 3 weeks of culture, MC3T3 cells could proliferate in the sterilized fibroin sponge. Thus, the fibroin sponge formed by this new process is applicable as a tissue-engineering scaffold because it is formed from biocompatible pure silk fibroin and offers both porous structure and mechanical properties that are suitable for cell growth and handling.

Wang, Y. *et.al.* [52]

In 2006, Yongzhong Wang *et.al.* studied the attachment, proliferation and differentiation of adult human chondrocytes (hCHs) in three-dimensional aqueous silk fibroin scaffolds. The results were compared with those using human bone marrow stem cells (hMSCs). Cell adhesion, proliferation and redifferentiation on the scaffolds based on cell morphology, levels of cartilage-related gene transcripts, and the presence of a cartilage-specific extra cellular matrix (ECM). The hCH-based constructs were significantly different than those formed from MSC-based constructs with respect to cell morphology, structure and initial seeding density needed to successfully generate engineered cartilage-like tissue. These results illustrated fundamental differences between stem cell-based (MSC) and primary cell-based (hCH) tissue engineering, as well as the importance of suitable scaffold features, in the optimization of cartilage-related outcomes *in vitro*.

Meechaisue, C. *et.al.* [53]

In 2007, Chidchanok Meechaisue *et.al.* fabricated the ultra-fine fibers of silk fibroin (SF) from cocoons of Thai silkworm (Nang-Lai) and Chinese/Japanese hybrid silkworms (DOAE-7). The results showed that the average diameter of electrospun (e-spun) SF fibers increased as increasing the solution concentration and the electrostatic field strength (EPS) value. The average diameter of the e-spun Thai SF fibers was between 217 and 610nm while that of the DOAE-7 fibers was between 183 and 810nm. *In vitro* cell culture was tested using mouse osteoblast-like cells (MC3T3-E1). MTT assay showed a monotonic increase in the absorbance values with the increase in the time in culture implying that the number of cells on the surface of the Nang-Lai SF fibrous scaffolds increased with the increase in the cell culture time. After 5 days of culture, cells appeared to fully cover the surface of the scaffold. This result showed that cells could adhere and proliferate on the surface of Nang-Lai SF fiber mats. The e-spun Nang-Lai SF fiber mats could be used as scaffolding materials for bone cell culture.

3.3 Preparation and characterization of silk fibroin blends

Kweon, H.Y. *et.al.* [54]

In 2001, Hae Yong Kweon *et.al.* reported the structural characteristics and thermal properties of *Antheraea pernyi* silk fibroin (SF)/chitosan blend films prepared by solution casting. The results demonstrated that the conformation of blend films was revealed to be a β -sheet structure, due to the effect of acetic acid used as a mixing solvent. According to the Fourier Transform Infrared (FTIR) spectra, NH groups of SF and C=O and NH₂ groups of chitosan have participated in a specific intermolecular interaction among themselves. The exotherm of SF was not exhibited in blend films due to the precrystallization of SF induced by acetic acid. The blend films showed decomposition temperatures at around 294°C (chitosan component) and 369°C (*A.pernyi* component) which could be indirect evidences of phase separation. This was confirmed by scanning electron microscopy (SEM) results. Blending with *A.pernyi* SF could enhance the thermal decomposition stability of chitosan.

Lv, Q. *et.al.* [2]

In 2005, Qiang Lv *et.al.* developed a new preparation for silk fibroin scaffolds with uniform pore distribution, controllable pore size and functional features by freeze-drying method. Collagen was added to fibroin solution to restrain unwanted fibroin aggregation in preparation processes. The results demonstrated that when collagen was added to fibroin solution, the viscosity of blend solution increased, and then it restrained unwanted fibroin leaf formation in freezing process. With methanol treatment, fibroin/collagen scaffolds became water-stable, following the transition from random and α -helix to β -sheet conformation. Aqueous-fibroin porous scaffolds had highly homogeneous and interconnected pores with pore sizes ranging from 127 to 833 μ m, depending on the fibroin concentration. The porosity of scaffolds was more than 90%, and the yield strength and modulus were up to 354 \pm 25 kPa and 30 \pm 0.1 MPa, respectively. Scanning electron microscopy (SEM) and MTT analyses

demonstrated that the adding of collagen evidently facilitated Human hepatocellular liver carcinoma (HepG2) attachment and proliferation *in vitro*.

Gil, E.S. *et.al.* [55]

In 2006, Eun S. Gil *et.al.* studied the effect of SF crystallization on properties of silk fibroin (SF)/type A gelatin (GA) blended membranes. When co-casting of solution, amorphous blends of these polymers appeared homogeneous, as discerned from visual observation, microscopy, and FTIR spectroscopy. After immersing in aqueous MeOH, the conformation of SF transformed from random coil to β -sheet. According to X-ray diffractometry and thermal calorimetry, this transformation occurred in pure SF as well as in each of the GA/SF blends. Thermal gravimetric analysis revealed that the presence of β -sheets in SF and GA/SF blends improves thermal stability. Extensional rheometry confirmed that SF crystallization enhanced the tensile properties of the blends. The formation of crystalline SF networks in GA/SF blends could be used to stabilize GA-based hydrogels for biomaterial and pharmaceutical purposes.

3.4 Preparation and characterization of hydroxyapatite-deposited biomaterials

Taguchi, T. *et.al.* [56]

In 1998, Tetsushi Taguchi *et.al.* introduced a method of hydroxyapatite (HAp) formation on/in a three-dimensional PVA hydrogel matrix. From the past study, the biomimetic process was used for HAp formation on/in hydrogel. The biomimetic method is basically divided into two stages: (1) nucleation, in which the substrate is immersed in a synthetic solution of simulated body fluid (SBF) and bioactive CaO–SiO₂ based glass particulates as a nucleating agent, and (2) precipitation and growth of the apatite layer. It can effectively prepare HAp composites on the surface of various kinds of material but it takes a long period of time (4 days for the first step

and another 4 days for the second step) to form a large amount of HAp on/in hydrogels. As a result, a novel HAp formation process was developed. This process was based on the widely-known wet synthesis of HAp. It employed alternate soaking process in 200mM CaCl₂/Tris-HCl (pH 7.4) at 37°C for 2 h and 120mM Na₂HPO₄ aqueous solutions at the same condition. The results illustrated that the HAp crystals could be formed on/in a PVA gel for a short amount of time (5 cycles correspond to 20 h).

Furuzono, T. *et.al.* [57]

In 2000, Tsutomu Furuzono *et.al.* applied alternate soaking process to silk fabric to prepare a composite of silk fabric and apatite and studied apatite deposited on the silk fabric. It was found that apatite weight increased with alternated soaking repetitions in calcium solution [200mM aqueous calcium chloride solution buffered with tris-(hydroxymethyl) aminomethane and HCl (pH 7.4)] and phosphate solution (120mM aqueous disodium hydrogenphosphate). Fresh solutions were used for each soaking. SEM showed that apatite deposited after 21 or more repeated soakings was over 20µm thick. XRD showed that the apatite crystals deposited on silk fabric elongated along the c axis. FTIR and XPS indicated the existence of carbonate, HPO₄²⁻, and Na⁺ ions in addition to constituent ions of hydroxyapatite. HPO₄²⁻ ions converted into PO₄³⁻ ions to form more stable hydroxyapatite crystals, which were associated with increasing apatite crystallinity. Apatite deposited on silk by the alternate soaking process was a deficient apatite containing carbonate, HPO₄²⁻, and Na⁺ ions as in a natural bone tissue. Thus, this apatite–silk composite material might be potentially bioactive.

Bigi, A. *et.al.* [10]

In 2002, Bigi *et.al.* reported that the presence of hydroxyapatite (HAp) inside the gelatin sponges could promote the deposition of apatite crystals from simulated body fluid (SBF). *In vitro* bioactivity of gelatin sponges and HAp/gelatin sponges was tested through evaluation of the variations in their composition and morphology after

soaking in SBF for periods up to 21 days at 37°C. It was found that HAp promotes the deposition of bonelike apatite crystals on gelatin sponges. The deposits were laid down as spherical aggregates with mean diameters increasing from about 1–2µm after 4 days of soaking in SBF solution and up to about 3.5µm in the samples soaked for 21 days. In addition, an amount of inorganic phase increased about 56wt% leading to a composite material with a composition quite close to that of bone tissue. The inorganic phase was a poor crystalline carbonated apatite similar to trabecular bone apatite.

Wang, L. *et.al.* [9]

In 2004, Li Wang *et.al.* prepared hydroxyapatite (HAp)–silk fibroin (SF) composites with various amounts of SF by a co-precipitation method in order to obtain well-dispersed HAp nanoparticles in a SF matrix. The effects of SF content on the microstructure and hardness of the composites were studied. A co-precipitation method, Phosphoric (H_3PO_4) solution was added into calcium hydroxide ($Ca(OH)_2$) suspension containing various amounts of SF powder. The mixture was stirred vigorously at room temperature for 3 h, followed by centrifugation and water-washing alternately for three cycles. The precipitates were dried in vacuum at 50°C for 24 h and subsequently ground into fine powders using an agate mortar. Meanwhile, pure HAp without SF was prepared as a control sample by the same process. When SF content increased up to 40wt%, the particle size distribution became narrower and the Vickers microhardness of the composites increased. The composites exhibited the porous microstructure with open porosity around 62–74%. About 70% of interconnective pores were between 40 and 115µm in diameter. The composite containing 30wt% of SF showed homogeneous form and a well dispersed state of HAp crystallites together with a highly developed three-dimensional network.

Taguchi, T. *et.al.* [11]

In 2004, Tetsushi Taguchi *et.al.* developed a novel bifunctional scaffold with calcium phosphate using alternate soaking process to form calcium phosphate in a

cartilage-like matrix of type II collagen gels. Characterization of calcium phosphate formed in type II collagen matrices was analyzed using X-ray diffraction (XRD), Fourier transform infrared spectroscopy (FT-IR), thermogravimetric and differential thermal analysis (TG-DTA), and scanning electron microscopy (SEM). The results from XRD and FT-IR analysis indicated that calcium phosphate formed in the matrix was hydroxyapatite (HAp), whose phosphate ions were partially replaced by carbonate ions. TG-DTA analysis showed that HAp content increased with increasing immersion cycle in calcium and phosphate solutions. SEM image showed that a calcium phosphate layer was deposited on one side of type II collagen gels. The composite with gradient calcium phosphate crystals should be useful in regenerating bone-cartilage interface.

Ijima, H. *et.al.* [12]

In 2004, Hiroyuki Ijima *et.al.* studied the characteristics of hydroxyapatite (HAp) formed on glass plates covered with polyvinyl alcohol (PVA) gel by the alternate soaking process and optimized the conditions of the alternate soaking process for animal cell culture with regard to cell attachment and proliferation. The results illustrated that HAp formation ratio depended on the reaction cycle number but was independent of the alternate soaking period per cycle. The Ca/P molar ratio of HAp formed at 10 reaction cycles was very close to the theoretical value of HAp, 1.67. From *in vitro* study using Chinese hamster ovary cell line (CHO-K1), the cell number was counted using the nucleus counting. Cell adhesion, proliferation and maximum cell density on HAp plates formed at two or five reaction cycles using 200mM CaCl₂ and 120mM Na₂HPO₄ solutions were better than on plates formed under other conditions. Furthermore, the adhesion ratio of CHO-K1 cells on HAp plates formed at 10 reaction cycles was about 60% of those at two or five reaction cycles. HAp provided an adequate substratum for CHO-K1 cell adhesion and proliferation.

Wang, L. *et.al.* [58]

In 2005, Li Wang *et.al.* prepared hydroxyapatite (HAp)/intact silk fibroin (SF) and HAp/alkali pretreated SF nanocomposite sol via a wet-mechanochemical route. The influence of the alkali pretreatment of SF on chemical states, microstructure, Vickers microhardness of the composite and gelation behavior of the composite sol was studied. A wet-mechanochemical route, Phosphoric (H_3PO_4) solution was added into calcium hydroxide ($Ca(OH)_2$) suspension containing various amounts of SF powder. The mixture was stirred vigorously at room temperature for 1h, and then milled by a multi-ring mill at 1250 rpm for 3 h. After that, the milled sol was centrifuged and water-washed alternately for three cycles. The precipitates were dried in vacuum at $50^\circ C$ for 24 h and subsequently ground into fine powders using an agate mortar. It was found that when the alkali pretreated SF involved, Vickers microhardness of the composite increased 57% and enhanced three-dimensional porous network with a homogenous particle form and a uniform pore size distribution. Not only, the alkali pretreatment of SF increased the viscosity and the rigidity of the composite sol but also promoted its gelation process, which was favorable for healing bone defects by an injection technique.

CHAPTER IV

EXPERIMENTAL WORK

The experimental work can be divided into three main parts:

1. Materials and reagents
2. Equipments
3. Experimental procedures

4.1 Materials and reagents

- 4.1.1 *Bombyx mori* cocoon (Nangnoi Srisaket from Nakhonratchasima province, Thailand)
- 4.1.2 Type A gelatin powder (116g bloom, pH 4.5, pI 9, lab grade, Ajax Finechem, Australia)
- 4.1.3 Type B gelatin powder (150g bloom, pH 5.6, pI 4.9, food grade, Erawan Chemical Co., Ltd., Thailand)
- 4.1.4 Sodium carbonate (Na_2CO_3 , Ajax Finechem, Australia)
- 4.1.5 Lithium bromide (LiBr , Sigma-Aldrich, Germany)
- 4.1.6 Mined salt (particle size 600-710 μm , Thai refined salt Co., Ltd., Nakhonratchasima, Thailand)
- 4.1.7 1-ethyl-3-(3-dimethylaminopropyl) carbodiimide hydrochloride (EDC, Nacalai Tesque, Inc., Japan)
- 4.1.8 N-hydroxysuccinimide (NHS, Nacalai Tesque, Inc., Japan)
- 4.1.9 Calcium chloride (CaCl_2 , Ajax Finechem, Australia)
- 4.1.10 Sodium dihydrogen phosphate monohydrate ($\text{NaH}_2\text{PO}_4 \cdot \text{H}_2\text{O}$, Sigma-Aldrich, Germany)
- 4.1.11 Sodium phosphate dibasic heptahydrate ($\text{Na}_2\text{HPO}_4 \cdot 7\text{H}_2\text{O}$, Sigma-Aldrich, Germany)
- 4.1.12 Ethanol (99.7-100%, VWR International Ltd., UK)

- 4.1.13 Modified eagle medium (α -MEM, Hyclone, USA)
- 4.1.14 Phosphate buffer saline without calcium, and magnesium (PBS, Hyclone, USA)
- 4.1.15 Trypsin-EDTA (0.25% trypsin with EDTA·Na, Gibco BRL, Canada)
- 4.1.16 3-(4,5-dimethylthiazol-2-yl)-2,5-diphenyltetrazolium bromide (MTT, USB corporation, USA)
- 4.1.17 Dimethyl sulfoxide (DMSO, Fisher Scientific, UK)
- 4.1.18 Glycine ($\text{NH}_2\text{CH}_2\text{COOH}$, Ajax Finechem, Australia)
- 4.1.19 Sodium chloride (NaCl, Analar, England)
- 4.1.20 Sodium hydroxide (NaOH, Analar, England)

4.2 Equipments

- 4.2.1 Seamless cellulose tubing (Molecular weight cut off 12000-16000, Viskase Companies, Inc., Japan)
- 4.2.2 -40°C freezer (Heto, PowerDry LL3000, USA)
- 4.2.3 Lyophilizer (Heto, PowerDry LL3000, USA)
- 4.2.4 Vacuum drying oven and pump (VD23, Binder, Germany)
- 4.2.5 Fourier transform infrared (FTIR) spectrophotometer from Perkin Elmer (Spectrum GX, UK)
- 4.2.6 Fine coat (JFC-1100E, JEOL Ltd., Japan)
- 4.2.7 Scanning Electron Microscopy (JSM-5400, JEOL Ltd., Japan)
- 4.2.8 Universal Testing Machine (Instron, No. 5567, USA)
- 4.2.9 Laminar Flow (HWS Series 254473, Australia)
- 4.2.10 CO_2 incubator (Series II 3110 Water Jacketed Incubator, Thermo Forma, USA)
- 4.2.11 UV-VIS spectrophotometer (Thermo Spectronic, Genesys 10UV scanning)
- 4.2.12 24-well polystyrene tissue culture plates (NUNC, Denmark)
- 4.2.13 Micropipette (Pipetman P20, P200, P1000 and P5000, USA)

4.3 Experimental procedures

All experimental procedures are summarized in Figure 4.1. In brief, there are three main steps comprised in this work; preparation of silk fibroin and gelatin solutions, preparation of silk and silk-based scaffolds, and characterization of scaffolds.

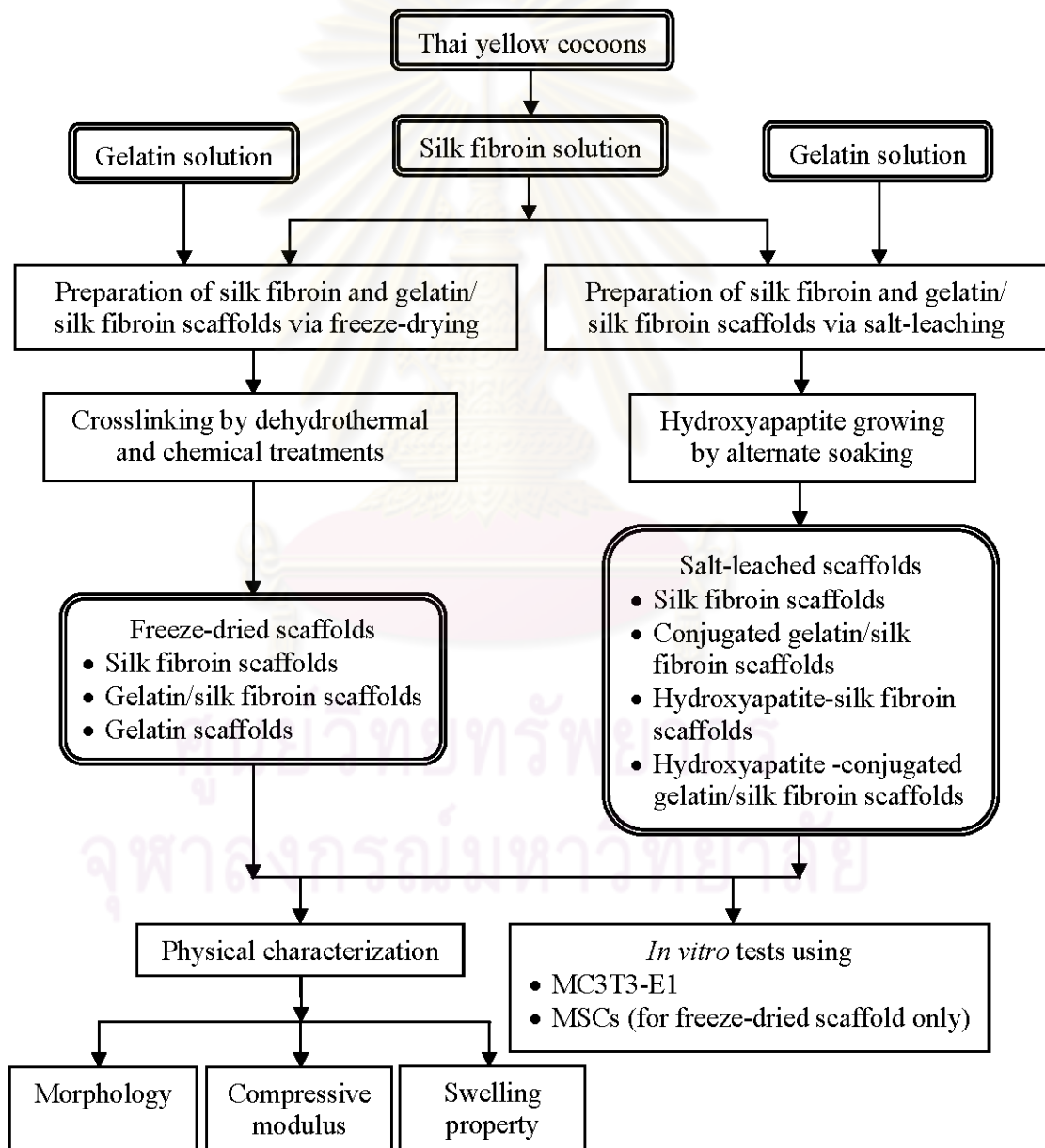


Figure 4.1 Diagram of experimental procedures.

4.3.1 Preparation of silk fibroin and gelatin solutions

4.3.1.1 Preparation of silk fibroin solution

Silk fibroin solution was prepared as described by Kim *et.al.* [1]. Cocoons were boiled in 0.02M Na₂CO₃ aqueous solutions and then rinsed thoroughly. This process was repeated until cocoon became colorless and the solution color remained the same to ensure complete removal of sericin or silk gum. The degummed silk fibroin was dissolved in 9.3M LiBr solutions at 60°C for 4 h to form 25wt% solution. The solution was dialyzed against deionized water at room temperature for 2 days and the conductivity of dialyzed water was the same as that of deionized water. After dialysis, 6.5wt% of aqueous silk fibroin solution, determined by weighing the remaining solid after drying, was obtained and further diluted to form 2wt% solution.

4.3.1.2 Preparation of gelatin solution

Type A and type B gelatin was suspended at the concentration of 2wt% in deionized water. The suspension was subsequently stirred at 40°C for 60 min to obtain gelatin solution.

4.3.2 Preparation of silk fibroin and silk fibroin-based scaffolds

4.3.2.1 Preparation of silk fibroin and gelatin/silk fibroin scaffolds via freeze-drying

Gelatin and silk fibroin solutions were blended under agitation at room temperature for 4 h. The blending weight ratios of gelatin/silk fibroin were 0/100, 20/80, 40/60, 60/40, 80/20 and 100/0. After mixing, 1ml of the 2wt% blended solution was poured into each well of 24-well plates and frozen at -50°C overnight prior lyophilized at -50°C for 48 h. The freeze dried scaffolds were treated by dehydrothermal (DHT) treatment at 140°C for 24 and 48 h in a vacuum oven. After that, the scaffolds were treated with carbodiimide solution (14mM 1-ethyl-3-(3-

dimethylaminopropyl) carbodiimide hydrochloride (EDC) and 5.5mM N-hydroxy-succinimide (NHS)) at room temperature for 2 h [59]. Treatment scaffolds were rinsed thoroughly with deionized water and freeze dried.

4.3.2.2 Preparation of silk fibroin and conjugated gelatin/silk fibroin scaffolds via salt-leaching

After dialysis, 3ml of 6.5wt% silk fibroin solution was added in a cylindrical container and 9 g of mined salt (particle size: 600-710 μ m) was added. The container was covered and left at room temperature for 24 h to allow the gelation of silk fibroin solution. Then, the container was immersed in water to leach out salt for 2 h. The scaffold was taken out from the container and washed under stirring for 4 h. The washing water was changed every 30 min. After that, the scaffold was left to be dried overnight. The silk fibroin scaffold was punched into 11mm in diameter, 2mm in height and immersed in 0.5wt% gelatin solution under vacuum for 2 h to allow gelatin coating on silk fibroin scaffolds. Gelatin was further conjugated via DHT and EDC treatments as previously described.

4.3.2.3 Preparation of hydroxyapatite/silk fibroin and hydroxyapatite-conjugated gelatin/silk fibroin scaffolds

Hydroxyapatite was deposited on the salt-leached scaffolds by an alternate soaking process [56]. The scaffold was immersed in 0.2M CaCl₂ at room temperature under vacuum for 30 min. After that, the scaffold was removed from CaCl₂ solution and rinsed with deionized water. The scaffold was then immersed in 0.12M Na₂HPO₄ at room temperature under vacuum for 30 min. After removing the scaffold from Na₂HPO₄ solution, it was rinsed with deionized water again. This was considered as one cycle of alternate soaking. Soaking process was performed for 2, 4, and 6 cycles. Fresh solutions, CaCl₂ and Na₂HPO₄ were used for each soaking cycle. After desired cycles of soaking process, the hydroxyapatite/silk fibroin and hydroxyapatite-conjugated gelatin/silk fibroin scaffolds were air-dried at room temperature for 24 h.

4.3.3 Characterization of scaffolds

4.3.3.1 Chemical characterization

The conformational structure of pure silk fibroin scaffolds before and after crosslinking was investigated using fourier transform infrared spectroscopic (FTIR) and X-ray diffraction (XRD) techniques.

4.3.3.1.1 Attenuated total reflection fourier transform infrared (ATR-FTIR) spectrophotometric measurements

The silk fibroin scaffolds were analyzed by ATR-FTIR technique using Perkin Elmer Spectrum GX (FTIR system). All spectra were recorded in the wavenumber range of $1800\text{-}900\text{cm}^{-1}$ at the resolution of 4cm^{-1} .

4.3.3.1.2 X-ray diffraction (XRD) measurements

X-ray diffraction patterns of silk fibroin scaffolds were recorded using a Bruker D8 X-ray diffractometer at 30kV and 30mA, with Cu $K\alpha$ radiation. The measurement was scanned at $2\theta = 10^\circ\text{-}50^\circ$. The scan speed used was 2.0 sec/step with the step size of 0.04° .

4.3.3.2 Physical characterization

4.3.3.2.1 Morphology

The morphology of scaffolds was investigated by scanning electron microscopy (SEM). In order to observe the inner structure of scaffolds, the scaffolds were cut vertically and/or horizontally with razor blades. The cut scaffolds were placed on the Cu mount and coated with gold prior to SEM observation.

4.3.3.2.2 Compressive modulus

The compression tests in a dry condition were performed on all scaffolds using a universal testing machine (Instron, No. 5567) at the constant compression rate of 0.5 mm/min. The compressive modulus of the scaffolds (dimension: d=12mm, h=3mm for freeze-drying and d = 11mm, h = 2mm for salt-leaching method) was determined from the slope of the compressive stress-strain curves during the strain range of 5%-30%. The reported values were the mean±standard deviation (n=5).

4.3.3.2.3 Swelling property

Scaffolds were immersed in phosphate buffered saline (PBS) at 37°C, pH 7.4 for 24 h. After excess water was removed, the wet weight of the scaffold was determined. The swelling ratio of the scaffold (W_{sw}) was calculated as follow:

$$W_{sw} = \frac{(W_t - W_o)}{W_o}$$

W_t represented the weight of the wet scaffolds, and W_o was the initial weight of the scaffolds. The values were expressed as the mean±standard deviation (n=5).

4.3.3.3 Biological characterization

In this work, primary bone-marrow derived mesenchymal stem cells (MSCs) and mouse osteoblast-like cells (MC3T3-E1) were used in *in vitro* tests. Cell proliferation on all scaffolds was studied using MC3T3-E1. However, due to a limit in MSCs isolation, the proliferation of MSCs was performed only on freeze-dried silk fibroin scaffolds.

4.3.3.3.1 MSCs isolation and culture

MSCs were isolated and cultivated according to the methods of Takahashi [59]. MSCs derived from the bone shaft of femurs of 3 week old wistar rats. Both ends of rat femurs were cut away from the epiphysis and the bone marrow was flushed out by a 26-gauge needle with 1 ml of phosphate buffer saline without calcium, and magnesium. The cell suspension was placed into tissue culture plates containing modified eagle medium (α -MEM) supplemented with 15% fetal bovine serum at 37°C in 5%CO₂ incubator. The medium was changed on the 4th day of culture and every 3 days thereafter. When the cells proliferated became subconfluent, after 10 days, the cells were detached with 0.25wt% of trypsin and 0.02wt% of ethylenediaminetetraacetic acid (EDTA). The first passage of MSCs was used in this study.

4.3.3.3.2 MC3T3-E1 culture

MC3T3-E1 were cultured in growth medium, α -MEM containing 10% FBS. They were incubated at 37°C in an atmospheric condition containing 5% CO₂. The culture medium was changed every 3 days. At confluence, MC3T3-E1 was harvested using 0.25% trypsin-EDTA and subcultivated in the same medium with 3 dilutions. The 23rd passage of MC3T3-E1 was used in this work.

4.3.3.3.3 *In vitro* cell proliferation tests

The scaffolds were placed into 24-well tissue culture plates and were sterilized in 70% (v/v) ethanol for 30 min. To remove ethanol, the scaffolds were rinsed 3 times with phosphate-buffered saline (PBS).

MC3T3-E1 were seeded at a density of 2×10^4 cells per scaffold onto each scaffold placed in medium and incubated at 37°C in 5%CO₂ incubator. After cultured for a desired day, the cells were then quantified by the 3-(4,5-dimethylthiazolyl)-2,5-diphenyltetrazolium bromide (MTT) assay. MTT solution (0.5mg/ml in DMEM without phenol red) was added into each scaffold and incubated for 30 min to

establish cell viability. DMSO was used to elute complex crystals and the absorbance of the solution was measured at 570nm using a spectrophotometer. The same treatment of the scaffolds without cells was used as a control. The culture medium was changed every 3 days. The cells viability was determined after 3rd and 7th days of seeding for MSCs and 7th and 14th days for MC3T3-E1. All data were expressed as mean±standard deviation (n = 3).

4.3.3.3.4 MC3T3-E1 migration and morphological observation

To study the cell migration into scaffolds and the morphology of cultured cells, freeze-dried gelatin/silk fibroin scaffolds with the blending composition of 20/80, and 0/100 were selected to observe its interaction with MC3T3-E1 because they did not collapse after dehydration. For salt-leached scaffolds, silk fibroin (control) and conjugated-gelatin/silk fibroin scaffolds were observed.

Scaffolds on which cells were cultured for 14 days were fixed with 2.5% glutaraldehyde solution in PBS for 1 h. Scaffolds were then serially dehydrated by a series of ethanol, which were 30%, 50%, 70%, 80%, 90%, 95% and 100%, for 5 min at each concentration. 200 µl of hexamethyldisilazane (HMDS) was added to dry the dehydrated scaffolds at room temperature. Dried scaffolds were cross-sectional cut and cell migration, including all morphology, was observed by SEM as schematically shown in Figure 4.2. The cell-seeding side was labeled as position 1 while position 2 and 3 represented further depth inside the scaffolds to the plate-exposed side (position 4).

4.3.4 Statistical analysis

Significant levels were determined by an independent two-sample t-test. All statistical calculations were performed on the Minitab system for Windows (version 14, USA). P-values of <0.05 was significantly considered.

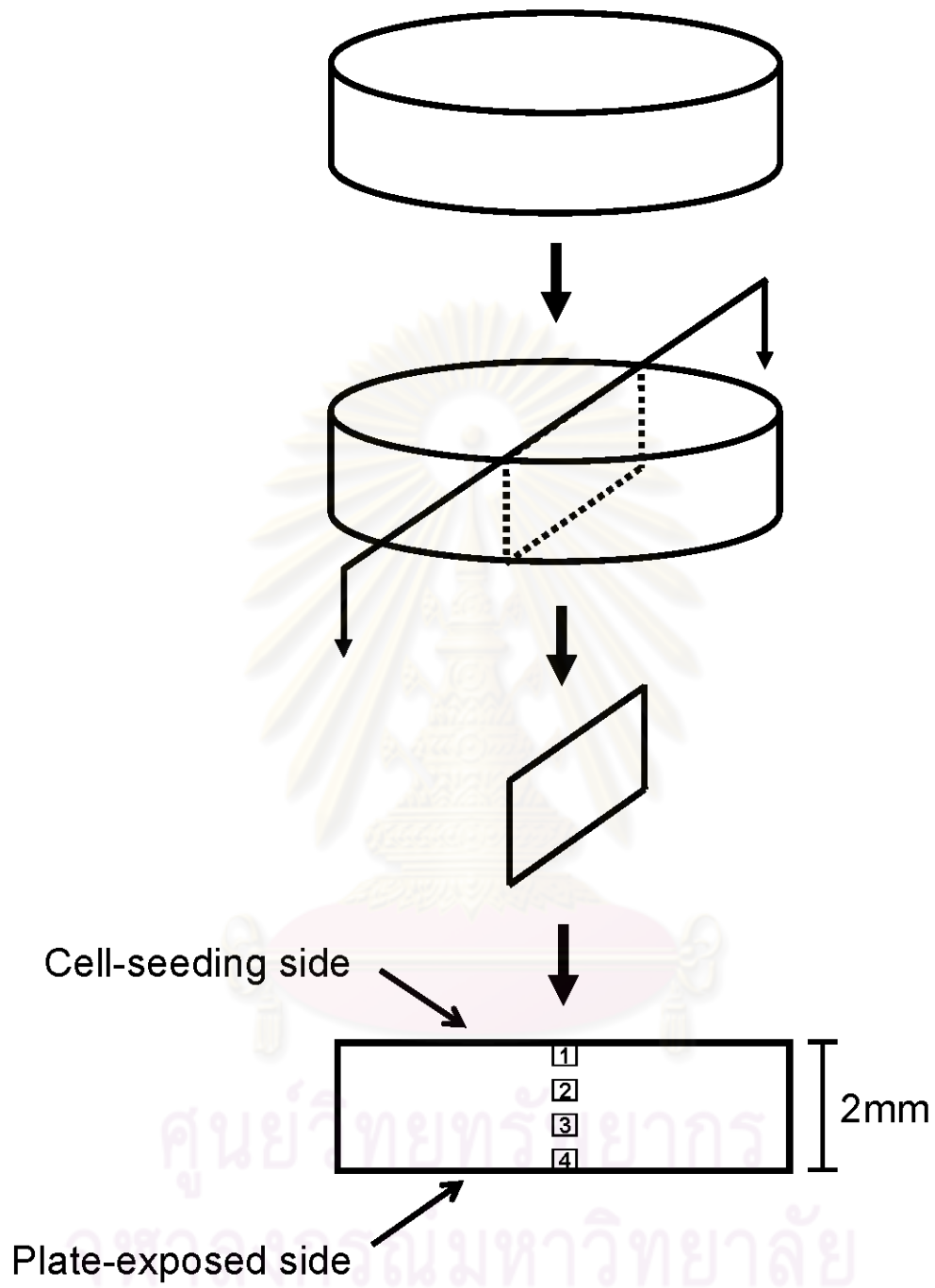


Figure 4.2 Schematic diagram of cross-sectional plane prior to the observation of cell migration and morphology.

CHAPTER V

RESULTS AND DISCUSSION

5.1 Degummed silk fiber

Silk consists of two main parts called silk sericin (silk gum) and silk fibroin. Silk sericin layer acts as an adhesive for the twin silk fibroin filaments and covers the luster of silk fibroin [6]. Many studies illustrated that the sericin glue-like proteins are the major cause of adverse problems with biocompatibility and hypersensitivity to silk [15]. Therefore, silk sericin must be removed to achieve pure silk fibroin fiber. Figure 5.1 showed SEM micrographs of silk fiber before and after degumming. Before degumming, the surface of cocoon fiber was rough (Figure 5.1(a)-(b)) which was the result of coated sericin layer. After sericin layer was removed by Na_2CO_3 [1], the surface of fiber was smooth as shown in Figure 5.1(c)-(d). Figure 5.1(e)-(f) showed the degummed silk fiber with NaOH [60]. The fiber surface was not smooth implying either an incomplete removal of sericin or damaged fibers by NaOH. From this qualitative result, degummed silk fiber using Na_2CO_3 was chosen for further uses.

ศูนย์วิทยทรัพยากร
จุฬาลงกรณ์มหาวิทยาลัย

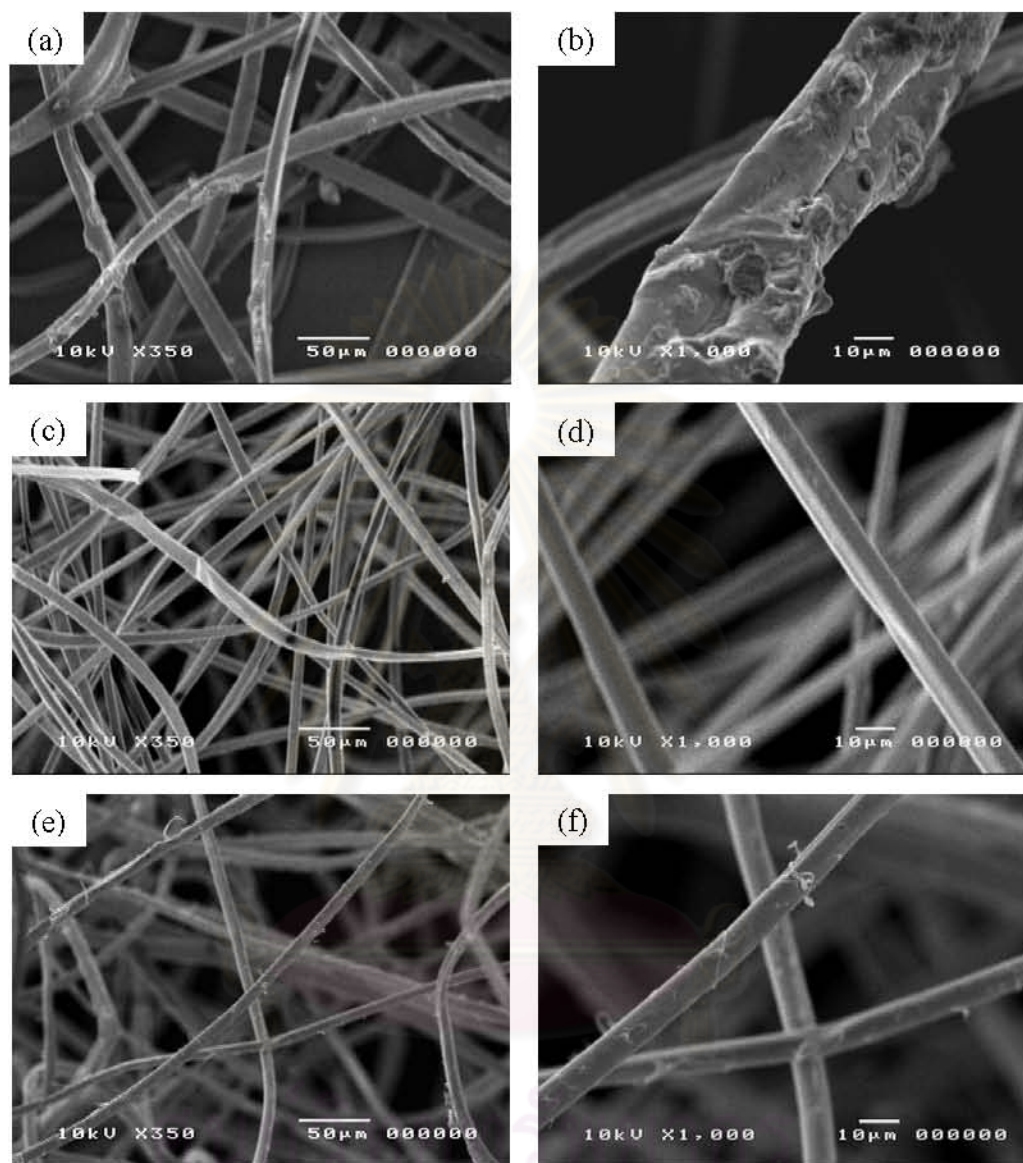


Figure 5.1 SEM micrographs of silk fiber: (a)-(b) cocoon fiber, (c)-(d) degummed silk fiber with Na_2CO_3 , and (e)-(f) degummed silk fiber with NaOH .

5.2 Chemical characteristics of silk fibroin scaffolds

After dialysis process, silk fibroin solution was fabricated into scaffolds by freeze-drying and salt-leaching methods. Chemical characteristics of silk fibroin scaffolds were examined by attenuated total reflection fourier transform infrared (ATR-FTIR) spectrophotometric and X-ray diffraction (XRD) techniques. In addition, LiBr residual in silk fibroin scaffolds was investigated by XRD.

5.2.1 Structural analysis of silk fibroin scaffolds

5.2.1.1 Attenuated total reflection fourier transform infrared (ATR-FTIR) spectrophotometric analysis

ATR-FTIR spectra of freeze-dried silk fibroin scaffolds were shown in Figure 5.2(a)-(c). It could be seen that the peak positions of amide I (C=O stretching), amide II (N-H deformation and C-N stretching), and amide III (C-N stretching and N-H deformation) were located at 1645, 1530, and 1238 cm^{-1} , respectively. These amide bands attributed to the primary structure (random coil) of silk fibroin [41]. This could be reflected from silk fibroin molecules in aqueous solution [44]. In other words, dehydrothermal (DHT) and chemical (EDC) treatments of silk fibroin scaffolds did not induce the transition of secondary structure of silk fibroin. Yamada *et.al.* [61] reported that the structural change of regenerated silk fibroin on heating occurred at approximately 200°C. Therefore, DHT treatment at 140°C was ineffective to structural transition of silk fibroin scaffolds. Generally, EDC was known as a crosslinking agent for proteins. EDC activates the carboxyl group of glutamic or aspartic acid to form an active O-acylisourea intermediate which reacts with an amino group [63]. Sofia *et.al.* [47] stated that EDC treatment led to more stable amide formation of silk fibroin. However, in our ATR-FTIR result, no change in structure of silk fibroin scaffolds due to EDC treatment was detected. Figure 5.2(d) showed ATR-FTIR spectrum of air-dried silk fibroin after gelling. The

absorption bands of amide I approximately at 1625 cm^{-1} , amide II at 1520 cm^{-1} , and amide III at 1265 cm^{-1} were observed. The peak positions of these amide bands reflected the secondary structure (β -sheet) of silk fibroin [55, 64]. This is consistent to several works demonstrated that the structure of silk fibroin was transformed from random coil to β -sheet after gelation process [1, 40, 49, 51]. Gelation process was believed to cause the shift of peak position of amide bands within silk fibroin molecules. ATR-FTIR results revealed that different fabrication process resulted in a difference in the secondary structure of silk fibroin scaffolds.

5.2.1.2 X-ray diffraction (XRD) analysis

Figure 5.3 showed X-ray diffraction patterns of freeze-dried silk fibroin and air-dried silk fibroin scaffolds after gelling. When silk fibroin aqueous solutions were freeze-dried, no peak was detected (Figure 5.3(a)) implying that freeze-dried silk fibroin scaffolds exhibited an amorphous structure [49]. Meanwhile silk fibroin scaffolds after DHT treatment displayed the same pattern as before the treatment as seen in Figure 5.3(b). This corresponded to ATR-FTIR results, e.g. freeze-drying and DHT treatment did not significantly influence the structure of silk fibroin. After treatment with EDC, the XRD peak appeared at $2\theta=20^\circ$ as presented in Figure 5.3(c). This might be the effect of the primary amines on the peptides formed a stable amide bond between the peptide of gelatin and silk fibroin [47]. Air-dried silk fibroin scaffolds after gelling showed a sharp peak at $2\theta=20.6^\circ$ and a small peak at $2\theta=24^\circ$. These peaks represented the β -sheet structure of silk fibroin [1, 40, 49, 51, 55]. The other peak at $2\theta=9^\circ$ that indicated β -sheet was not observed in our result due to the limitation of the equipment.

From the results of X-ray diffraction, the gelation of silk fibroin solutions induced a transition from random coil to β -sheet structure. This result corresponded to the ATR-FTIR spectra of silk fibroin scaffolds as discussed in section 5.2.1.1. The results on ATR-FTIR and XRD rendered that the structure of freeze-dried silk fibroin scaffolds was random coil while that of air-dried silk fibroin scaffolds after gelling was β -sheet.

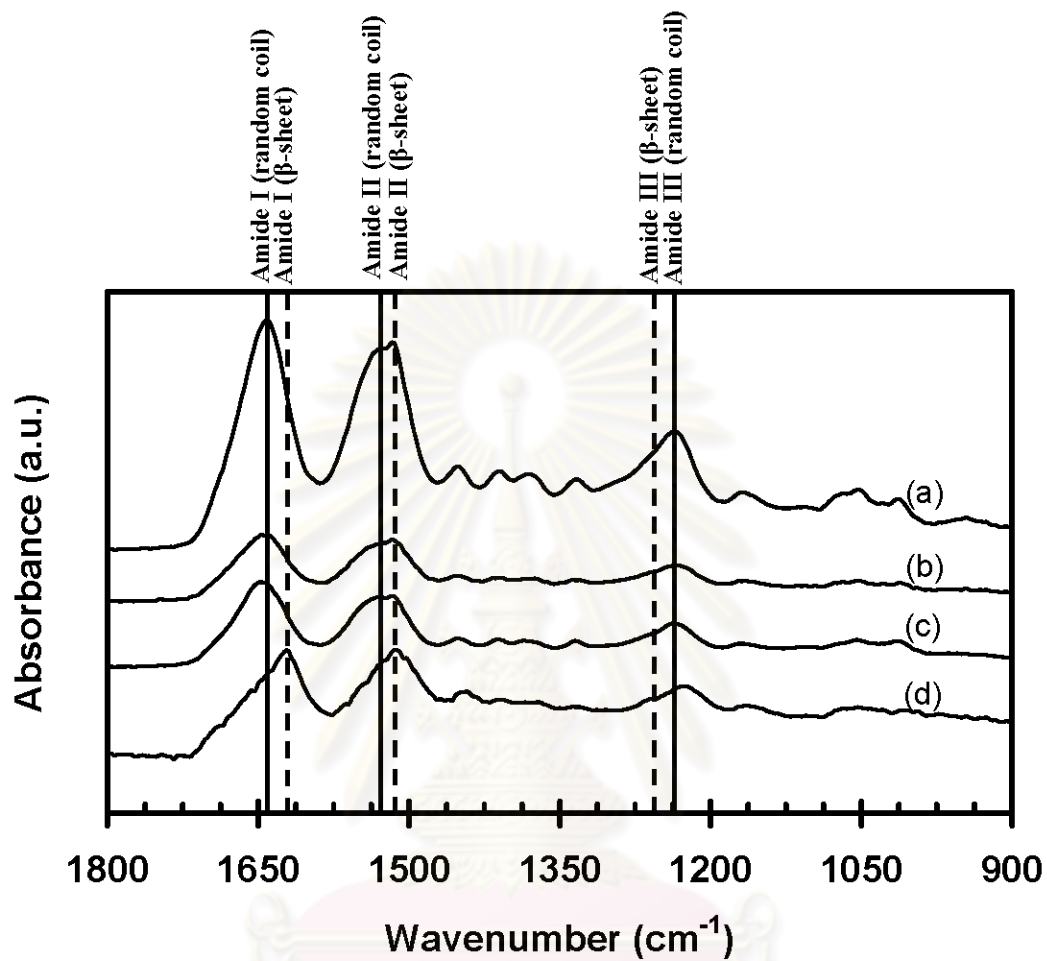


Figure 5.2 ATR-FTIR spectra of freeze-dried silk fibroin scaffolds from dialyzed solution (a) after freeze-drying (before any treatments), (b) after DHT treatment for 48 h, (c) after DHT and EDC treatments, and (d) air-dried silk fibroin obtained after gelling.

จุฬาลงกรณ์มหาวิทยาลัย

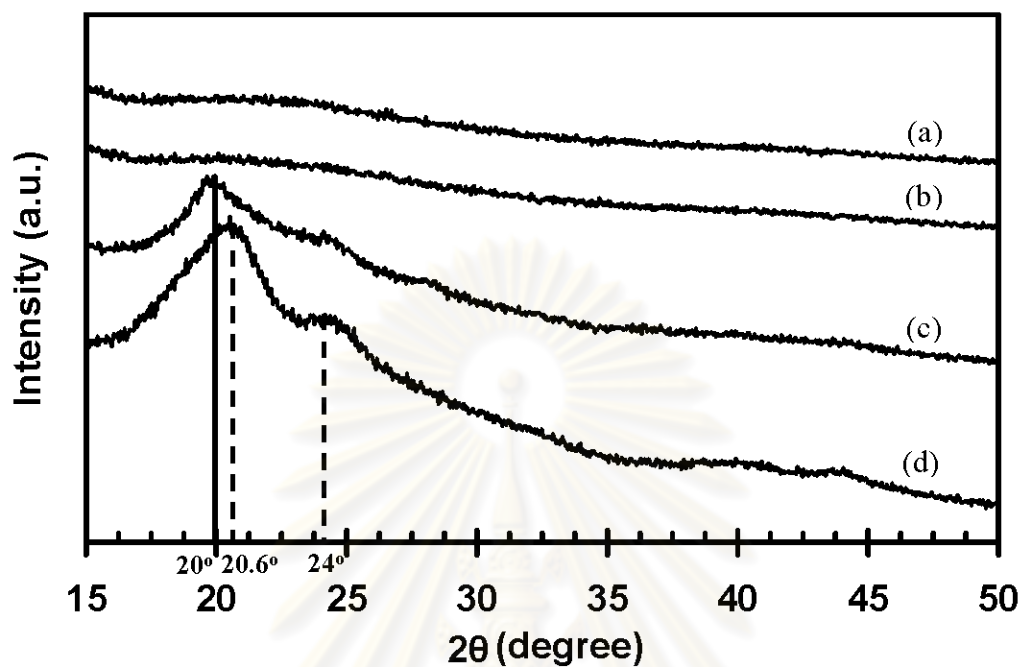


Figure 5.3 XRD patterns of freeze-dried silk fibroin scaffolds from dialyzed solution (a) after freeze-drying (before any treatments), (b) after DHT treatment for 48 h, (c) after DHT and EDC treatments, and (d) air-dried silk fibroin obtained after gelling.

5.2.2 LiBr residual in silk fibroin scaffolds

Figure 5.4 showed X-ray diffraction pattern of lithium bromide (LiBr) powder. The peak position appeared at $2\theta=27, 32,$ and 46° . These positions could not be observed in the XRD patterns of silk fibroin scaffolds (Figure 5.3). This confirmed that there was no LiBr residual in silk fibroin scaffolds.

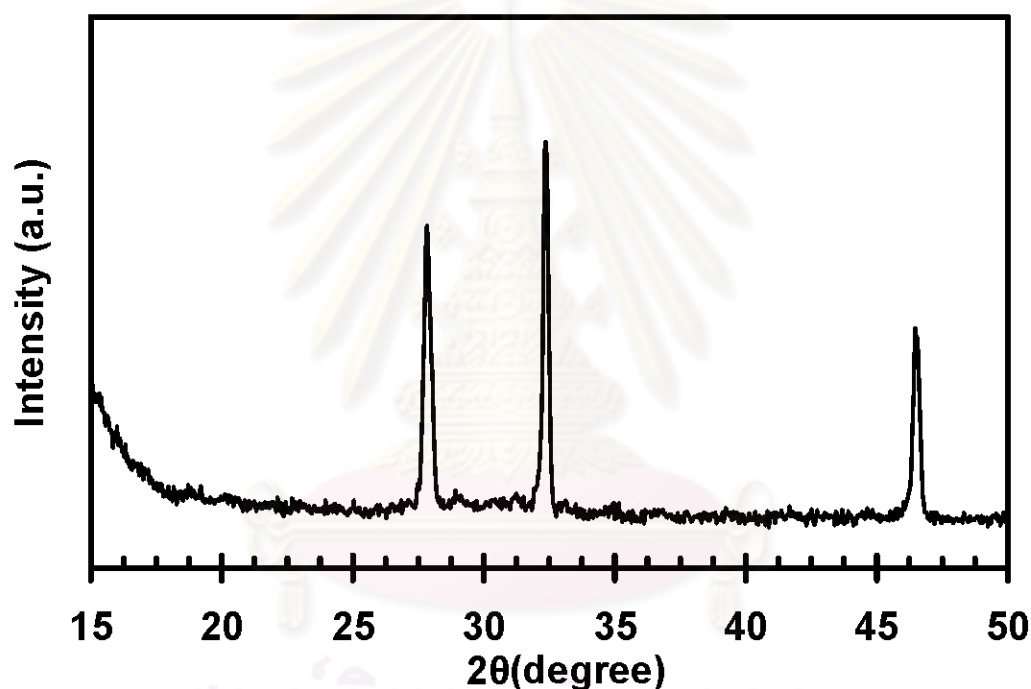


Figure 5.4 XRD pattern of lithium bromide (LiBr) powder.

5.3 Comparison of type A and type B gelatin blending in silk fibroin

After silk fibroin aqueous solution was obtained from dialysis process, the blending of silk fibroin solution with each type of gelatin was investigated and the resulting scaffolds were compared. Either type A or type B gelatin was blended with silk fibroin solution at various blending weight ratios and gelatin/silk fibroin scaffolds were

obtained by freeze-drying. After DHT and EDC treatments, silk fibroin and gelatin/silk fibroin scaffolds were cross-sectional cut in order to observe the morphology under SEM. Figure 5.5 demonstrated SEM micrographs of type B gelatin/silk fibroin scaffold. It could be seen that pure silk fibroin scaffolds possessed highly interconnected porous network, as presented in Figure 5.5(a)-(b), while pure gelatin scaffolds, presented in Figure 5.5(o)-(p), showed leave-like porous structure with very low interconnection.

When silk fibroin was blended with type B gelatin as shown in Figure 5.5(c)-(n), non-uniform porous structure of scaffolds was observed. Two layers were distinguished in cross-sectional scaffolds; the upper layer consisted of a lot of small fibrous pores around big leave-like pores while the lower layer was mainly leave-like porous structure. This implied an incompatibility of silk fibroin and type B gelatin.

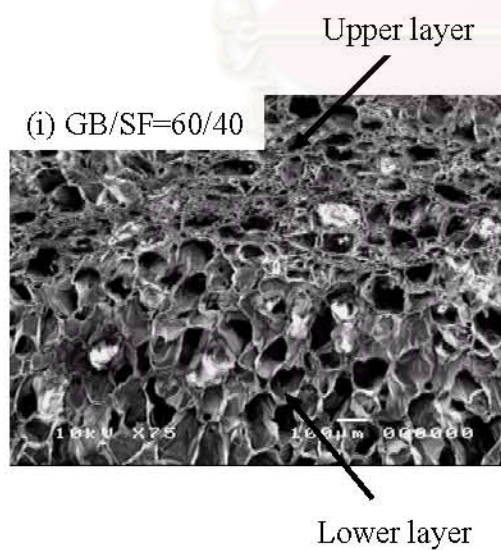
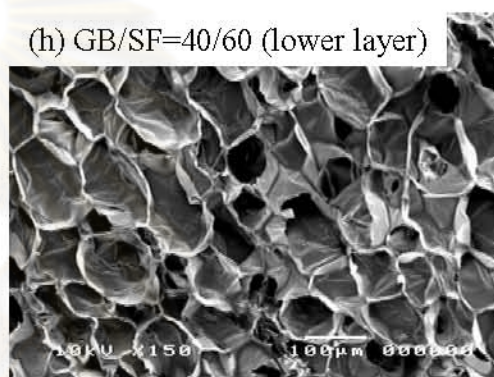
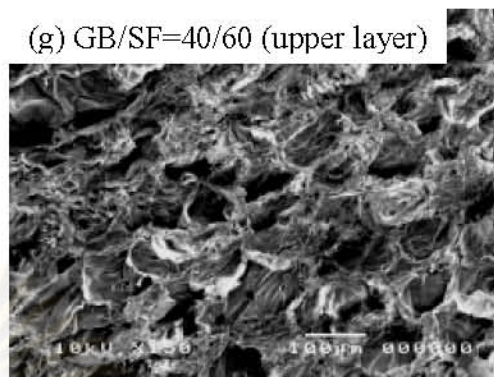
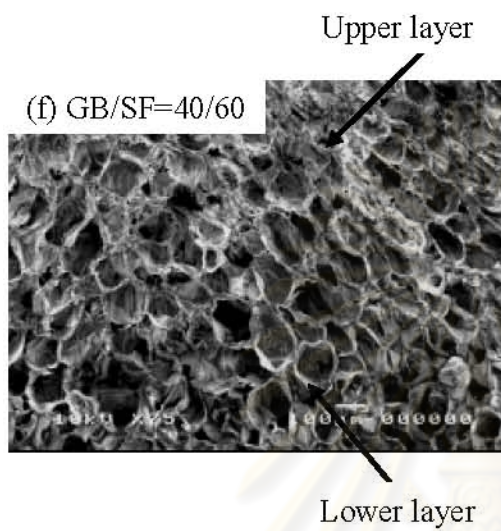
Figure 5.6 depicted SEM micrographs of type A gelatin/silk fibroin scaffolds. It could be noticed that the porous structure of type A gelatin/silk fibroin scaffolds at each blending ratio was uniform. The interconnected porous network of type A gelatin/silk fibroin scaffolds was less than that of pure silk fibroin scaffolds. A more amount of gelatin in the scaffolds resulted in less fibrous network, less interconnection, and bigger pores similar to the leave-like porous structure of type A gelatin (pore size $\sim 50\text{-}150\mu\text{m}$).

The morphology of gelatin/silk fibroin scaffolds revealed in Figure 5.5 and 5.6 proved that only type A gelatin could be homogeneously blended with silk fibroin. This was a result from the charges of materials which depended upon pH and pI, as illustrated in Table 5.1.

Table 5.1 pI and charges of silk fibroin and gelatin

Materials	pI	Charge at pH $\sim 5.5\text{-}6$
Silk fibroin	~ 3	Anionic
Type A gelatin	~ 9	Cationic
Type B gelatin	~ 5	Anionic

At the working pH $\sim 5.5\text{-}6$, silk fibroin and type B gelatin have anionic charges while type A gelatin employs cationic charge. An electrostatic interaction between silk



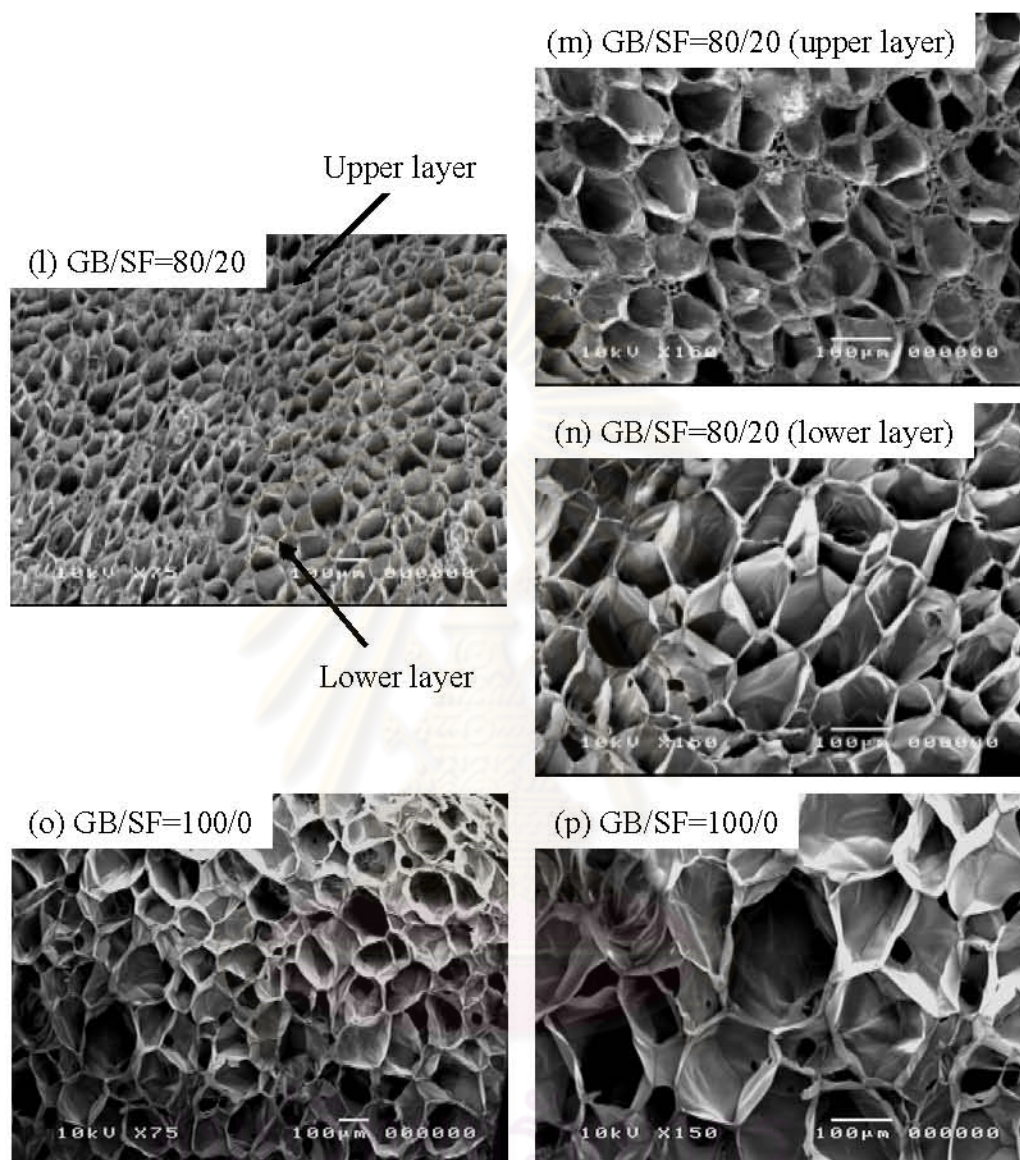


Figure 5.5 SEM micrographs of freeze-dried type B gelatin/silk fibroin (GB/SF) scaffolds (a), (b) 0/100, (c)-(e) 20/80, (f)-(h) 40/60, (i)-(k) 60/40, (l)-(n) 80/20, and (o), (p) 100/0.

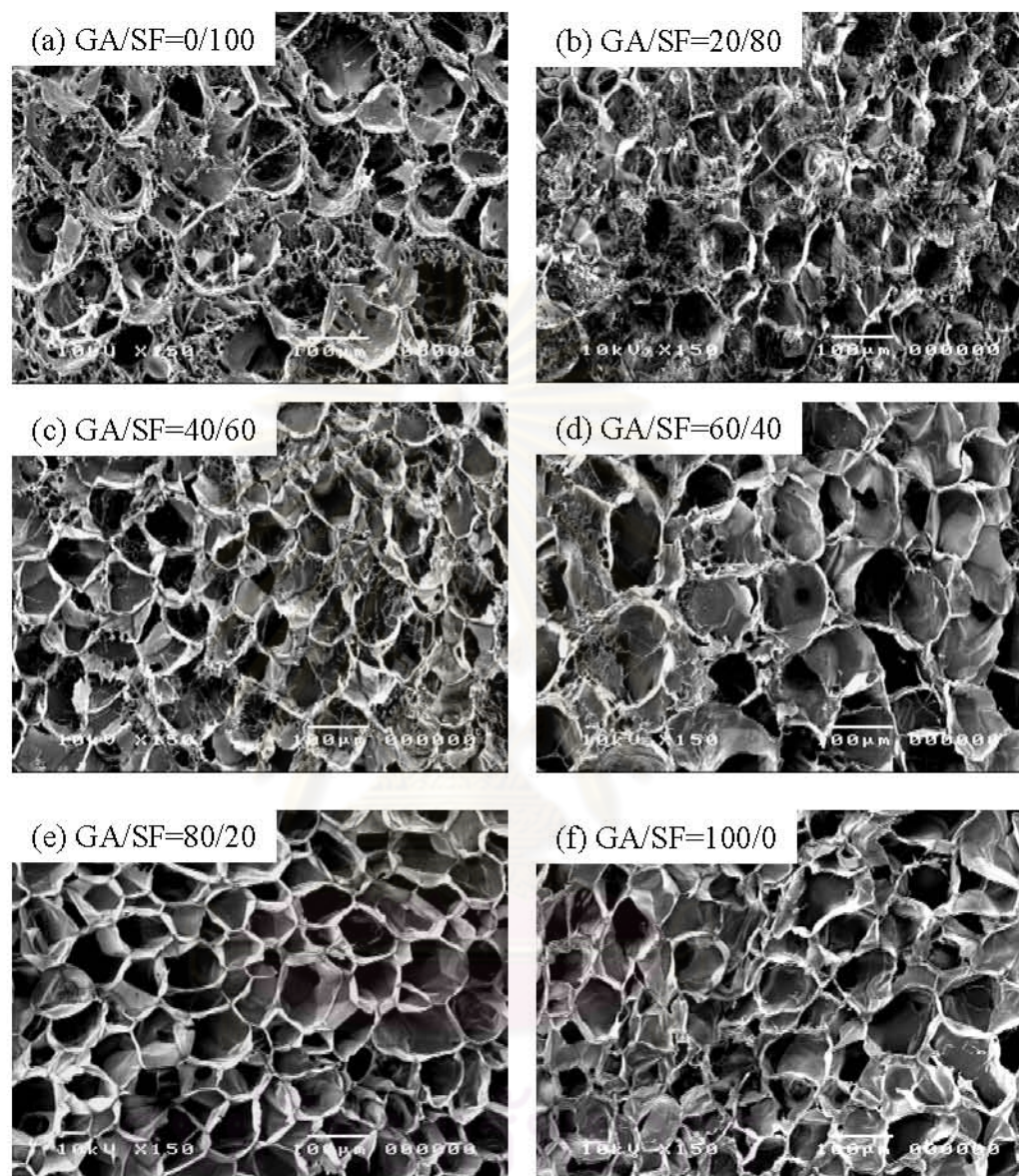


Figure 5.6 SEM micrographs of freeze-dried type A gelatin/silk fibroin (GA/SF) scaffolds (a) 0/100, (b) 20/80, (c) 40/60, (d) 60/40, (e) 80/20, and (f) 100/0.

5.4 Silk fibroin and gelatin/silk fibroin scaffolds via freeze-drying

As the morphology of type A gelatin/silk fibroin blended scaffolds at various blending weight ratios has been presented and discussed in section 5.3. In this section, other characterizations of these blends were presented and discussed. Furthermore, the effects of the dehydrothermal treatment periods at 140°C for 24 and 48 h prior to EDC treatment were investigated.

5.4.1 Compressive modulus of scaffolds

The compressive modulus of gelatin/silk fibroin scaffolds with various dehydrothermal treatment periods was illustrated in Figure 5.7. When the scaffolds were DHT treated for 24 h prior to EDC treatment, the compressive modulus of freeze-dried pure silk fibroin and gelatin scaffolds were 442.50 ± 66.52 and 302.50 ± 34.03 kPa, respectively. It was found that the compressive modulus of pure silk fibroin scaffolds was higher than that of pure gelatin and all gelatin/silk fibroin scaffolds except gelatin/silk fibroin scaffold at blending ratio 20/80 which possessed the highest compressive modulus among all freeze-dried scaffolds. There was a significant difference in the compressive modulus of scaffolds at all blending ratio relative to pure gelatin scaffolds. When the scaffolds were DHT treated for a longer period of 48 h prior to EDC treatment, the compressive modulus of freeze-dried pure silk fibroin and gelatin scaffolds were 350.00 ± 102.31 and 337.14 ± 143.96 kPa, respectively. These are about the same as those scaffolds DHT treated for 24 h. Additionally, the compressive modulus of all blended scaffolds were similar to those processed in DHT treatment for 24 h. In other words, there was no significant difference in the compressive modulus of each type of scaffolds when DHT treated for 24 and 48 h.

Generally, the mechanical characteristic of scaffolds depended upon the type of materials and the structure of scaffolds. The results indicated that the blending ratio

affected the compressive modulus of the scaffolds. Scaffolds with high silk fibroin content (80-100%) possessed relatively high compressive modulus.

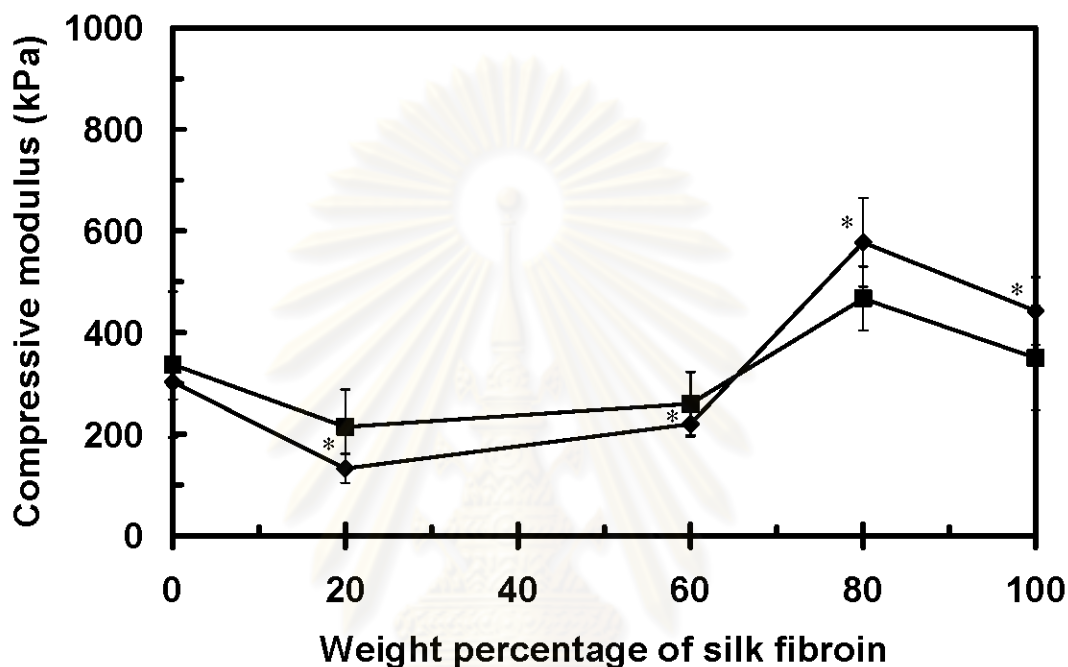


Figure 5.7 Compressive modulus of freeze-dried gelatin/silk fibroin scaffolds with various DHT treatment periods: (◆) 24 h, and (■) 48 h.

* represent the significant difference ($p < 0.05$) relative to gelatin scaffolds.

§ represent the significant difference ($p < 0.05$) relative to the same weight percentage of silk fibroin.

5.4.2 Swelling property of scaffolds

The swelling ratios of the scaffolds represented the amount of water uptake to the dry weight of scaffolds. Swelling ability was an important property for tissue engineering to absorb cell and transport nutrient into scaffolds. Figure 5.8 showed swelling ratios of gelatin/silk fibroin scaffolds with various DHT treatment periods. While 24 h of DHT treatment was employed, it could be seen that swelling ratios of freeze-dried pure silk

fibroin and gelatin scaffolds were 9.19 ± 1.34 and 12.01 ± 0.60 , respectively. The result on the swelling ratio of gelatin scaffolds corresponded to the work of Ratanavaraporn [8]. She reported that the swelling ratios of 0.8wt% freeze-dried type A gelatin scaffolds was 16.64 ± 6.09 and this ration decreased as decreasing gelatin concentration. The swelling ratio of pure silk fibroin scaffolds was significantly lower than that of pure gelatin scaffolds. This could due to the hydrophobic property of silk fibroin. As expected, swelling ratios of gelatin/silk fibroin scaffolds tended to slightly decrease as increasing silk fibroin content. Similarly, the swelling ratios of scaffolds DHT treated for 48 h were closed to those with 24 h of DHT treatment. This result demonstrated that DHT treatment period had no effects on the swelling property of scaffolds.

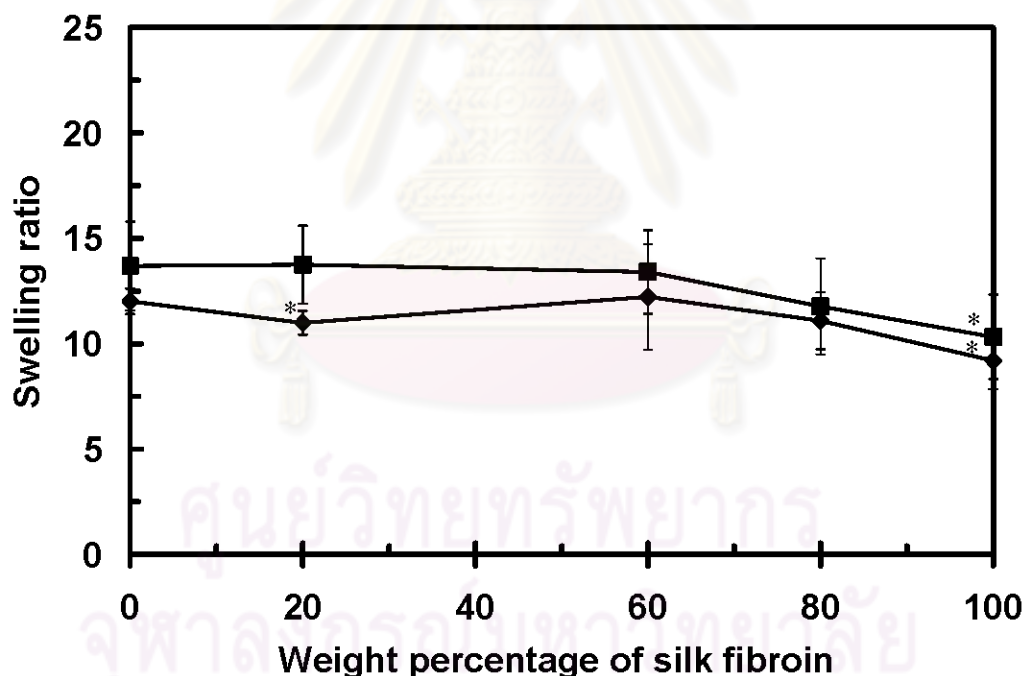


Figure 5.8 Swelling ratios of freeze-dried gelatin/silk fibroin scaffolds with various DHT treatment periods: (◆) 24 h, and (■) 48 h.

* represent the significant difference ($p < 0.05$) relative to gelatin scaffolds.

§ represent the significant difference ($p < 0.05$) relative to the same weight percentage of silk fibroin.

5.4.3 Biological property of scaffolds

To evaluate biocompatibility of scaffolds, each scaffold was seeded with MSCs and MC3T3-E1 at a density of 2×10^4 cells per scaffold. Cell proliferation on scaffolds was investigated using MTT assay.

5.4.3.1 MSCs proliferation tests

The results on *in vitro* cell proliferation of MSCs on gelatin/silk fibroin scaffolds were shown in Figure 5.9. Due to a limit in the number of MSCs, the viability of cells on all scaffolds was determined only after 3 and 7 days of the culture. At 3 days after seeding, the number of cells on pure silk fibroin scaffold was less than pure gelatin and all blended scaffolds. There was no significant difference in the number of cells among various types of scaffolds. After 7 days of seeding, there were more MSCs on each type of scaffolds comparing to those at 3 days of culture. The highest increase in the number of MSCs from the 3rd to 7th date after seeding was obviously noticed for pure silk fibroin scaffolds. There was still no significant difference in the number of cells on all scaffolds after 7 days of culture. However, pure silk fibroin tended to have a slightly more proliferated MSCs comparing to gelatin/silk fibroin and gelatin scaffolds even it was not statistically different. This could due to the morphology of scaffolds (Figure 5.6). Freeze-dried pure silk fibroin scaffolds were a porous network with highly interconnection. This might support cell proliferation.

5.4.3.2 MC3T3-E1 proliferation tests

Figure 5.10 showed the numbers of MC3T3-E1 on gelatin/silk fibroin scaffolds after 1, 7 and 14 days of the culture. At 1 day after seeding, the number of cells on pure silk fibroin scaffold was higher than that of pure gelatin and all gelatin/silk fibroin scaffolds except gelatin/silk fibroin scaffold at blending ratio 20/80. This could be a

result from the morphology of scaffolds (Figure 5.6). Scaffolds with high silk fibroin content (80-100%) had highly interconnected porous network. This might support cell migration. At 7 days after seeding, there was more MC3T3-E1 on each type of scaffolds comparing to those at 1 days of culture. The number of cell on pure silk fibroin and gelatin scaffolds increased 140%, and 2400%, respectively. However, there was no significant difference in the number of osteoblast-like cells on all types of scaffolds. This implied that, in this case, blending of gelatin that was known to contain RGD-like sequence could not promote cell proliferation. The pattern of the number of osteoblast cells grown on all scaffold after 7 days of seeding was similar to that noticed when using MSCs (Figure 5.9). At 14 days after MC3T3-E1 seeding, the same trend as that after 7 days of seeding was observed. Nevertheless, the number of cells tended to slightly decrease in blended scaffolds as increasing silk fibroin content.

This result demonstrated that both cell types can proliferate on freeze-dried gelatin/silk fibroin scaffolds with a similar number.

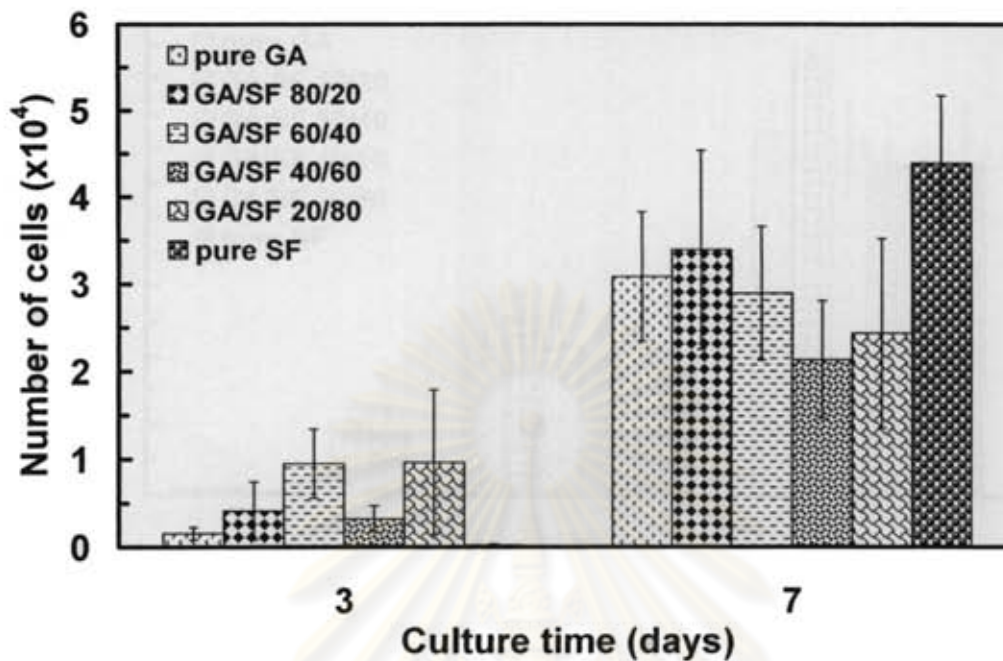


Figure 5.9 Number of MSCs on freeze-dried gelatin/silk fibroin scaffolds after 3 and 7 days of the culture (seeding: 2×10^4 cells/scaffold).

* represent the significant difference ($p < 0.05$) relative to gelatin scaffolds in each periods.

ศูนย์วิทยทรัพยากร
จุฬาลงกรณ์มหาวิทยาลัย

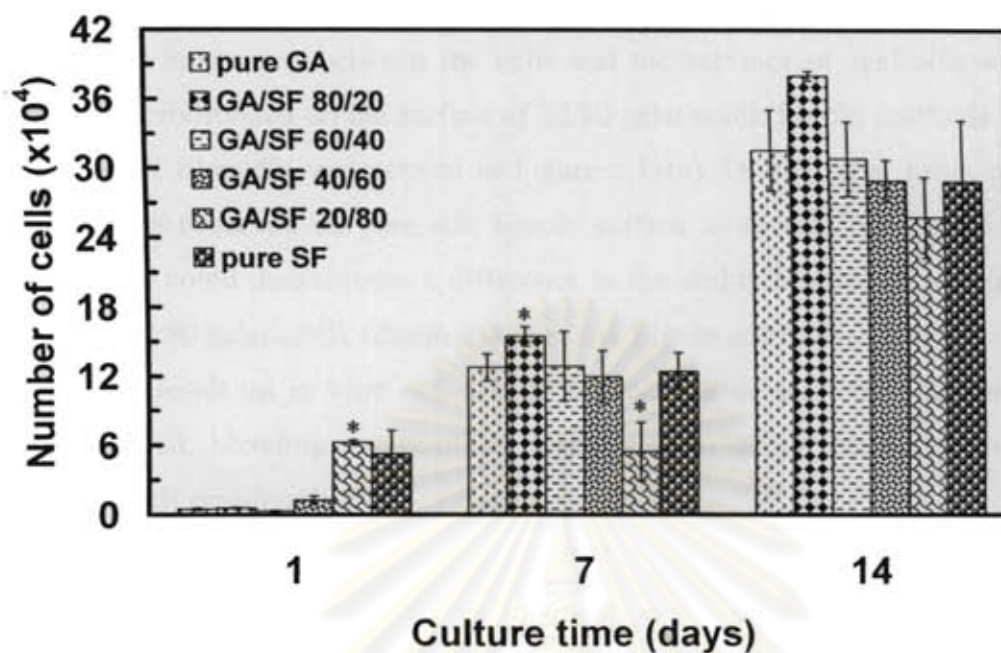


Figure 5.10 Number of MC3T3-E1 on freeze-dried gelatin/silk fibroin scaffolds after 1, 7, and 14 days of the culture (seeding: 2×10^4 cells/scaffold).

* represent the significant difference ($p < 0.05$) relative to gelatin scaffolds in each periods.

5.4.3.3 MC3T3-E1 migration and morphological observation

The morphology of MC3T3-E1 cultured on 20/80 gelatin/silk fibroin and pure silk fibroin scaffolds for 14 days were depicted in Figure 5.11 and 5.12, respectively. These two were selected for cell-material morphological observation since they did not collapse after dehydration with ethanol and hexamethyldisilazane (HMDS). MC3T3-E1 migration was investigated from the cell seeding side (position 1-Figure 5.11(a) and Figure 5.12(a)) down to the plate-exposed side (position 4-Figure 5.11(d) and Figure 5.12(d)). The micrographs demonstrated that MC3T3-E1 could penetrate through the thickness of both scaffolds. Cells could be observed on the scaffold from cell seeding side toward bottom side. Using higher magnification, cell morphology on 20/80

gelatin/silk fibroin and pure silk fibroin scaffolds after 14 days of culture was shown in Figure 5.13. Interaction between the cells and the surfaces of scaffolds was noticed. MC3T3-E1 proliferated on the surface of 20/80 gelatin/silk fibroin scaffolds were round and a sign of filopodia was noticed in Figure 5.13(a). On the other hand, no filopodia evidence was observed on pure silk fibroin surface as shown in Figure 5.13(b). This phenomenon could demonstrate a difference in the ability of cells to proliferate on the surface of 20/80 gelatin/silk fibroin and pure silk fibroin scaffolds.

This result on in vitro cell culture of freeze-dried scaffolds illustrated that cell types, material, blending composition of material including morphology of scaffolds influenced cell proliferation.

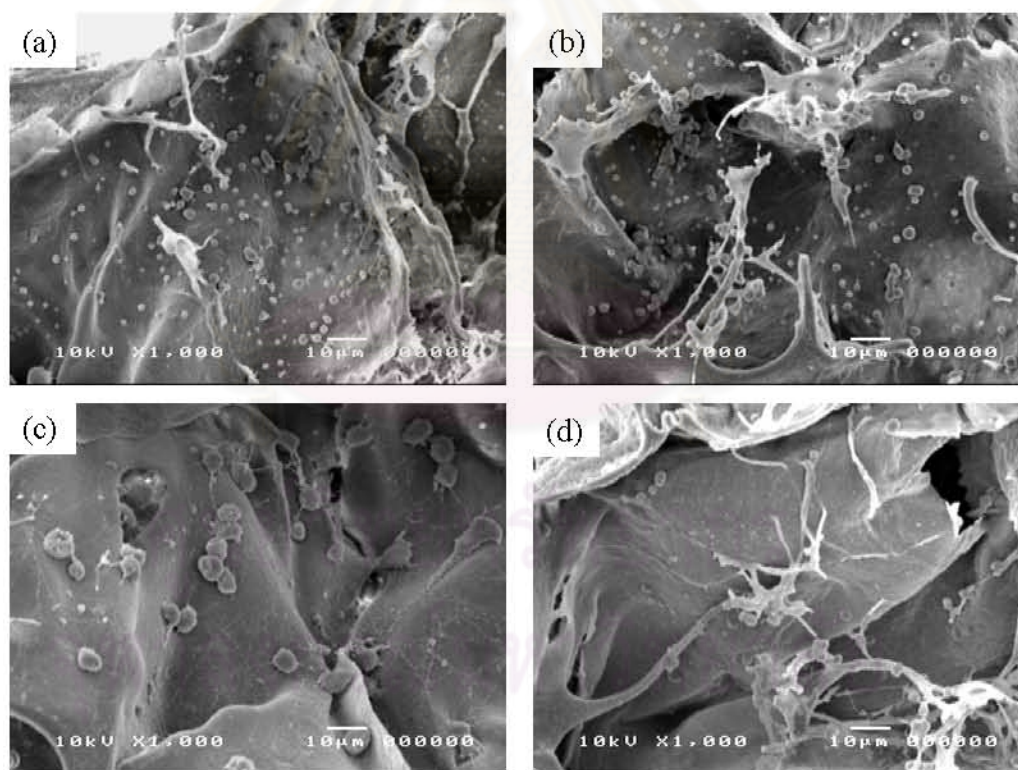


Figure 5.11 SEM micrographs of cross-sectional plane of freeze-dried 20/80 gelatin/silk fibroin scaffolds at position (a) 1 (cell seeding side), (b) 2, (c) 3, and (d) 4 (plate-exposed side) after 14 days of MC3T3-E1 culture.

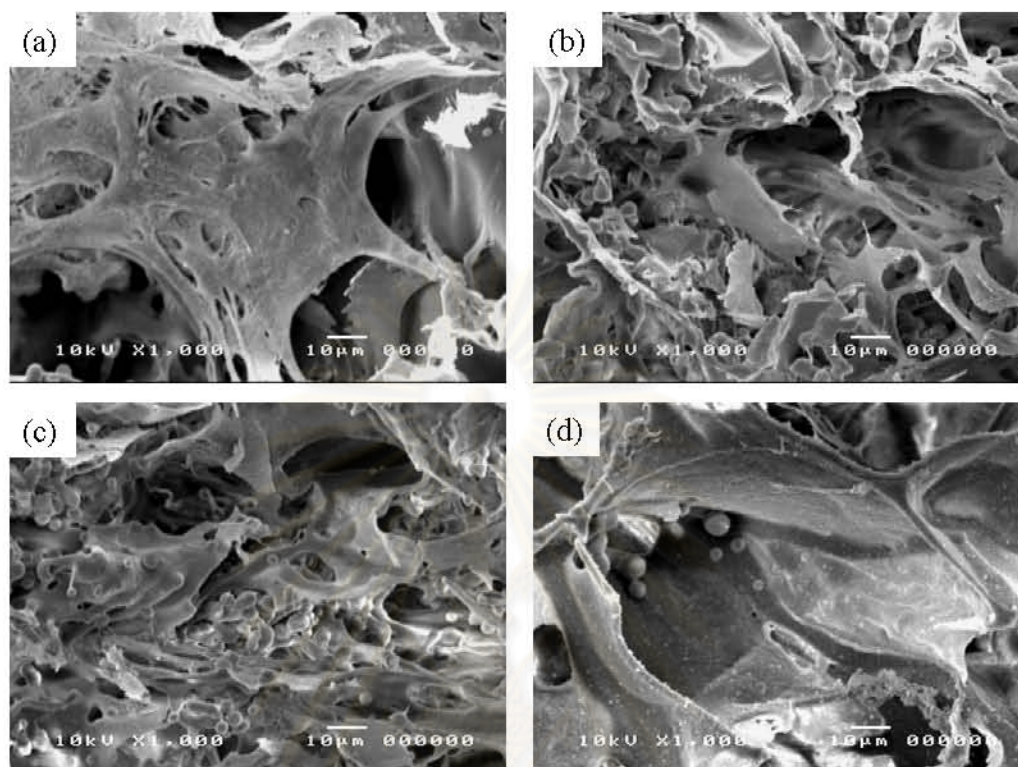


Figure 5.12 SEM micrographs of cross-sectional plane of freeze-dried pure silk fibroin scaffolds at position (a) 1 (cell seeding side), (b) 2, (c) 3, and (d) 4 (plate-exposed side) after 14 days of MC3T3-E1 culture.

ศูนย์วิจัยทรัพยากร
จุฬาลงกรณ์มหาวิทยาลัย

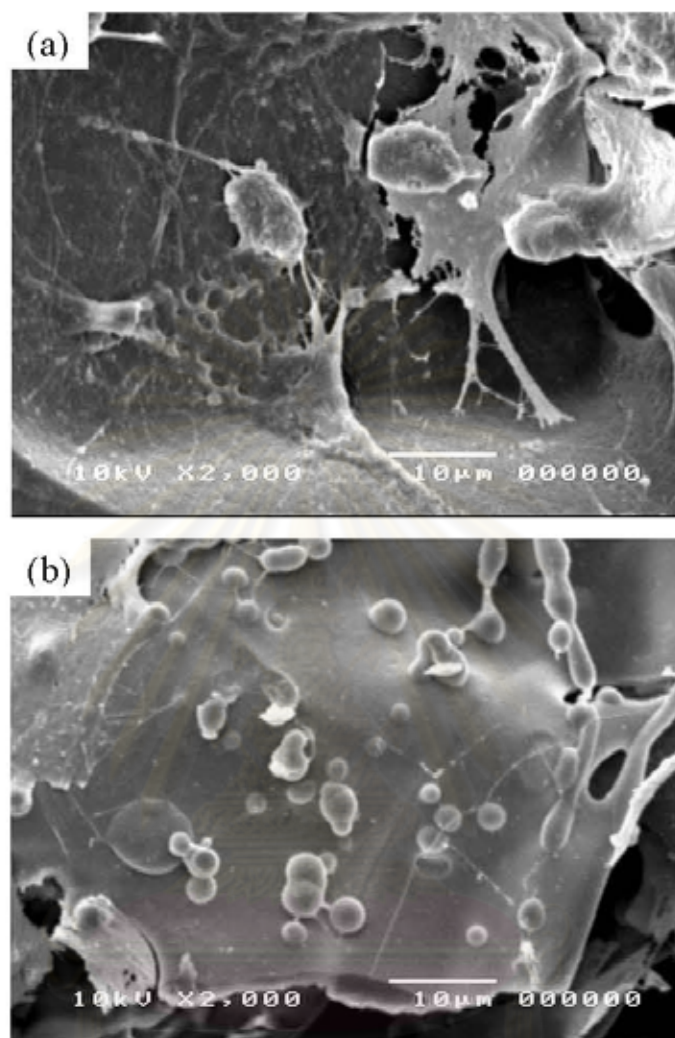


Figure 5.13 SEM micrographs of MC3T3-E1 morphology after 14 day cultured on freeze-dried gelatin/silk fibroin scaffolds: (a) 20/80, and (b) 0/100.

จุฬาลงกรณ์มหาวิทยาลัย

5.5 Silk fibroin and conjugated gelatin/silk fibroin scaffolds via salt-leaching

In this section, porous silk fibroin scaffolds were prepared using salt-leaching method. The pore size of scaffolds could be regulated by the size of granular NaCl added into the silk fibroin aqueous solution. In this work, the size of granular NaCl used was 600-710 μm (Figure 5.14) due to local availability.

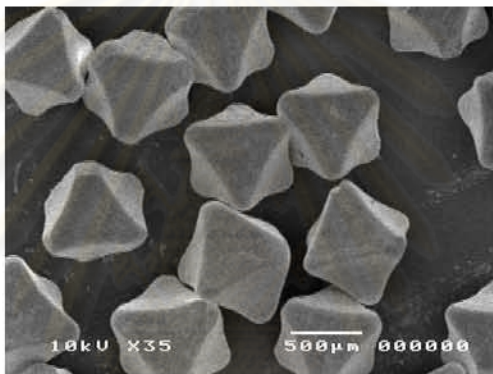


Figure 5.14 SEM micrograph of NaCl crystals.

After salt-leached silk fibroin scaffolds were obtained, surface was modified by conjugating with type A gelatin. Furthermore, silk fibroin and conjugated gelatin/silk fibroin scaffolds were alternately immersed in calcium and phosphate solution to allow the deposition of hydroxyapatite compound on the surface of scaffolds. This method was employed to grow hydroxyapatite compound on various surface of substrates [11, 56-57]. All types of salt-leached scaffolds prepared were listed in Table 5.2.

Table 5.2 Salt-leached scaffolds prepared in this work

Scaffolds	Number of alternate soaking cycles	Notation
Silk fibroin scaffolds	0	SF0
	2	SF2
	4	SF4
	6	SF6
Conjugated gelatin/silk fibroin scaffolds	0	CGSF0
	2	CGSF2
	4	CGSF4
	6	CGSF6

5.5.1 Morphology of scaffolds

5.5.1.1 Hydroxyapatite/silk fibroin scaffolds

Figure 5.15 showed the cross sectional morphology of hydroxyapatite/silk fibroin scaffolds. Before hydroxyapatite growing, porous structure with smooth surface of silk fibroin scaffolds was noticed as illustrated in Figure 5.15(a)-(b). The pore size of scaffold structure represented the size of salt crystals used (600-710 μ m). The outer surface of salt-leached silk fibroin scaffolds before hydroxyapatite growing, shown in Figure 5.15(c), was similar to the inner surface of scaffolds as presented in Figure 5.15(a). After alternate soaking in calcium and phosphate solutions, the pore size of scaffolds decreased as seen from both inner surface (Figure 5.15(d), (g), and (j)) and outer surface (Figure 5.15(f), (i), and (l)). This due to the infusion of calcium and phosphate solutions throughout the scaffolds leading to the deposition of hydroxyapatite on the surface of scaffolds. The accumulated hydroxyapatite resulted in the rough surface of porous structure as seen in Figure 5.15(e), (h), and (k). After 6 cycles of alternate soaking, the outer structure of scaffolds was covered with hydroxyapatite. As a result, the alternate soaking process

could not be further performed; i.e. calcium and phosphate solutions hardly diffused into the scaffolds.

Considering the hydroxyapatite crystals grown on the scaffold surface after 2, 4, and 6 cycles of alternate soaking (Figure 5.16), it was found that the hydroxyapatite formed inside the scaffolds looked to be less than that grown on the outer surface. Size of hydroxyapatite crystal seemed to increase as increasing the number of alternate soaking cycles from 2 to 4 cycles as shown in Figure 5.16(b), and (d). After 6 cycles of alternate soaking (Figure 5.16(f)), the more accumulation of hydroxyapatite crystals led to a thick layer of hydroxyapatite fully filled the porous structure as discussed earlier.

5.5.1.2 Hydroxyapatite-conjugated gelatin/silk fibroin scaffolds

Figure 5.17 showed the cross sectional morphology of hydroxyapatite-conjugated gelatin/silk fibroin scaffolds. The structure of CGSF0 was very fibrous (Figure 5.17(a)-(b)). Conjugated gelatin was partly formed fibers inside the pores of silk fibroin scaffolds resulting in fiber-like structure with highly interconnection which was different from the porous structure of silk fibroin as shown in Figure 5.15(a)-(b). Figure 5.17(c) showed the outer surface of CGSF0 which obviously differed from the inner surface of CGSF0 in Figure 5.17(a) and the outer surface of SF0 in Figure 5.15(c). Gelatin conjugating caused a less opened-surface of scaffolds. This partly limited the infusion of calcium and phosphate solution into the scaffolds. After hydroxyapatite growing, the interconnected porous network tended to decrease comparing to CGSF0 (Figure 5.17(d), (g), and (j)). The deposition of hydroxyapatite was observed along gelatin fiber and scaffold surface leading to a rough surface (Figure 5.17(e), (h), and (k)). More hydroxyapatite accumulation was noticed upon the increasing number of alternate soaking cycles. The accumulation of hydroxyapatite over the outer surface of scaffolds was clearly noticed which caused the porous structure disappeared as presented in Figure 5.17(f), (i), and (l). This result revealed that gelatin conjugating on silk fibroin scaffolds influenced the morphology of silk fibroin scaffolds and the pattern of hydroxyapatite growing.

Figure 5.18 elucidated the hydroxyapatite crystals grown on the conjugated gelatin/silk fibroin scaffold surface after 2, 4, and 6 cycles of alternate soaking. It confirmed that the hydroxyapatite deposition inside the scaffolds was less than that formed on the outer surface of the scaffolds. The hydroxyapatite crystal aggregation increased as increasing the number of alternate soaking cycles as shown in Figure 5.18(b), (d), and (f).

Comparing the hydroxyapatite crystals grown in SF (Figure 5.16) and CGSF (Figure 5.18), it was noted that crystal sizes of hydroxyapatite in SF were larger than those in CGSF. This could be a result from a difference in the morphology of both scaffolds. Moreover, the surface area of fibrous CGSF was relatively more than that of SF, while the pore volume of CGSF was less as noticed from an increased weight of scaffolds (~13%) after gelatin conjugating. This ensured that gelatin conjugating of silk fibroin scaffolds influenced hydroxyapatite growing including the size and distribution of hydroxyapatite.

Additionally, after the silk fibroin and conjugated gelatin/silk fibroin scaffolds were immersed in calcium and phosphate solutions, i.e. hydroxyapatite growing, the average weight of the scaffolds was increased as depicted in Figure 5.19. The increasing weight of silk fibroin and conjugated silk fibroin scaffolds after various numbers of alternate soaking cycles was obviously the weight of grown hydroxyapatite in the scaffolds. It was clearly seen that the weight of hydroxyapatite deposited in the scaffolds was progressively increased upon the increasing number of alternate soaking cycles.

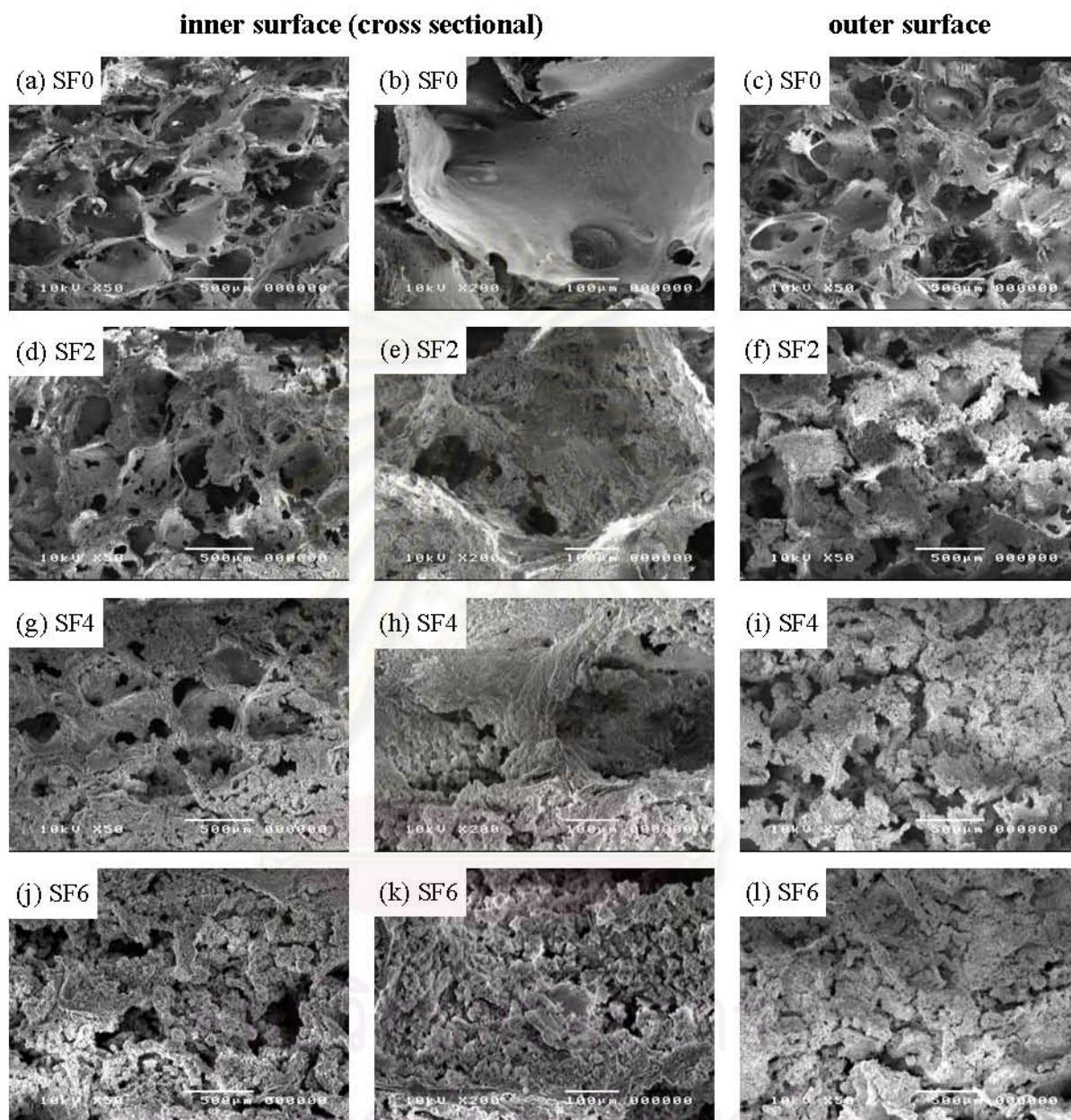


Figure 5.15 SEM micrographs of silk fibroin scaffolds (a)-(c) before soaking, after (d)-(f) 2 cycles, (g)-(i) 4 cycles, and (j)-(l) 6 cycles of alternate soaking in calcium and phosphate solutions.

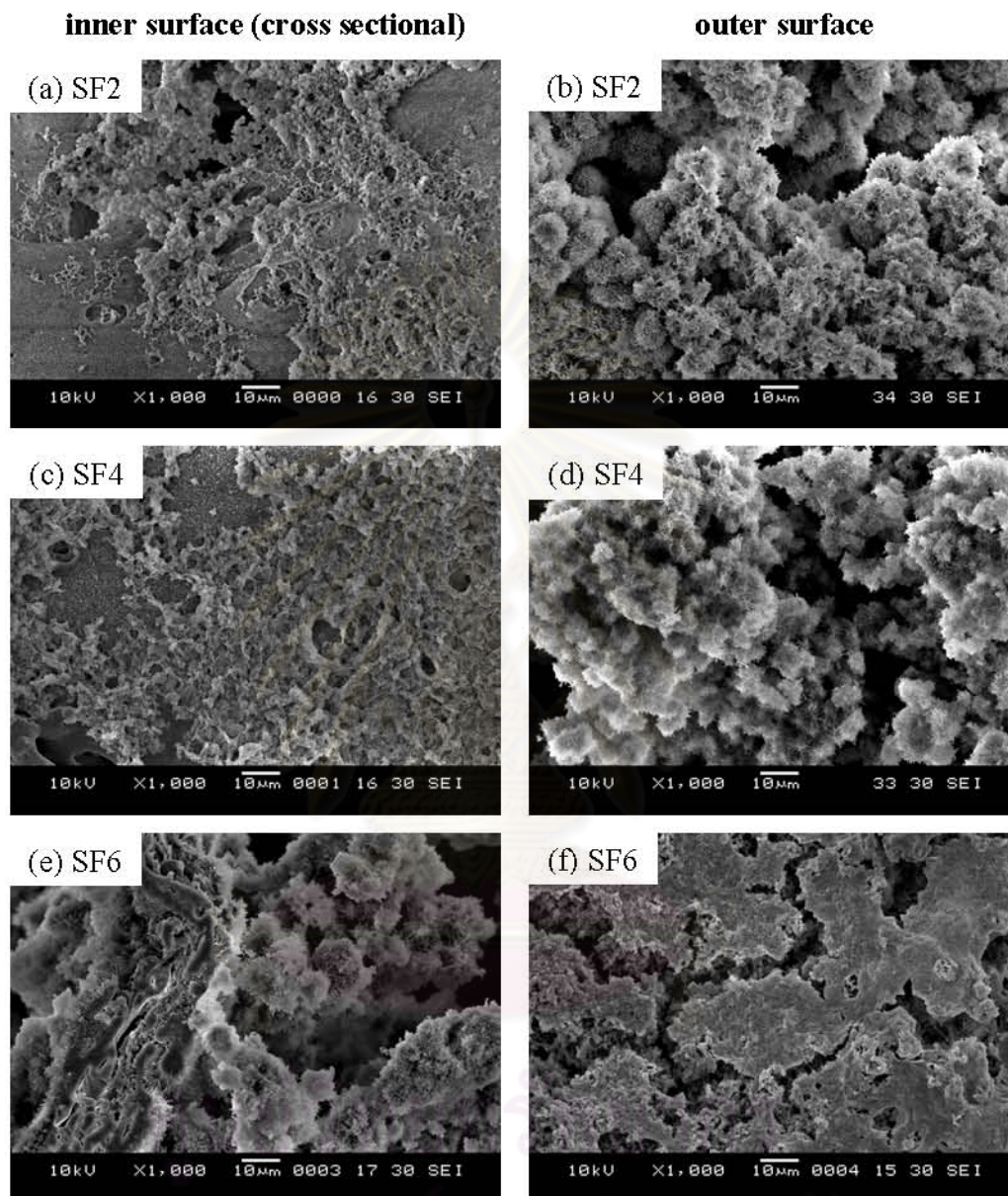


Figure 5.16 SEM micrographs of hydroxyapatite crystals in silk fibroin scaffolds (a)-(b) 2 cycles, (c)-(d) 4 cycles, and (e)-(f) 6 cycles of alternate soaking.

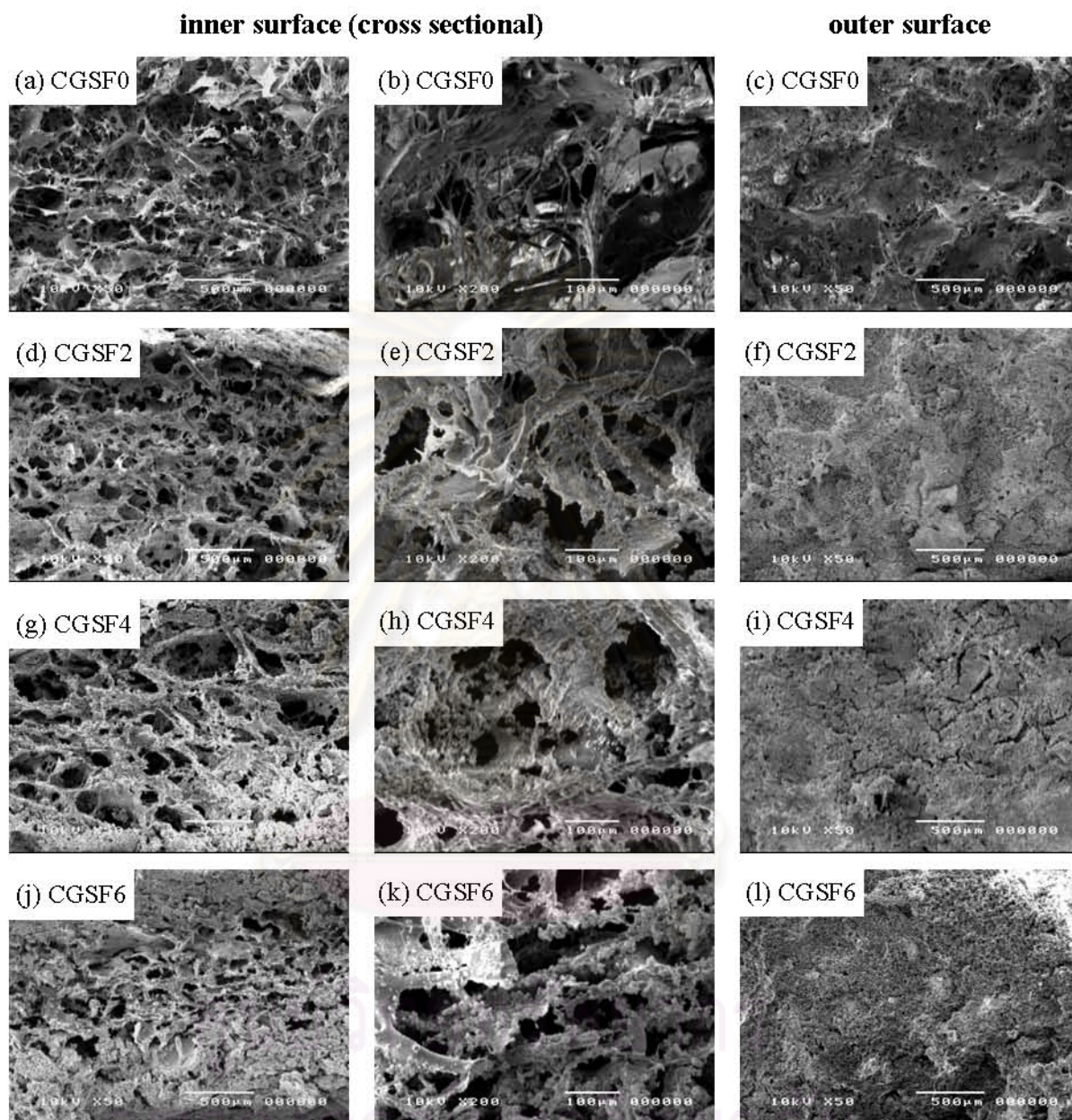


Figure 5.17 SEM micrographs of conjugated gelatin/silk fibroin scaffolds (a)-(c) before soaking, after (d)-(f) 2 cycles, (g)-(i) 4 cycles, and (j)-(l) 6 cycles of alternate soaking in calcium and phosphate solutions.

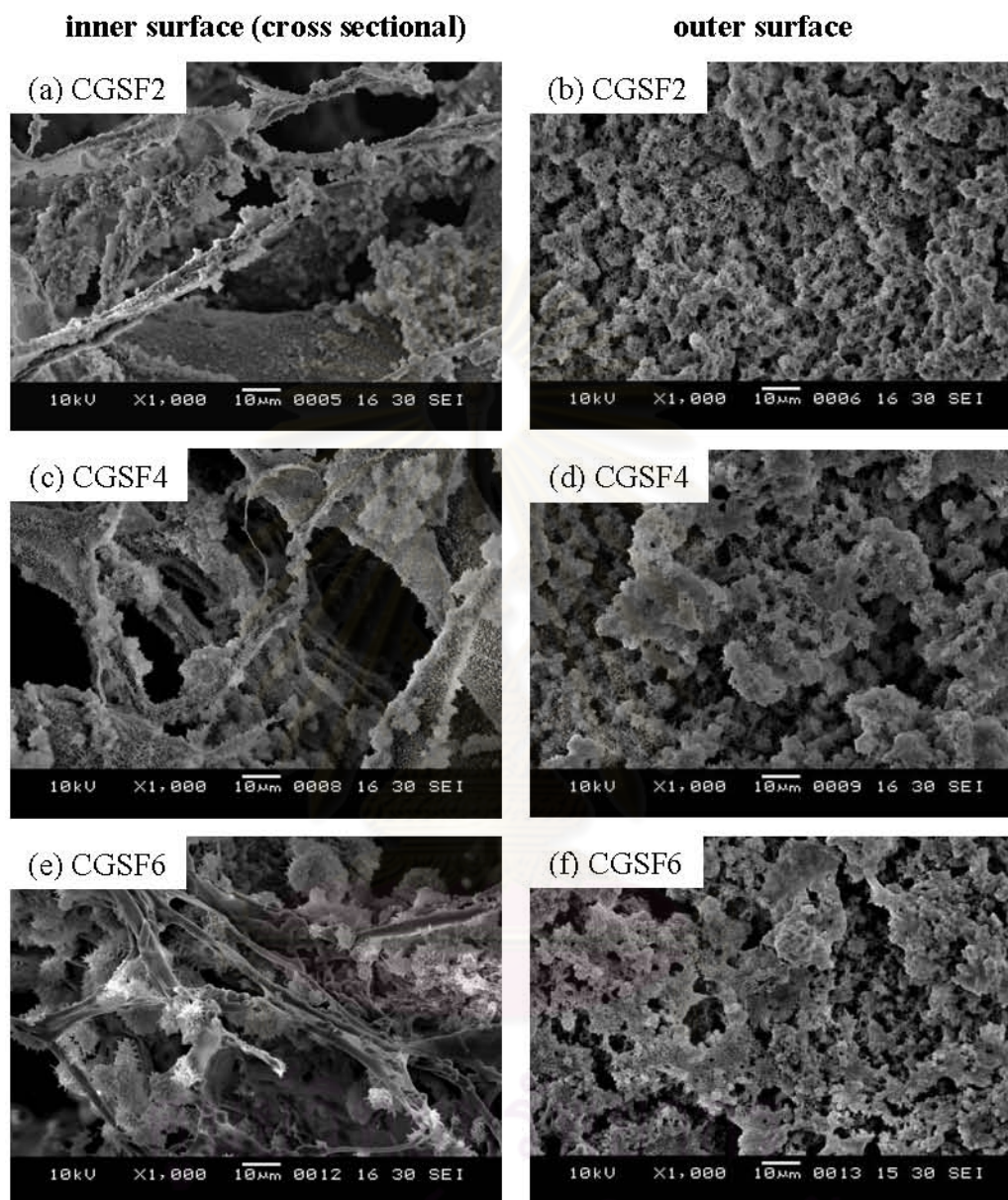


Figure 5.18 SEM micrographs of hydroxyapatite crystals in conjugated gelatin/silk fibroin scaffolds (a)-(b) 2 cycles, (c)-(d) 4 cycles, and (e)-(f) 6 cycles of alternate soaking.

The comparison between SF and CGSF exhibited that the increasing weight of hydroxyapatite in SF was higher than CGSF and the difference tended to be more as increasing the cycles of alternate soaking process. The weight of both scaffolds was increased about 80-95% after 2 cycles of alternate soaking. At 6 cycles of alternate soaking, hydroxyapatite deposited in SF and CGSF scaffolds were 230% and 190% of initial weight of scaffolds, respectively. When SF was conjugated with gelatin, the ability of hydroxyapatite growing via solution infusion into the scaffolds was reduced. This was in agreement with the results on SEM micrographs of both types of scaffolds discussed previously.

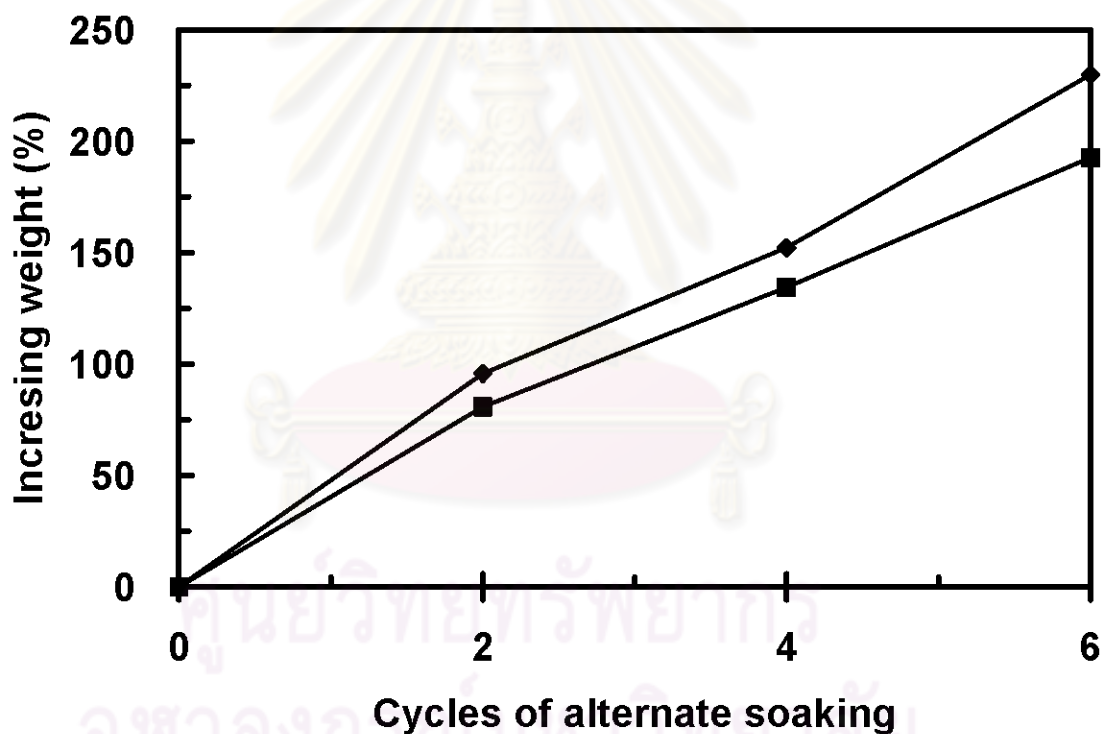


Figure 5.19 Increasing weights of scaffolds as a function of alternate soaking cycles (◆) silk fibroin scaffolds, and (■) conjugated gelatin/silk fibroin scaffolds.

Our results corresponded to a recent report by Furuzono *et.al.* [57] which showed the increasing of apatite weight on the silk fabric with alternated soaking repetitions. Taguchi *et.al.* [11] also reported that hydroxyapatite content increased with increasing immersion cycle in calcium and phosphate solutions.

5.5.2 Compressive modulus of scaffolds

The compressive modulus of hydroxyapatite/silk fibroin and hydroxyapatite-conjugated gelatin/silk fibroin scaffolds was shown in Figure 5.20. The compressive modulus of SF0 and CGSF0 were 262.50 ± 61.85 and 506.00 ± 151.10 kPa, respectively. This could be a result from the morphology of both scaffolds. Morphology of CGSF was more fibrous structure and the surface area of CGSF was more than SF. This supported compressive ability of scaffolds. Moreover, CGSF was treated by DHT and EDC. DHT brings about chemical bonding between the amino and carboxyl groups within molecule of polypeptide. It was well-known that crosslinking could enhance mechanical properties of scaffolds. Further treated with EDC, the primary amines on the peptides formed a stable amide bond between the peptide of gelatin and silk fibroin [47] causing an increasing in compressive modulus of scaffolds.

Comparing the compressive modulus of salt-leached silk fibroin scaffolds to the other work reported [1], it was found that the compressive modulus of SF0 was lower than that reported (770 ± 50 kPa). This might due to different testing condition and the size of scaffolds. Our scaffolds were rather small (~ 11 mm in diameter, ~ 2 mm in height) comparing to those used in Kim *et.al.*'s work (12mm in diameter, 10mm in height). Another possible reason might be the different source of *Bombyx mori* silkworm. Our Thai silkworm (yellow cocoon) possessed lower molecular weight (~ 253.4 kDa) than that of Japanese race (white cocoon, ~ 515.1 kDa) [65].

After hydroxyapatite growing, compressive modulus of both scaffolds increased with an increasing numbers of alternate soaking cycles. At 6 cycles of alternate soaking, compressive modulus of SF increased by 100% while that of CGSF increased 60%. This

might be the influence of the hydroxyapatite deposited in SF which was more than in CGSF. However, the absolute compressive modulus of SF6 (535.00 ± 93.99 kPa) was still lower than that of CGSF6 (826.00 ± 388.63 kPa). These results confirmed that gelatin conjugating and hydroxyapatite growing on silk fibroin scaffolds enhanced the compressive modulus of silk fibroin scaffolds.

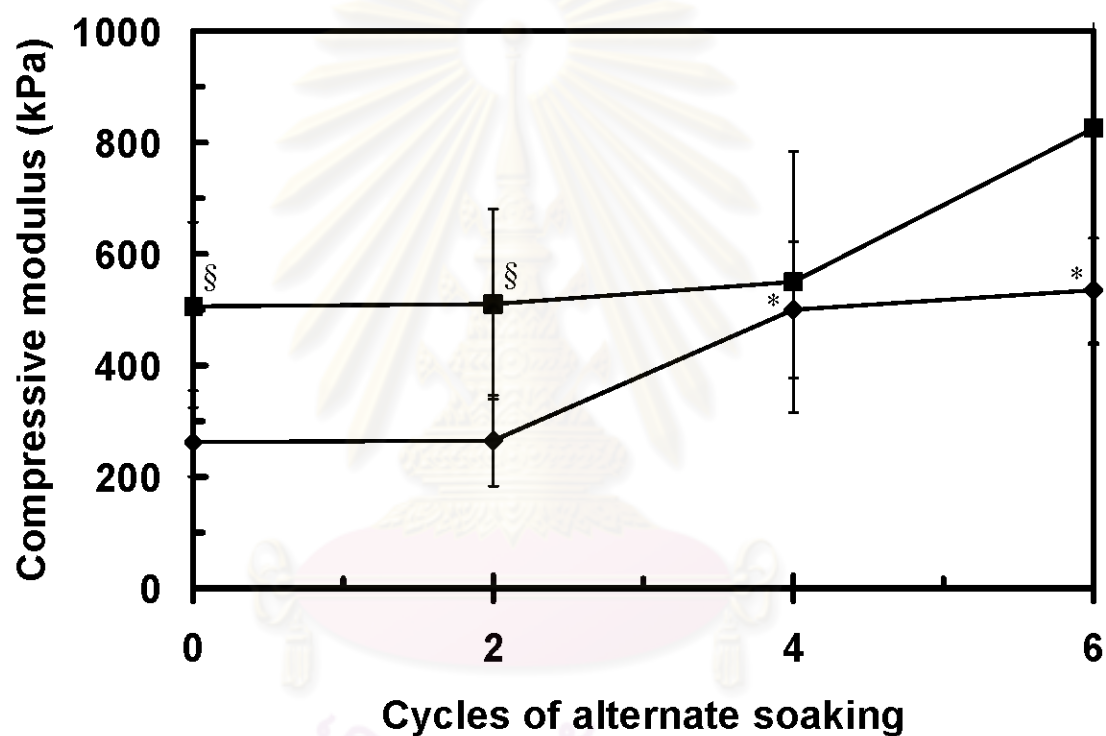


Figure 5.20 Compressive modulus of (♦) hydroxyapatite/silk fibroin scaffolds, and (■) hydroxyapatite-conjugated gelatin/silk fibroin scaffolds.

* represent the significant difference ($p < 0.05$) relative to each scaffold before alternate soaking (0 cycle).

§ represent the significant difference ($p < 0.05$) relative to the scaffold at the same number of alternate soaking cycles

5.5.3 Swelling property of scaffolds

Figure 5.21 showed the swelling ratio of hydroxyapatite/silk fibroin scaffolds and hydroxyapatite-conjugated gelatin/silk fibroin scaffolds at various numbers of alternate soaking cycles. The swelling ratios of SF0 and CGSF0 were 11.02 ± 1.46 and 10.32 ± 1.37 , respectively. The swelling ratio of SF was very similar to that of CGSF0. This result showed that gelatin conjugating did not affect the swelling property of scaffolds.

After hydroxyapatite growing, swelling ratio of both SF and CGSF decreased significantly with an increasing numbers of alternate soaking cycles. At 6 cycles of alternate soaking, swelling ratio of SF and CGSF decreased about 50-60%. It was a result from the accumulation of hydroxyapatite on the surface of scaffolds obstructed the swelling ability of scaffolds and possibly the less pore volume in the scaffolds as seen from SEM micrographs.

Comparing the swelling property of salt-leached silk fibroin scaffolds to the other work reported [1], it was found that the swelling ratio of SF0 was lower than that prepared from Japanese white silkworm (28.4 ± 2.7). The discrepancy might be attributed by different source of silk fibroin as well as the testing condition. Before the swelling test, our scaffolds were not dried in a vacuum oven to reduce the humidity. This could reduce the swelling ability of our silk fibroin scaffolds. In addition, our scaffolds were rather small (~ 11 mm in diameter, ~ 2 mm in height) comparing to those used in Kim *et.al.*'s work (12mm in diameter, 10mm in height).

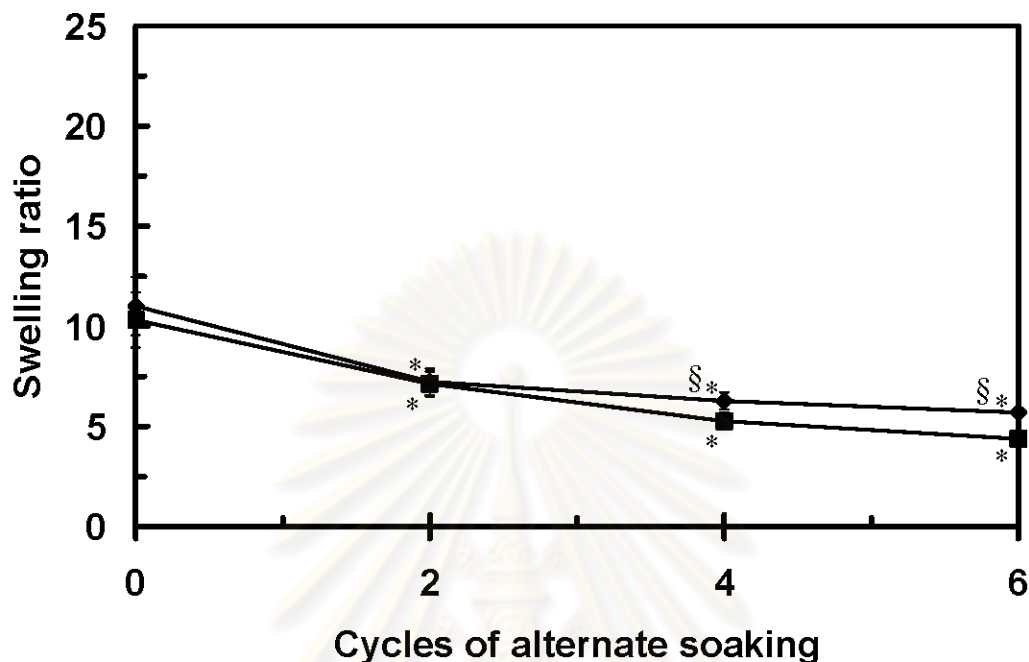


Figure 5.21 Swelling properties of (♦) hydroxyapatite/silk fibroin scaffolds, and (■) hydroxyapatite-conjugated gelatin/silk fibroin scaffolds.

* represent the significant difference ($p < 0.05$) relative to each scaffold before alternate soaking (0 cycle).

§ represent the significant difference ($p < 0.05$) relative to the scaffold at the same number of alternate soaking cycles

5.5.4 Biological property of scaffolds

5.5.4.1 MC3T3-E1 proliferation tests

Figure 5.22 presented the numbers of MC3T3-E1 on hydroxyapatite/silk fibroin scaffolds, and hydroxyapatite-conjugated gelatin/silk fibroin scaffolds after 1, 7 and 14 days of the culture. At 1 day after seeding, no significant difference in the number of cells among various scaffolds was noticed except CGSF4. At 7, and 14 days after seeding, the number of cells tended to decrease in all scaffolds except in CGSF0. This might be the

result of fibrous morphology of CGSF0 which was reported to support the proliferation of MC3T3-E1 [66]. In addition, hydrophilic property of gelatin promoted cell proliferation of CGSF0. Calvert *et.al.* [67] reported that MC3T3-E1 could adhere better on hydrophilic surfaces than hydrophobic surfaces. Moreover, gelatin contains arginine-glycine-aspartic acid (RGD)-like sequence that promotes cell adhesion and migration [46, 68]. For the case of hydroxyapatite/silk fibroin and hydroxyapatite-conjugated gelatin/silk fibroin scaffolds, cells might not be able to proliferate on scaffolds due to a high deposition of hydroxyapatite on the cell-seeding surface of scaffolds.

The other work reported on the use of Thai silk fibroin in tissue engineering by Meechaisue *et.al.* [53] have showed that MC3T3-E1 could adhere and proliferate on the electrospun Nang-Lai silk fibroin fiber mats similar to that on electrospun silk fibroin fiber mats from Chinese/Japanese hybrid silkworms. They suggested that the electrospun Nang-Lai silk fibroin fiber mats could be used as scaffolding materials for bone cell culture.

5.5.4.2 MC3T3-E1 migration and morphological observation

Figure 5.23-5.25 showed SEM micrographs of spreading behavior of MC3T3-E1 mouse osteoblast-like on silk fibroin scaffolds, and conjugated gelatin/silk fibroin scaffolds after 14 days of culture. Conjugated gelatin/silk fibroin scaffolds which showed the highest cell proliferation were selected to observe the cell interaction and morphology. Furthermore, silk fibroin scaffolds, as control, were investigated. For silk fibroin scaffold as shown in Figure 5.23, MC3T3-E1 was found throughout the thickness of scaffolds (position 1 to 4) though there were fewer cells found at the deepest position (position 4). For the case of conjugated gelatin/silk fibroin scaffolds, the surfaces were decorated with cells. In addition, the porous structure in the upper half of conjugated gelatin/silk fibroin scaffolds (Figure 5.24(a)-(b)) was disappeared as it was possibly covered with neo-extracellular matrix deposited by MC3T3-E1. Comparing the cell morphology proliferated on both types of scaffolds shown in Figure 5.25, it was evident

that cells on silk fibroin surface were round. No filopodia was observed as shown in Figure 5.25(a). Meanwhile, the extension of cytoplasm on conjugated gelatin/silk fibroin surfaces was noticed as seen in Figure 5.25(b). Cell morphology implied that cells were more active on conjugated gelatin/silk fibroin surfaces. For the case of hydroxyapatite/silk fibroin and hydroxyapatite-conjugated gelatin/silk fibroin scaffolds, no cells inside scaffolds were noticed. This confirmed that the hydroxyapatite accumulation on the outer surface of scaffolds obstructed the cell migration into the scaffolds. This possibly ceased the cell growth resulting in a decreasing trend in the number of living cells as noticed in previous section (Figure 5.22)

This result indicated that gelatin conjugating on silk fibroin scaffolds promoted the proliferation and biological activity of mouse osteoblast-like cells. Further investigations are required to fully understand the biological activity of cells on these scaffolds.



ศูนย์วิจัยทรัพยากร
จุฬาลงกรณ์มหาวิทยาลัย

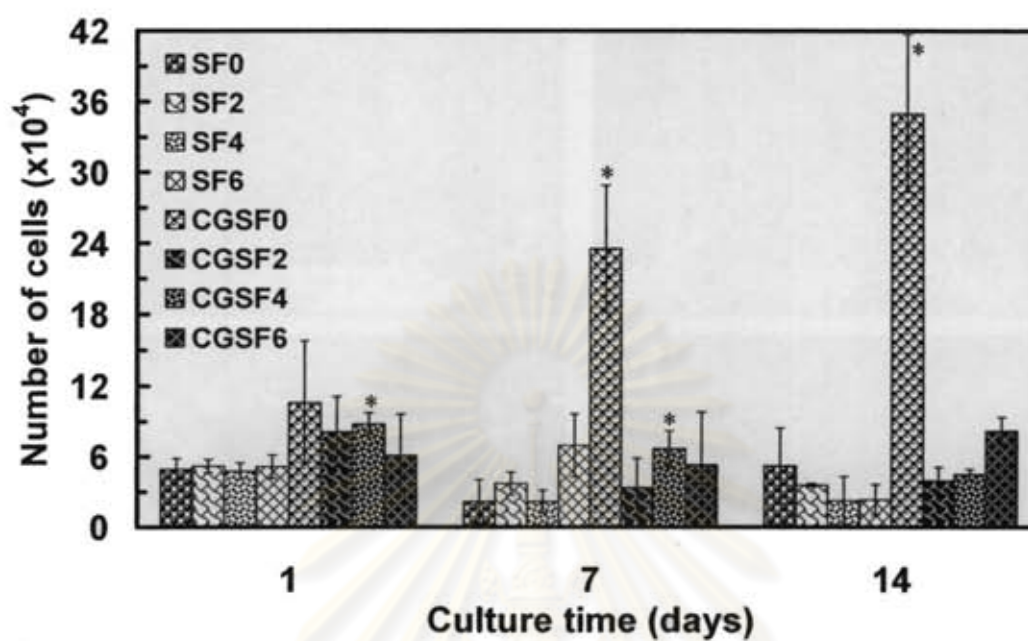


Figure 5.22 Number of MC3T3-E1 on hydroxyapatite/silk fibroin scaffolds, and hydroxyapatite-conjugated gelatin/silk fibroin scaffolds after 1, 7, and 14 days of the culture (seeding: 2×10^4 cells/scaffold).

* represent the significant difference ($p < 0.05$) relative to silk fibroin (SF0) scaffolds in each periods.

ศูนย์วิทยทรัพยากร
จุฬาลงกรณ์มหาวิทยาลัย

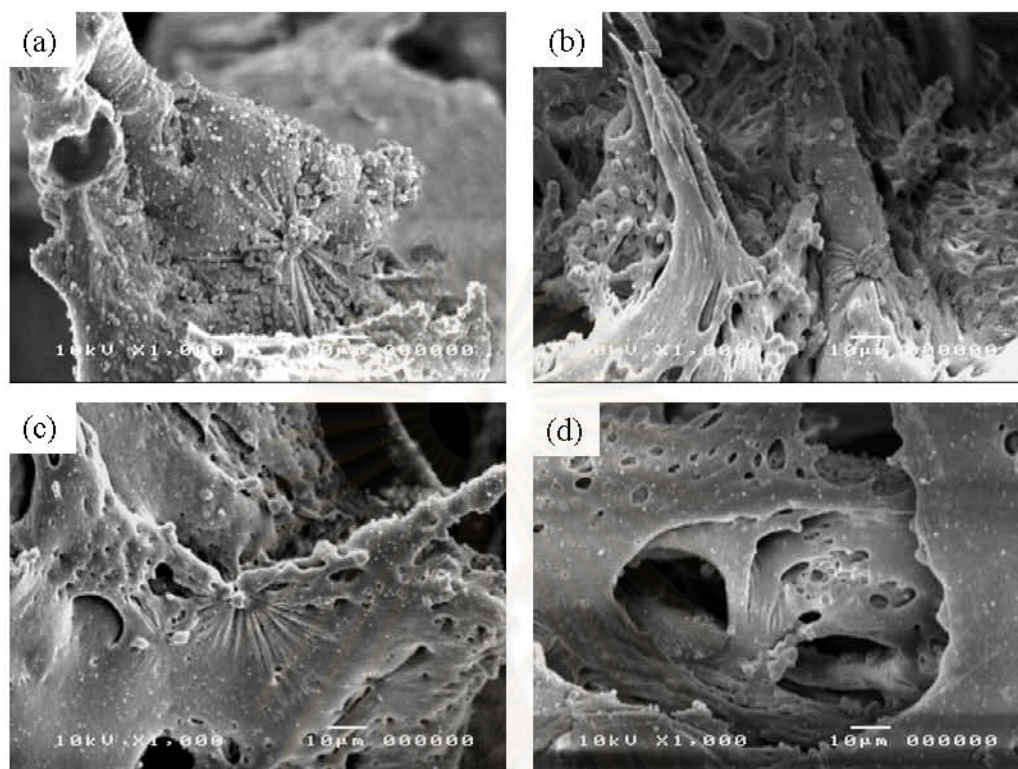


Figure 5.23 SEM micrographs of cross-sectional plane of silk fibroin scaffolds at position (a) 1 (cell seeding side), (b) 2, (c) 3, and (d) 4 (plate-exposed side) after 14 days of MC3T3-E1 culture.

ศูนย์วิทยทรัพยากร
จุฬาลงกรณ์มหาวิทยาลัย

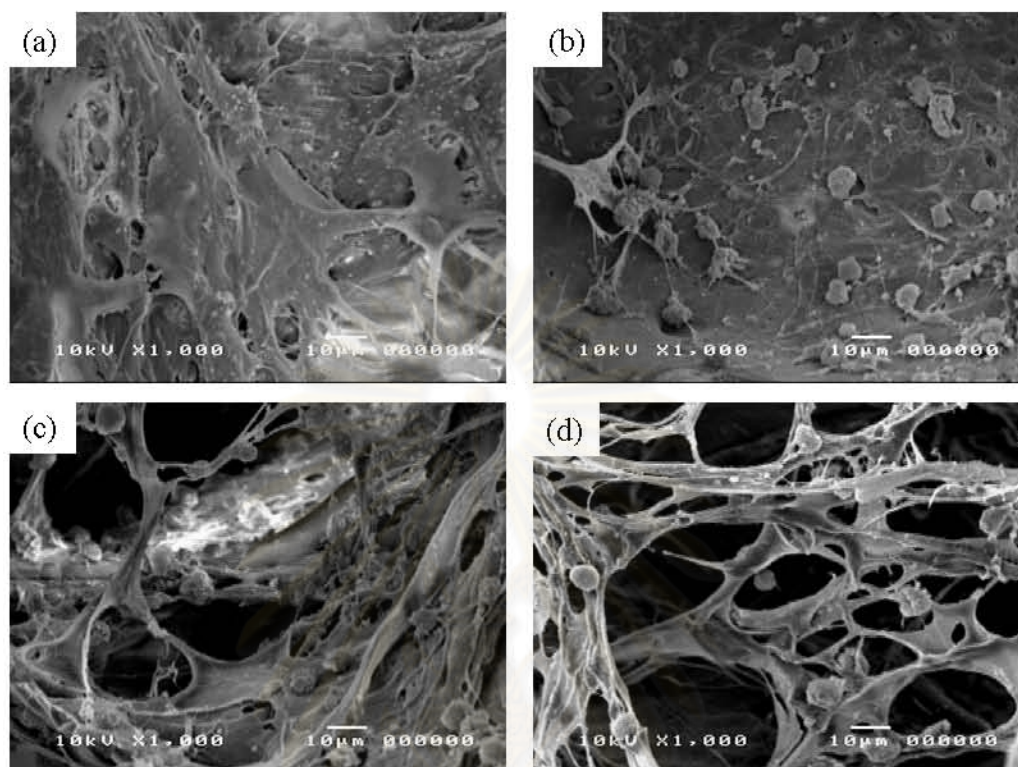


Figure 5.24 SEM micrographs of cross-sectional plane of conjugated-gelatin silk fibroin scaffolds at position (a) 1 (cell seeding side), (b) 2, (c) 3, and (d) 4 (plate-exposed side) after 14 days of MC3T3-E1 culture.

ศูนย์วิทยทรัพยากร
จุฬาลงกรณ์มหาวิทยาลัย

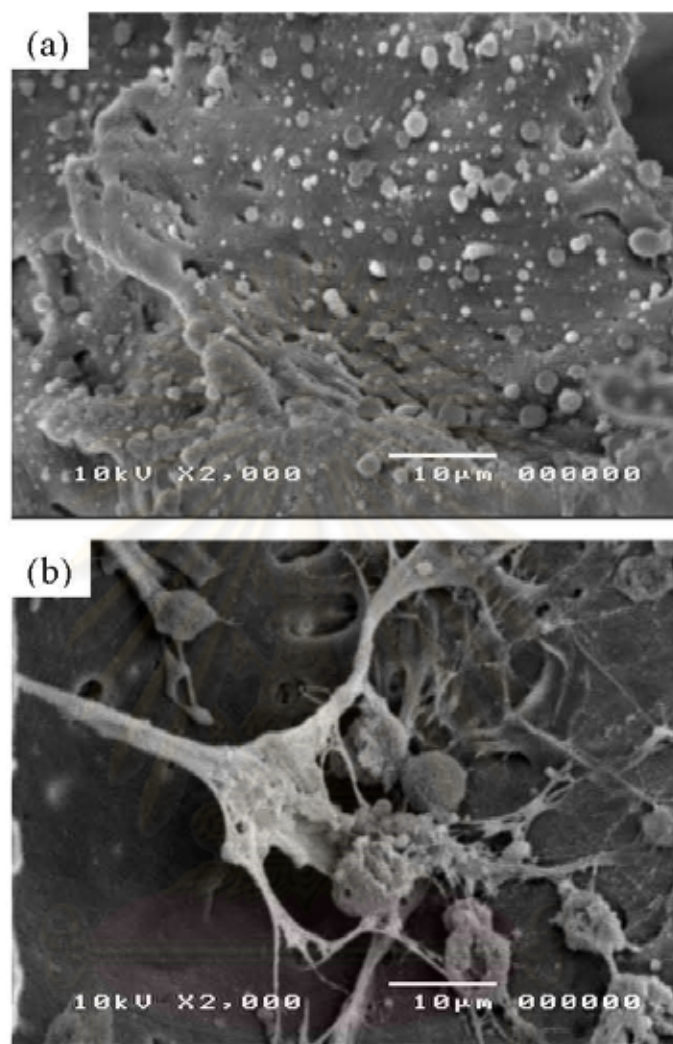


Figure 5.25 SEM micrographs of MC3T3-E1 morphology after 14 days cultured on scaffolds: (a) silk fibroin, and (b) conjugated-gelatin silk fibroin scaffolds.

จุฬาลงกรณ์มหาวิทยาลัย

CHAPTER VI

CONCLUSIONS AND RECOMMENDATIONS

6.1 Conclusions

Three-dimensional porous scaffolds prepared from Thai silk fibroin were developed via freeze-drying and salt-leaching methods. Gelatin was used to incorporate into Thai silk fibroin using two various techniques. To obtain freeze-dried scaffolds, gelatin solution was blended with aqueous silk fibroin solution prior to freeze-drying. Type of gelatin suitable to incorporate with silk fibroin was evaluated. After that, porous scaffolds were treated by dehydrothermal and chemicals. Morphology of type A gelatin/silk fibroin scaffolds showed a uniform structure compared to type B gelatin/silk fibroin scaffolds due to the electrostatic force of both materials. As a result, type A gelatin was selected to incorporate with silk fibroin in this work and the effects of blending weight ratio and DHT treatment period on physical and biological properties of the freeze-dried scaffolds were investigated.

The different fabrication process resulted in a difference in the secondary structure of silk fibroin scaffolds. The structure of freeze-dried silk fibroin scaffolds was random coil while that of air-dried silk fibroin scaffolds after gelling was β -sheet.

Blending ratio was formed to affect the compressive modulus of the scaffolds. Scaffolds with high silk fibroin content (80-100wt%) possessed relatively high compressive modulus (~350 kPa). Swelling ability of gelatin/silk fibroin scaffolds tended to slightly decrease as increasing silk fibroin content due to the hydrophobic property of silk fibroin. There was no significant difference in the compressive modulus and swelling ability of each type of blended scaffolds when DHT treated for 24 and 48 h. *In vitro* culture showed that freeze-dried pure silk fibroin scaffolds tended to have a slightly more MSCs proliferated comparing to gelatin/silk fibroin and gelatin scaffolds. MC3T3-E1 cells culture indicated that the number of

proliferated cells decreased in all blended scaffolds as increasing silk fibroin content. This could be due to the hydrophobic property of silk fibroin.

For the case of salt-leached silk fibroin scaffolds, gelatin was used to conjugate on the surface of silk fibroin scaffolds. Furthermore, the deposition of hydroxyapatite on silk fibroin and conjugated gelatin/silk fibroin scaffolds via alternate soaking in calcium and phosphate solutions was performed. After conjugating with gelatin, the structure of scaffolds were more fibrous with highly interconnection. The compressive modulus of conjugated gelatin/silk fibroin scaffold was higher than silk fibroin scaffold. In addition, hydroxyapatite growing on both scaffolds, with and without gelatin conjugating, resulted in less porous network and less interconnection as increasing the number of alternate soaking cycles. The hydroxyapatite deposition on the scaffolds was more upon the more cycles of alternate soaking resulting in higher compressive modulus but less swelling ability comparing to each initial scaffold without hydroxyapatite. Conjugated-gelatin/silk fibroin scaffolds showed a markedly increase in the number of MC3T3-E1 comparing to other scaffolds. In addition, the morphology of cells after 14 days culture of conjugated gelatin/silk fibroin scaffold indicated the extension of cytoplasm on surfaces. This revealed that gelatin conjugating was favorable to cell proliferation. Hydroxyapatite growing did not affect the number of proliferated cells. This was possibly due to the closed surface of scaffolds after hydroxyapatite deposition.

6.2 Recommendations

Although the effects of gelatin type, blending composition, DHT treatment time, effect of fabrication method, and effect of hydroxyapatite growing on chemical, physical and biological properties of the gelatin/silk fibroin scaffolds have been investigated in this work, there are other interesting points which should be further considered as follows:

1. The detailed evaluation on the activity of proliferated MC3T3-E1, such as ALP activity, immunohistochemistry staining, on silk fibroin and conjugated gelatin/silk fibroin scaffolds should be performed to fully understand the biological characteristics of these scaffolds
2. Biodegradation property should be investigated in order to understand the degradation rate of silk fibroin scaffolds.
3. Further study on differentiation of mouse osteoblast-like MC3T3-E1 with induced medium should be explored in order to evaluate the potential of silk fibroin for bone tissue engineering application.

References

- [1] Kim, U.J.; Park, J.; Kim, H.J.; Wada, M.; and Kaplan, D.L. Three-dimensional aqueous-derived biomaterial scaffolds from silk fibroin. Biomaterials 26 (2005): 2775–2785.
- [2] Lv, Q.; Feng, Q.; Hu, K.; and Cui F. Three-dimensional fibroin/collagen scaffolds derived from aqueous solution and the use for HepG2 culture. Polymer 46 (2005): 12662–12669.
- [3] Cai, K.; Yao, K.; Lin, S.; Yang, Z.; Li, X.; Xie, H.; Qing, T.; and Gao, L. Poly(D,L-lactic acid) surfaces modified by silk fibroin: effects on the culture of osteoblast *in vitro*. Biomaterials 23 (2002): 1153–1160.
- [4] Veparia, C.; and Kaplan, D.L. Silk as a biomaterial. Progress in Polymer Science 32 (2007): 991–1007.
- [5] Wang, Y.; Kim, H.J.; Novakovic, G.V.; and Kaplan, D.L. Stem cell-based tissue engineering with silk biomaterials. Biomaterials 27 (2006): 6064–6082.
- [6] http://www.en.rmut.ac.th/prd/Journal/Silk_with_figuresnew.pdf (October 8, 2005).
- [7] Huang, Y.; Onyeri, S.; Siewe, M.; Moshfeghian, A.; and Madihally, S.V. *In vitro* characterization of chitosan–gelatin scaffolds for tissue engineering. Biomaterials 26 (2005): 7616–7627.
- [8] Ratanavaraporn, J. Physical and biological properties of collagen/gelatin scaffolds. Master thesis Department of Chemical Engineering Chulalongkorn University, 2005.
- [9] Wang, L.; Nemoto, R.; and Senna, M. Changes in microstructure and physico-chemical properties of hydroxyapatite–silk fibroin nanocomposite with varying silk fibroin content. Journal of the European Ceramic Society 24 (2004): 2707–2715.
- [10] Bigi, A.; Boanini, E.; Panzavolta, S.; Roveri, N.; and Rubini, K. Bonelike apatite growth on hydroxyapatite–gelatin sponges from simulated body fluid. Journal of Biomedical Material Research 59 (2002): 709–714.

- [11] Taguchi, T.; Sawabe, Y.; Kobayashi, H.; Moriyoshi, Y.; Kataoka, K.; and Tanaka, J. Preparation and characterization of osteochondral scaffold. Materials Science and Engineering C 24 (2004): 881–885.
- [12] Ijima, H.; Ohchi, T.; Ono, T.; and Kawakami, K. Hydroxyapatite for use as an animal cell culture substratum obtained by an alternate soaking process Biochemical Engineering Journal 20 (2004): 155–161.
- [13] Ratner, B.D.; Hoffman, A.S.; Schoen, F.J.; and Lemons, J.E. Biomaterials. Science Academic Press (1996): 360-370.
- [14] Mori, H.; and Tsukadab, M. New silk protein: modification of silk protein by gene engineering for production of biomaterials. Reviews in Molecular Biotechnology 74 (2000): 95-103.
- [15] Altman, G.H.; Diaz, F.; Jakuba, C.; Calabro, T.; Horan, R.L.; Chen, J.; Lu, H.; Richmond, J.; and Kaplan, D.L. Silk-based biomaterials. Biomaterials 24 (2003): 401–416.
- [16] <http://www.nd.edu/~aseriann/silk.html>. (June 4, 2006)
- [17] <http://dspace.library.drexel.edu/retrieve/4251/CHAPTER+2.pdf> (March 30, 2006)
- [18] Baker, R.W. Other membrane processes. Membrane Technology and Applications. 491-520. New York: John Wiley & Sons, (2004).
- [19] <http://www.moac.go.th/builder/mu/index.php?page=415&clicksub=415&sub=1> 26 (June 11, 2007)
- [20] Young, S.; Wong, M.; Tabata, Y.; and Mikos, A.G. Gelatin as a delivery vehicle for the controlled release of bioactive molecules. Journal of Controlled Release 109 (2005): 256–274.
- [21] <http://en.wikipedia.org/wiki/Gelatin>. (June 3, 2006)
- [22] http://www.gmap-gelatin.com/about_gelatin_phys.html. (June 4, 2006)
- [23] <http://www.lsbu.ac.uk/water/hygel.html>. (June 4, 2006)
- [24] http://www.gelatin-gmia.com/html/gelatine_health.html. (June 4, 2006)
- [25] <http://www.csrc.com.tw/content-application.html>. (June 4, 2006)
- [26] Ma, P.X. Scaffolds for tissue fabrication. Materialtoday (2004)
- [27] Sachlos, E.; and Czernuszka, J.T. Making tissue engineering scaffolds work. European cells and materials 5 (2003): 29-40.

- [28] Rezwan, K.; Chen, Q.Z.; Blaker, J.J.; and Boccaccini, A.R. Biodegradable and bioactive porous polymer/inorganic composite scaffolds for bone tissue engineering. Biomaterials 27 (2006): 3413–3431
- [29] Ozeki, M.; and Tabata, Y. *In vivo* degradability of hydrogels prepared from different gelatins by various crosslinking method. Journal of Biomaterial Science Polymer Edition (2004).
- [30] Damink, L.H.H.; Dijkstra, P.J.; Feijen, J.; Luyn M.J.A.; Wachem, P.B.; and Nieuwenhuis, P. Cross-linking of dermal sheep collagen using a water-soluble carbodiimide Biomaterials 17 (1996): 765–73.
- [31] Grabarek, Z.; and Gergely, J. Zero-length crosslinking procedure with the use of active esters. Analytical Biochemistry 185 (1990): 131-135.
- [32] Davey, J.; and Lord, M. Essential cell biology Volume 1: Cell structure A practical approach. Oxford University Press, (2003).
- [33] http://www.vetscite.org/issue1/reviews/sultan_2_0800.htm.
- [34] <http://www.chemicon.com/webfiles/PDF/ECM810.pdf> (August, 2007)
- [35] Takahashi, Y.; Yamamoto, M.; and Tabata, Y. Osteogenic differentiation of mesenchymal stem cells in biodegradable sponges composed of gelatin and β -tricalcium phosphate. Biomaterials 26 (2005): 3587–3596.
- [36] Meinel, L.; Karageorgiou, V.; Hofmann, S.; Fajardo, R.; Snyder, B.; Li, C.; Zichner, L.; Langer, R.; Novakovic, G.V.; and Kaplan, D.L. Engineering bone-like tissue *in vitro* using human bone marrow stem cells and silk scaffolds. Journal of Biomedical Material Research 71A (2004): 25–34.
- [37] Kim, H.J.; Kim, U.J.; Novakovic, G.V.; Min, B.H.; and Kaplan, D.L. Influence of macroporous protein scaffolds on bone tissue engineering from bone marrow stem cells. Biomaterials 26 (2005): 4442-4452.
- [38] Mosmann, T. Rapid colorimetric assay for cellular growth and survival: application to proliferation and cytotoxicity assays. Journal of Immunological Methods 65 (1983): 55-63.
- [39] <http://www.atcc.org/common/products/MttCell.cfm>.
- [40] Tsukada M.; Gotoh, Y.; Nagura, M.; Minoura, N.; Kasai, N.; and Freddi, G. Structural changes of silk fibroin membranes induced by immersion in methanol aqueous solution. Journal of Polymer Science 32 (1994): 961-968.

- [41] Chen, X.; Knight, D.P.; Shao, Z.; and Vollrath, F. Regenerated Bombyx silk solutions studied with rheometry and FTIR. Polymer 42 (2001): 9969-9974.
- [42] Li, M.; Wu, Z.; Zhang, C.; Lu, S.; Yan, H.; Huang, D.; and Ye, H. Study on porous silk fibroin materials. II. Preparation and characteristics of spongy porous silk fibroin material. Journal of Applied Polymer Science 79 (2001): 2192-2199.
- [43] Yamada, H.; Nakao, H.; Takasu, Y.; and Tsubouchi, K. Preparation of undegraded native molecular fibroin solution from silkworm cocoons. Materials Science and Engineering C 14 (2001): 41-46.
- [44] Wang, H.; Zhang, Y.; Shao, H.; and Hu, X. A study on the flow stability of regenerated silk fibroin aqueous solution. International Journal of Biological Macromolecules 36 (2005): 66-70.
- [45] Horan, R.L.; Antle, K.; Collette, A.L.; Wang, Y.; Huang, J.; Moreau, J.E.; Volloch, V.; Kaplan, D.L.; and Altman, G.H. *In vitro* degradation of silk fibroin. Biomaterials 26 (2005): 3385-3393.
- [46] Minoura, N.; Aiba, S.I.; Higuchi, M.; Gotoh, Y.; Tsukada M.; and Imai Y. Attachment and growth of fibroblast cells on silk fibroin. Biochemical and Biophysical Research Communications 28 (1995): 511-516.
- [47] Sofia, S.; McCarthy, M.B.; Gronowicz, G.; and Kaplan, D.L. Functionalized silk-based biomaterials for bone formation. Journal of Biomedical Materials Research 54 (2001): 139-148.
- [48] Panilaitis, B.; Altman, G.H.; Chen, J.; Jin, H.J.; Karageorgiou, V.; and Kaplan, D.L. Macrophage responses to silk. Biomaterials 24 (2003): 3079-3085.
- [49] Kim, U.J.; Park, J.; Li, C.; Jin, H.J.; Valluzzi, R.; and Kaplan, D.L. Structure and properties of silk hydrogels. Biomacromolecules 5 (2004): 786-792.
- [50] Meinel, L.; Hofmann, S.; Karageorgiou, V.; Head, C.K.; McCool, J.; Gronowicz, G.; Zichner, L.; Langer, R.; Novakovic, G.V.; and Kaplan, D.L. The inflammatory responses to silk films *in vitro* and *in vivo*. Biomaterials 26 (2005): 147-155.
- [51] Tamada, Y. New process to form a silk fibroin porous 3-D structure. Biomacromolecules 6 (2005): 3100-3106.

- [52] Wang, Y.; Blasioli, D.J.; Kim, H.J.; Kim H.S.; and Kaplan D.L. Cartilage tissue engineering with silk scaffolds and human articular chondrocytes. Biomaterials 27 (2006): 4434-4442.
- [53] Meechaisue, C.; Wutticharoenmongkol, P.; Waraput, R.; Huangjing, T.; Ketbumrung, N.; Pavasant, P.; and Supaphol, P. Preparation of electrospun silk fibroin fiber mats as bone scaffolds: a preliminary study Biomedical Materials 2 (2007): 181–188.
- [54] Kweon, H.Y.; Um, I.C.; and Park, Y.H. Structural and thermal characteristics of *Antheraea pernyi* silk fibroin/chitosan blend film. Polymer 42 (2001): 6651-6656.
- [55] Gil, E.S.; Frankowski, D.J.; Bowman, M.K.; Gozen, A.O.; Hudson, S.M.; and Spontak, R.J. Mixed protein blends composed of gelatin and *Bombyx mori* silk fibroin: effects of solvent-induced crystallization and composition. Biomacromolecules 7 (2006): 728-735.
- [56] Taguchi, T.; Kishida, A.; and Akashi, M. Hydroxyapatite Formation on/in poly(vinyl alcohol) hydrogel matrices using a novel alternate soaking process. Chemistry Letters (1998): 711-712.
- [57] Furuzono, T.; Taguchi, T.; Kishida, A.; Akashi, M.; and Tamada, Y. Preparation and characterization of apatite deposited on silk fabric using an alternate soaking process. Journal of Biomedical Material Research 50 (2000): 344–352.
- [58] Wang, L.; Ning, G.L.; and Senna, M. Microstructure and gelation behavior of hydroxyapatite-based nanocomposite sol containing chemically modified silk fibroin. Colloids and Surfaces A 254 (2005): 159–164.
- [59] Pek, Y.S.; Spector, M.; Yannas, I.V.; and Gibson, L.J. Degradation of a collagen–chondroitin-6-sulfate matrix by collagenase and by chondroitinase. Biomaterials 25 (2004): 473–482.
- [60] Takahashi, Y.; Yamamoto, M.; and Tabata, Y. Osteogenic differentiation of mesenchymal stem cells in biodegradable sponges composed of gelatin and β -tricalcium phosphate. Biomaterials 26 (2005): 3587–3596.
- [61] Kaplan, D.; Adams, W.W.; Farmer, B.; and Viney, C. silk polymers. Washington DC: American Chemical Society, 1993.

- [62] Saitoh, H.; Ohshima, K.; Tsubouchi, K.; Yoko Takasu, Y.; and Yamada, H. X-ray structural study of noncrystalline regenerated *Bombyx mori* silk fibroin. International Journal of Biological Macromolecules 34 (2004): 259–265.
- [63] Grabarek, Z.; and Gergely, J. Zero-length crosslinking procedure with the use of active esters. Analytical Biochemistry 185 (1990): 131-135.
- [64] Gil, E.S.; Frankowski, D.J.; Hudson, S.M.; and Spontak, R.J. Silk fibroin membranes from solvent-crystallized silk fibroin/gelatin blends: Effects of blend and solvent composition. Materials Science and Engineering C 27 (2007): 426–431.
- [65] Motta, A.; Moschini, L.; Chamchongkaset, J.; Kanokpanont, S.; and Damrongsakkul, S. Characterization of silk proteins: A comparison of different cocoon sources. (In preparation)
- [66] Wutticharoenmongkol, P.; Pavasant, P.; and Supaphol, P. Osteoblastic phenotype Expression of MC3T3-E1 cultured on electrospun polycaprolactone fiber mats filled with hydroxyapatite nanoparticles. Biomacromolecules 8 (2007): 2602-2610.
- [67] Calvert, J.W.; Marra, K.G.; Cook, L.; Kumta, P.N.; DiMilla, P.A.; and Weiss, L.E. Characterization of osteoblast-like behavior of cultured bone marrow stromal cells on various polymer surfaces. Journal of Biomedical Materials Research 52 (2000): 279.
- [68] Huang, Y.; Onyeri, S.; Siewe, M.; Moshfeghian, A.; and Madihally, S.V. *In vitro* characterization of chitosan–gelatin scaffolds for tissue engineering. Biomaterials 26 (2005): 7616–7627.



APPENDICES

ศูนย์วิทยทรัพยากร
จุฬาลงกรณ์มหาวิทยาลัย

APPENDIX A

Raw data of compressive modulus

Table A-1 Mean and SD of compressive modulus of gelatin/silk fibroin scaffolds with DHT treatment for 24 h.

Weight percentage of silk fibroin	Compressive modulus (kPa)	
	mean	SD
0	337.14	143.96
20	214.29	73.68
60	260.00	62.45
80	467.14	62.91
100	350.00	102.31

Table A-2 Mean and SD of compressive modulus of gelatin/silk fibroin scaffolds with DHT treatment for 48 h.

Weight percentage of silk fibroin	Compressive modulus (kPa)	
	mean	SD
0	302.50	34.03
20	132.50	28.72
60	220.00	24.49
80	577.50	87.32
100	442.50	66.52

Table A-3 Mean and SD of compressive modulus of hydroxyapatite/silk fibroin scaffolds.

Cycles of alternate soaking	Compressive modulus (kPa)	
	mean	SD
0	262.50	61.85
2	265.00	81.85
4	500.00	121.93
6	535.00	93.99

Table A-4 Mean and SD compressive modulus of hydroxyapatite-conjugated gelatin/silk fibroin scaffolds.

Cycles of alternate soaking	Compressive modulus (kPa)	
	mean	SD
0	506.00	151.10
2	510.00	170.88
4	550.00	234.09
6	826.00	388.63



APPENDIX B

Raw data of swelling ratios

Table B-1 Mean and SD of swelling ratios of gelatin/silk fibroin scaffolds with DHT treatment for 24 h.

Weight percentage of silk fibroin	Compressive modulus (kPa)	
	mean	SD
0	12.01	0.60
20	10.99	0.56
60	12.22	2.50
80	11.09	1.35
100	9.19	1.34

Table B-2 Mean and SD of swelling ratios of gelatin/silk fibroin scaffolds with DHT treatment for 48 h.

Weight percentage of silk fibroin	Compressive modulus (kPa)	
	mean	SD
0	13.69	2.10
20	13.75	1.85
60	13.40	1.97
80	11.77	2.28
100	10.32	2.00

Table B-3 Mean and SD of swelling ratios of hydroxyapatite/silk fibroin scaffolds.

Cycles of alternate soaking	Compressive modulus (kPa)	
	mean	SD
0	11.02	1.46
2	7.23	0.66
4	6.28	0.42
6	5.70	0.15

Table B-4 Mean and SD of swelling ratios of hydroxyapatite-conjugated gelatin/silk fibroin scaffolds.

Cycles of alternate soaking	Compressive modulus (kPa)	
	mean	SD
0	10.32	1.37
2	7.13	0.62
4	5.27	0.42
6	4.38	0.20



ศูนย์วิทยทรัพยากร
จุฬาลงกรณ์มหาวิทยาลัย

APPENDIX C

Standard curve of *in vitro* cell culture test

Table C-1 Absorbance at 570 nm from MTT assay for standard curve of bone-marrow derived mesenchymal stem cells (MSCs).

Replication no.	Number of cells				
	5,000	10,000	20,000	40,000	80,000
1	0.066	0.103	0.144	0.320	0.562
2	0.068	0.081	0.158	0.339	0.544
3	0.066	0.094	0.147	0.316	0.544
4	0.064	0.069	0.123	0.203	0.637
mean	0.066	0.087	0.143	0.295	0.572
SD	0.002	0.015	0.015	0.062	0.044

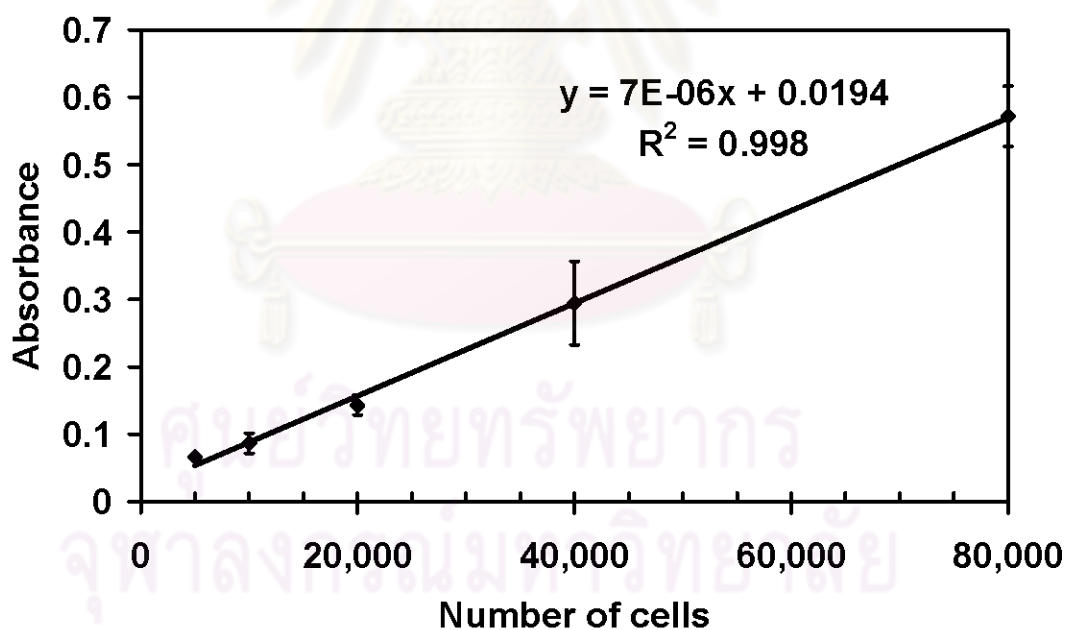


Figure C-1 Standard curve for MSCs.

Table C-2 Absorbance at 570 nm from MTT assay for mouse osteoblast-like cells (MC3T3-E1).

Replication no.	Number of cells				
	10,000	20,000	40,000	80,000	160,000
1	0.033	0.052	0.08	0.185	0.319
2	0.036	0.049	0.093	0.181	0.299
3	0.052	0.061	0.082	0.152	0.273
mean	0.040	0.054	0.085	0.173	0.297
SD	0.010	0.006	0.007	0.018	0.023

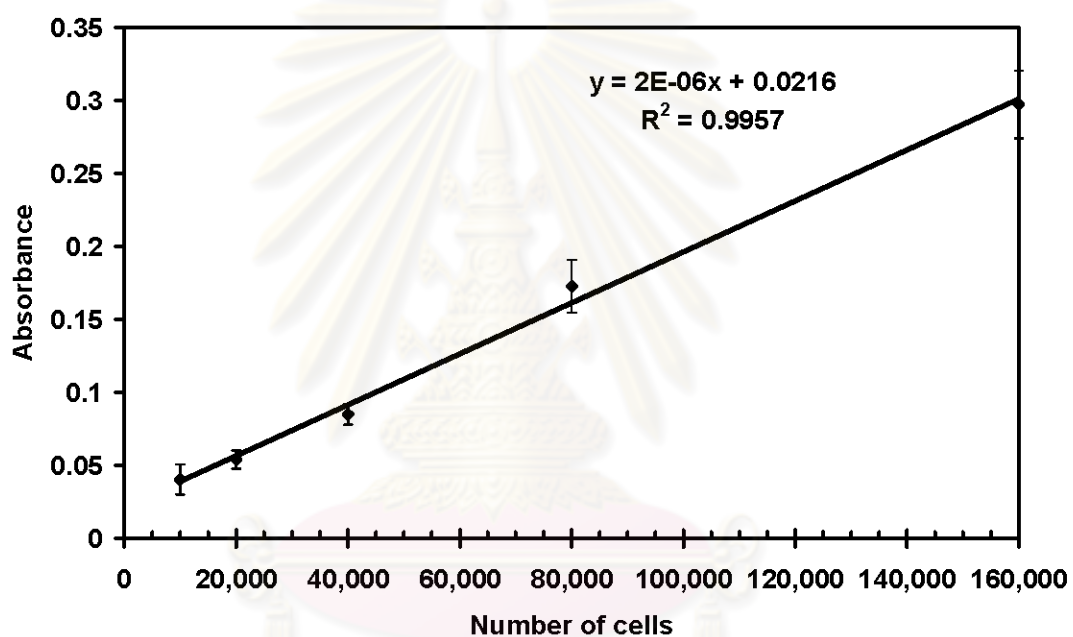


Figure C-2 Standard curve for MC3T3-E1.

ศูนย์วิทยุโทรพยากร
จุฬาลงกรณ์มหาวิทยาลัย

VITAE

Miss Jitima Chamchongkaset was born in Bangkok, Thailand on February 7, 1983. She finished the high school education in 2000 from Bodindecha (Sing Singhaseni) school. In 2004, she received her Bachelor Degree of Engineering with a major of Chemical Engineering from Faculty of Engineering, Mahidol University. After the graduation, she pursued her graduate study to a Master of Engineering (chemical engineering), the Faculty of Engineering, Chulalongkorn University.

Some parts of this work were presented at the conferences as follows;

- Chamchongkaset, J.; Kanokpanont, S.; and Damrongsakkul, S. Morphology and biological properties of Thai silk fibroin-based scaffolds. Poster presentation in biomedical polymer at ABC2006: The Sixth Asian BioCeramics Symposium 2006, 7-10 November 2006, The Sofitel Central Plaza, Bangkok, Thailand (ABC poster presentation award)

- Chamchongkaset, J.; Kanokpanont, S.; and Damrongsakkul, S. *In vitro* study using mesenchymal stem cell on gelatin/Thai silk fibroin scaffolds. Oral presentation in biomaterials at NCBME2007: The 5th National Conference on Biomedical Engineering, 8 July 2007, The Twin Tower Hotel, Bangkok, Thailand.

ศูนย์วิทยทรัพยากร
จุฬาลงกรณ์มหาวิทยาลัย